New mechanistic insight into replication fork reversal and resart

Matteo Berti

This thesis is submitted for the degree of Doctor of Philosophy in Molecular Genetics and Biotechnologies

Scuola Normale Superiore, Pisa, Italy.

Genome Stability
International Centre for Genetic Engineering and Biotechnology (ICGEB),
Trieste, Italy

Scientific Supervisor: Prof. Alessandro Vindigni

March 2013

ABSTRACT

An emerging model of how stalled or damaged forks are processed is that replication forks can reverse to aid repair of the damage. The first evidence that replication forks regress in human cells came from a recent study with topoisomerase I (Top1) inhibitors, an important class of anticancer drugs currently in clinical use. Their cytotoxicity, and thus their efficacy, has been generally linked to their ability to cause the accumulation of DNA nicks, which are later converted into double-stranded breaks (DSBs) by the collision of the DNA replication fork with the primary lesion. The discovery that replication forks can regress upon Top1 inhibition provided new insight into the molecular basis of Top1 cytotoxicity by showing that clinically relevant, nanomolar doses of Top1 poisons induce replication fork slowing and reversal in a process that can be uncoupled from DSB formation and requires poly(ADP-ribose) polymerase 1 (PARP1) activity. However, whether reversed forks can efficiently restart and which factors are involved in this mechanism was still unknown. In this thesis, using a combination of biochemical and cellular approaches, we provided the first evidence that regressed forks can restart *in vivo* and identified a key role for the human RECQ1 helicase in promoting efficient replication fork restart after Top1 inhibition that is not shared by other human RecQ members. Our data also provided the first insight into the molecular role of PARP1 in fork reversal by showing that the poly(ADP-ribosyl)ation activity of PARP inhibits RECQ1 activity on replication forks after Top1 inhibition. Thus, PARP activity is not required to form, but rather to "accumulate" reversed fork structures by maintaining/protecting them from a counteracting activity (RECQ1), which would otherwise cause an untimely restart of reversed forks, leading to DSB formation. The identification of a specific and controlled biochemical activity that drives the restart of reversed forks strongly supports the physiological relevance of this DNA transaction during replication stress in human cells. Moreover, our studies provide new mechanistic insights into the roles of RECQ1 and PARP1 in DNA replication and offer molecular perspectives to potentiate chemotherapeutic regimens based on Top1 inhibition.

CONTENTS

LIST OF FIGURES AND TABLES

1 INTRODUCTION

Genomic instability is one of the hallmarks of almost all human cancers [1]. In contrast to normal tissues precancerous cells are characterized by accumulation of DNA lesions and activation of the DNA damage response (DDR), which induces senescence and apoptosis, thus representing an active barrier to tumorigenesis [2, 3]. The major source of genomic instability associated with cancer development arises from oncogene-induced replication stress [4]. Indeed cells are particularly vulnerable during DNA replication and several cellular factors are needed to ensure the correct duplication of the genome. However, hereditary or acquired mutations targeting DNA repair or checkpoint genes lead to aberrant DNA replication and genomic instability contributing to the tumorigenesis process. Cancer cells, in turn, become genetically "addicted" to these error-prone repair pathways to actively proliferate, contributing to their mutator phenotype [5, 6]. Unraveling the mechanisms by which the cells cope with replication stress is critical not only to understand the basis of tumor development, but also to optimize and design novel therapies that target those specific repair pathways needed for cancer cell survival.

1.1 DNA replication initiation

The replication of genomic DNA is a well-conserved and tightly regulated process to ensure that the genome is replicated just once for every cell cycle [7]. In higher eukaryotes replication initiates from multiple and generally clustered genomic regions termed origins of replication, unlike bacteria, which replicate their small genome from a single origin. The first step of the DNA replication is the formation of a pre-replicative complex (pre-RC) at each origin in G1 phase, through the binding of the origin recognition complex (ORC) to the chromatin, followed by the recruitment of additional replication factors, such as cell division control protein 6 (Cdc6), chromatin licensing and dna replication factor 1 (Cdt1) and the mini-chromosome maintenance (MCM) 2-7 helicase complex [8]. There are several mechanisms that finely tune the "licensing" process in order to prevent re-replication: cyclin-dependent kinases (CDKs) activation inhibits the assembly of new origins and, most importantly, geminin binds to Cdt1 blocking MCM recruitment [9]. During the G1/S

transition state the pre-RC becomes phosphorylated by the cyclin E/CDK2 (cyclin-dependent kinase 2) and DDK (Dbf4/Drf1-dependent S-phase-promoting kinase Cdc7), promoting loading of Cdc45 and the GINS complex, which are essential for origin firing and fork progression. The MCM2-7 and Cdc45 form the active replicative helicase required for DNA unwinding, while the GINS complex maintains their structural association (CMG complex). In addition, their assembly depends on additional factors well-defined in yeast, such as Sld2 and Sld3. These two factors interact with and activate Dpb11 upon CDK phosphorylation, which in turn seems to be required to facilitate Cdc45 loading [10]. The mammalian orthologs of Sld2 and Sld3 have not been identified as far. However, the RECQ4 helicase, MCM10, and Ctf4/AND-1 are needed for the CMG complex assembly in mammalian cells, as recently demonstrated using Bimolecular fluorescence complementation assay [11].

The replisome is a multicomponent protein complex that contains different elongation proteins evolved to ensure the bidirectional semi-discontinuous DNA synthesis. The clamp loader replication factor C (RFC) helps the loading of the sliding clamp PCNA (proliferating cell nuclear antigen) that in turn tethers the DNA polymerases to the chromosome, enabling highly processive DNA replication. On the leading strand the DNA nucleotides are added continuously by the polymerase ε to the 3' end of the RNA primer synthesized by the polymerase α-primase. On the lagging strand short DNA fragments called Okazaki fragments are built by the polymerase δ on the RNA primer, processed by the FEN1 and Dna2 nucleases, and ligated to the previous fragment by DNA ligase I.

Unwinding of the duplex DNA induces positive and negative torsional stress both in front and behind the replication fork that cannot simply diffuse by the swiveling of the long chromosomes. Specialized nucleases called DNA Topoisomerases (Top) relieve the positive supercoils ahead and the precatenates that intertwine the two replicated duplexes behind the replication fork by introducing either single (Top1) or double-stranded breaks (Top2) into the backbone of the DNA [12 13]. In a chromatin context histones are evicted ahead of the fork by the histone chaperone FACT and recycled on to the daughter strands by ASF1 and CAF1 ensuring a proper epigenetic transmission [14, 15].

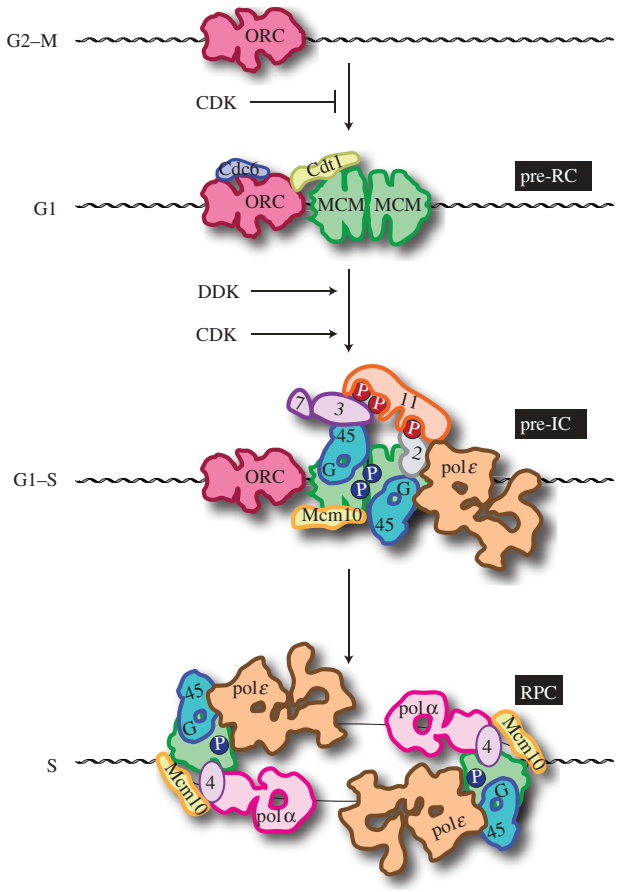

Figure 1.1. Assembly of DNA replication complexes. The individual steps leading to the assembly of bidirectional replisomes in yeast is outlined. Names associated with each of the complexes are shown on the right: pre-RC, pre-replication complex; pre-IC, pre-initiation complex; RPC, replisome progression complex. Cell cycle phases permissive for the individual steps are shown on the left. For simplicity, some of the protein names have been abbreviated: 11, Dpb11; 3, Sld3; 7, Sld7; 2, Sld2; G, GINS; 45, Cdc45; 4, Ctf4. Cyclin-dependent kinase (CDK) phosphorylation sites are shown in red, Dbf4-dependent kinase (DDK) phosphorylation sites are shown in blue. Adapted from J.F.X. Diffley, 2011 [10].

1.2 Replication stress

Replication fork progression can be impaired by several obstacles, such as the presence of non-nucleosomal protein-DNA interactions, head-on collision with the transcription machinery, secondary structures that may arise in repeated A-T- or G-C- rich sequences or spontaneous DNA damage. A halted replication fork is called "stalled" when is structurally able to resume progression, while is called "collapsed" when it becomes inactivated following the dissociation of the replication machinery [16]. In bacteria a recombination-like process allows the origin-independent loading of the replication

machinery in order to resume DNA synthesis after replication collapse [17]. In higher organisms a similar mechanism has not been identified yet; however, because of the presence of multiple origins, replication can be completed by an adjacent replication fork or by the firing of nearby "dormant" origins. Indeed, the MCM complex is loaded on chromatin in large excess relative to the effective fired replication forks, ensuring a reservoir of origin backup [18, 19]. Moreover, cells accumulate DNA damage and chromosome instability in conditions of "limited licensing" due to MCM downregulation, [20]. Despite that, if both converging forks collapse or at regions of low density of origins such as fragile sites or telomeres, replication must restart in order to complete DNA synthesis.

Upon transient fork stalling generated by replication inhibitors, such as hydroxyurea (HU) or aphidicolin, stabilization of replication forks by checkpoint signaling is crucial for maintaining the replisome in a replication-competent state and keeping DNA polymerases at the site of nucleotide incorporation [21]. The ATR branch is the main checkpoint pathway during the S-phase and its ablation is early embryonic lethal in the mouse [22]. Stalled forks generated by helicase-polymerase uncoupling generally presents exposed ssDNA regions coated by the single-strand binding protein RPA (replication protein A), which in turn recruits the active ATR-ATRIP (ATR-interacting protein) complex [23]. In spite of the numerous substrates, the main signal arising from the ATR cascade is the phosphorylation-activation of Chk1, a serine-threonine kinase. Globally Chk1 activation leads to cell cycle arrest by phosphorylation-modulation of CDK regulators CDC25-A, CDC25-B, CDC25-C, and p53 activation. In addition, the ATR pathway promotes local fork stabilization through phosphorylation of several targets such as replication components, nucleases, and DNA helicases, which are required to maintain replisome integrity and prevent fork collapse [23, 24]. In yeast, UV-irradiated or HU-treated checkpoint mutants accumulate aberrant replication structures such as long gaps and four-ways branched molecules resembling reversed forks [25, 26]. A set of not essential, but evolutionary conserved proteins named TIM, TIPIN, AND-1, and Clapsin are important structural components of the replication machinery, by physically linking the helicase and the polymerase activities and preventing their uncoupling upon fork stalling. In addition, they provide a platform for DNA damage signaling and checkpoint activation, and ensure proper chromosome segregation by promoting sister chromatid cohesion [27].

1.3 Homologous recombination and DNA replication.

Double strand-breaks (DSBs) are the major source of genomic instability and cell death. During DNA replication DSBs can arise from unscheduled nuclease processing of collapsed replication forks or from the replication run-off at nicks or gaps on the DNA template. While the Non-Homologous End-Joining (NHEJ) pathway processes and seals DSBs in non-proliferating cells during the G1 phase, Homologous Recombination (HR) is an highly accurate repair pathway that uses the intact sister chromatid as template to fix DSBs during the S and G2 phases [28]. The central HR factors are RecA in bacteria and RAD51 in eukaryotes. They form a nucleofilament on 3'-single-stranded DNA ends and catalyzes homologous DNA search, strand invasion and pairing to form a displacement loop (D-loop), where the 3'-end of the invading strand primes DNA synthesis off the template duplex DNA. If the DSB is two-sided (frank), after branch migration of the D-loop, the other end of the DSB is engaged by another invasion event or by DNA annealing. The resultant double Holliday junction is a substrate for dissolution into non-crossover products by BLM-Top3α or for resolution into crossover products by structure-specific endonucleases, such as Mus81-Eme1, Slx1-Slx4 and Gen endonuclease homologue 1 (GEN-1) (Figure 2). Mitotic recombination in contrast to meiosis preferentially leads to non-crossover products; crossover events can be cytogenetically detected in metaphase as sister chromatid exchanges (SCEs). Alternatively, after partial DNA synthesis, the D-loop is dissolved and the displaced invading 3'-end reanneals with the second end of the DSB. This process, called synthesis-dependent strand annealing (SDSA) always leads to non-crossover products, thus reducing the potential for genetic rearrangement [29] (Figure 2). ATP-dependent dissolution of D-loops by motor proteins is the key step in this HR sub-pathway. Recently, FANCM, one of the 13 proteins linked to the rare human genetic disease *Fanconi Anemia* (FA) [30], as well as its yeast orthologs Mph1 (*Saccharomyces cerevisiae*) [31] and Fml1 (*Schizosaccharomyces pombe*) [32], were shown biochemically and genetically to dissolve D-loops. This dissolution activity channels HR repair (HRR) into the SDSA sub-pathway, thus preventing crossover formation and maintaining the genome stability.

Replication fork collapse triggered by nick formation on the template DNA, especially on the leading strand, or generated by endonucleolytic processing of stalled forks, leads to the

formation of one-sided DSB, where, in the absence of a converging forks, the D-loop accumulated by the RAD51-mediated nucleofilament invasion cannot be processed by the two HR subpathways described above. Bacteria has an efficient system to reload the replisome on these D-loops, in an origin-independent manner, and resume DNA synthesis thanks to the action of specialized 3'-5' helicases such as PriA [17]. Although a PriA homolog is missing in eukaryotes, recent studies showed that Mre11 and RAD51 facilitate the reassembly of the CMG complex at broken replication forks in *Xenopus laevis* egg extract, suggesting the presence of a similar recombination-dependent (and origin-independent) mechanism in vertebrates [33].

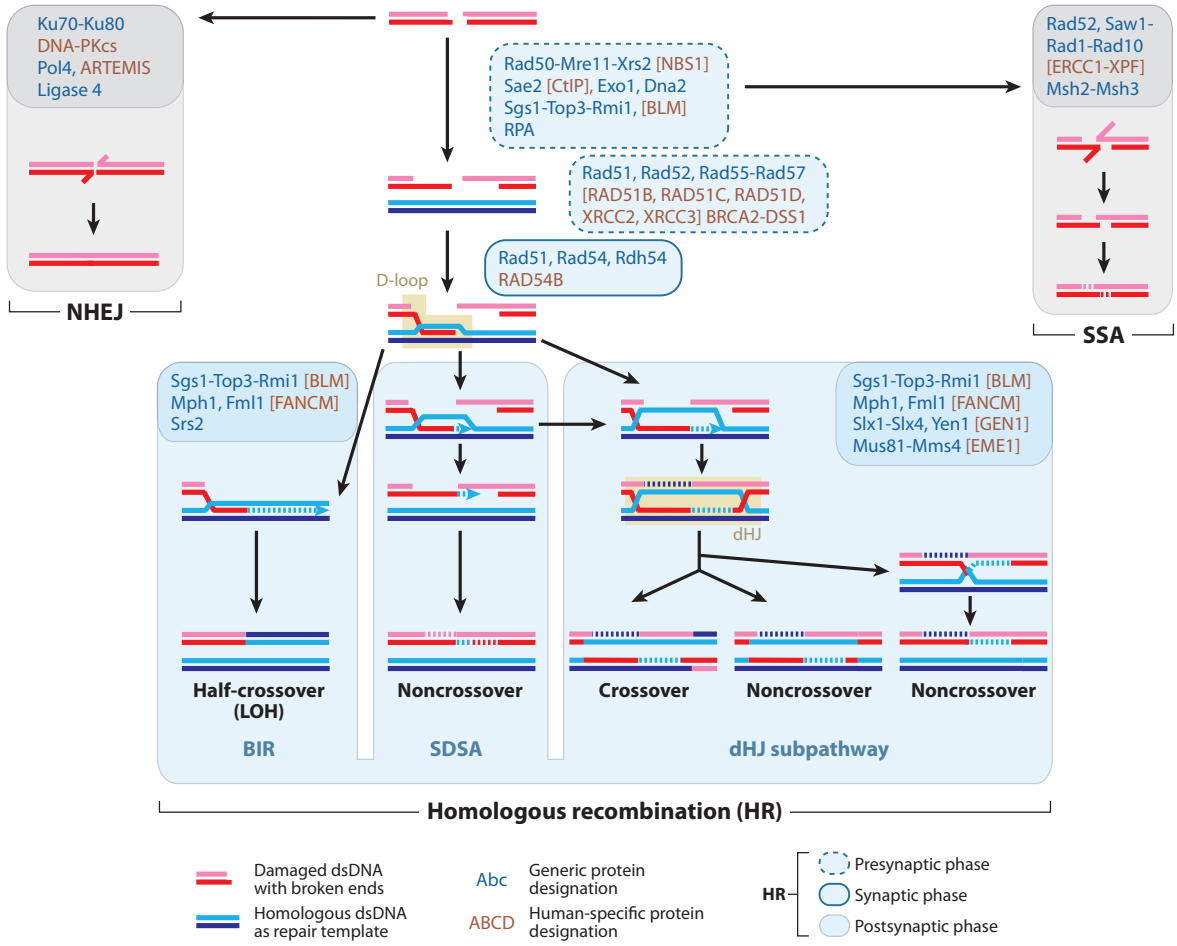

Figure 1.2. Pathways of double-strand break repair. Protein names refer to the budding yeast *Saccharomyces cerevisiae* (blue). Where different in human, names (brown) are given in brackets. For proteins without a yeast homolog, brackets for human proteins are omitted. Broken lines indicate new DNA synthesis and stretches of heteroduplex DNA that upon mismatch repair (MMR) can lead to gene conversion. Abbreviations: BIR, break-induced replication; dHJ, double Holliday junction; NHEJ, non-homologous end joining; LOH, loss of heterozygosity; SDSA, synthesis-dependent strand annealing; SSA, single-strand annealing. Adapted form W.D. Heyer, 2010 [29].

This process resembles a particular HR sub-pathway called Break-induced replication (BIR), which has been extensively studied in yeast, where the invading strand generated at one-sided DSB is thought to establish a replication fork and to copy the entire distal arm of the template chromosome, resulting in loss of heterozygoty (LOH) (Figure 2 and Figure 3h). In principle, this process might have a more relevant role in vertebrates than in lower eukaryotes due to the elevated presence of repetitive sequences that allow invasions on non-homologous template and fork restart. However, because of its non-conservative nature, the BIR process is characterized by several rounds of invasion and template switching, which trigger replication slippage and gross chromosomal rearrangements (GCR) [34, 35]. Moreover, BIR-mediated DNA synthesis is highly inaccurate leading to a frameshift mutagenesis rate 2,800-fold higher than during normal replication, probably because of the lack of essential replicative factors [36]. While this process is well defined in yeast, it has not been identified in mammalian cells to date.

All the HR pathways described above are finely regulated by several mechanisms in order to ensure accurate recombination and prevent mutations, deletions and gene amplifications. The requirement of a 3'-ssDNA overhangs for RAD51 loading makes HR repair dependent on a first step of nucleolytic resection by the coordinated action of specific nucleases and helicases [37]. First, DSBs are recognized and processed by the Mre11-Rad50-Nbs1 (MRN) complex, the tumor suppressor BRCA1 and CtBP-interacting protein (CtIP) [38]. Their assembly is under the control of CDK activity, therefore restricted to S-phase and G2-phase [39] and it is counteracted by the high affinity for double-strand ends of the Ku heterodimer that prevents resection and promote NHEJ during G1 [40]. Then extensive, long-range resection is taken over by the action of nucleases or nuclease-helicase complexes such as BLM and Dna2, or Exo1 [41, 42, 43, 44]. The resected 3'-end becomes coated by RPA that is subsequently replaced by RAD51 to form the presynaptic filament. Since RPA has a higher affinity for ssDNA than RAD51, cells have evolved mediator proteins such as Rad52 in yeasts and the tumor suppressor protein BRCA2 in vertebrates to overcome the RPA inhibitory barrier and promote RAD51 filament assembly [45, 46, 47]. The central role of BRCA1 and BRCA2 in homologous recombination have been extensively studied and exploited for cancer therapy since mutations in these two genes confer genomic instability

and predispose to a high risk for breast and ovarian cancer [48]. In addition to these two proteins, other factors are critical for the positive regulation of the RAD51-ssDNA filament assembly. Indeed mutations in genes coding for the RAD51 paralogs (*RAD51C*, *RAD51B*, *RAD51D*, *XRCC2*, *XRCC3*), a group of proteins important for RAD51 filament stabilization, have been recently demonstrated to recapitulate the tumorigenic potential of *BRCA* dysfunction ("BRCAness") [49, 50, 51].

On the other hand excess of HR-dependence for survival leads to a hyper-recombination phenotype and chromosomal instability. Increasing evidences suggest that HR is an inaccurate process, particularly due to the complex architecture of the vertebrate genome. Lee *et al.* demonstrated that a microhomology-based, nonallelic homologous recombination (NAHR) mechanism between low-copy number repeats or repetitive elements located at different replication forks, brought nearby by chromatin looping, is responsible for the complex nonrecurrent rearrangements of *PLP1 (proteolipid protein 1)* gene, observed in the dysmyelinating disorder *Pelizaeus-Merzbacher disease* (PMD) [52]. Moreover, when the homologous sequences are in inverted-repeat orientation, NAHR-mediated replication restart results in dicentric chromosome intermediates, which, on segregation, lead to breakage and further chromosome rearrangements [53, 54]. Following these findings, a growing number of genetic disorders have been associated with GCRs arising from inaccurate recombination events at stalled replication forks in the last years [55, 56]. For this reasons, HR is a tightly regulated process and non-recombinogenic mechanisms are generally favored to restart stalled replication forks. In addition, organisms have also evolved a set of motor proteins with the specialized function of limiting HR by removing RAD51 from ssDNA, such as Srs2 in yeast and RTEL1 (regulator of telomere elongation helicase 1), FBH1 (F-Box helicase 1), PARI (PCNA-associated recombination inhibitor), and RecQ helicases in mammals [57], whose depletion leads to unscheduled recombination and genomic instability.

Recent studies suggested that HR proteins play a complex role at replication forks that goes beyond their repair and restart activity. Indeed, the loss of crucial homologous recombination and/or Fanconi anemia (FA) factors, such as RAD51, BRCA2, and FANCD2, leads to Mre11-dependent degradation of nascent strands at stalled replication fork and accumulation of ssDNA gaps [58, 59]. These studies uncovered a DSB-independent

role of RAD51 nucleofilament formation in protecting stalled replication forks from unscheduled nucleolytic resection. Interestingly, this function does not seem to help directly cells in resuming replication, but partially explains the chromosomal abnormalities and the cancer-prone phenotype associated with *BRCA* and *FANC* dysfunction [60, 61].

Besides DSBs, replication fork can be halted by bulky lesions arising from exogenous DNA damage, such as UV irradiation and alkylating agents, or from endogenous processes, such as oxidative stress, spontaneous depurination, and ribonucleotide incorporation. These template lesions, particularly if posed at the leading strand, impede further nucleotide incorporation by replicative DNA polymerases but usually they do not represent an obstacle for helicase unwinding [62] (Figure 3b). Given the inherent plasticity of the replication processes, DNA synthesis can proceed discontinuously on both strands in the presence of DNA damage, without replisome dissociation from the fork. For example the leading-strand polymerase can use a primer synthetized by the primase in *Escherichia coli* [63, 64], or even the mRNA transcript during in-line collision with the transcriptional machinery [65], to re-initiate DNA synthesis downstream a template lesion (Figure 3c). The resulting ssDNA gaps behind the fork are substrates for the RAD51 strand invasion and error-free, post-replicative recombination-mediated gap filling. This process uses the daughter strand posed on the sister duplex to copy the damaged template and it is thought to require the formation of a sister chromatid junction (SCJ) (Figure 3f and 3f') or a double Holliday junction (dHJ) (Figure 3e and 3e') which are subsequently resolved by the action of BLM and Top3. This notion is supported by the observation that the depletion of Sgs1, the yeast homolog of BLM, leads to the toxic accumulation of X-shape recombination intermediates upon methyl methanesulfonate (MMS) treatment, in a RAD51-dependent manner [66]. In addition, cells can use an alternative mechanism driven by a group of low-fidelity, non-replicative polymerases, called Translesion Synthesis (TLS) polymerases, which are able to copy lesions-containing DNA because they have a larger active site than replicative polymerases that is able to accommodate damaged or distorted templates. However, because of their lower ability to discriminate the correct base and their lack of 3'-5' exonuclease proofreading activity, these polymerases copy the template in an error-prone manner, increasing the risk of mutagenesis (Figure 3d) [67]. The main event orchestrating the choice between these two pathways is the differential addition of

ubiquitin- and SUMO-related moieties on the replication sliding clamp PCNA [68]. In general, PCNA K164-monoubiquitination by Rad6/Rad18 recruits TLS polymerases through their ubiquitin binding motifs and promotes the error-prone repair pathway, whereas Ubc13-Mm2 and Rad5 dependent PCNA polyubiquitination drives the error-free repair by a mechanism that is still poorly understood [69]. Moreover in yeast SUMOylation of PCNA keeps certain potentially deleterious HR pathways in check by recruiting the antirecombinase Srs2, which disrupts RAD51 nucleofilament [70].

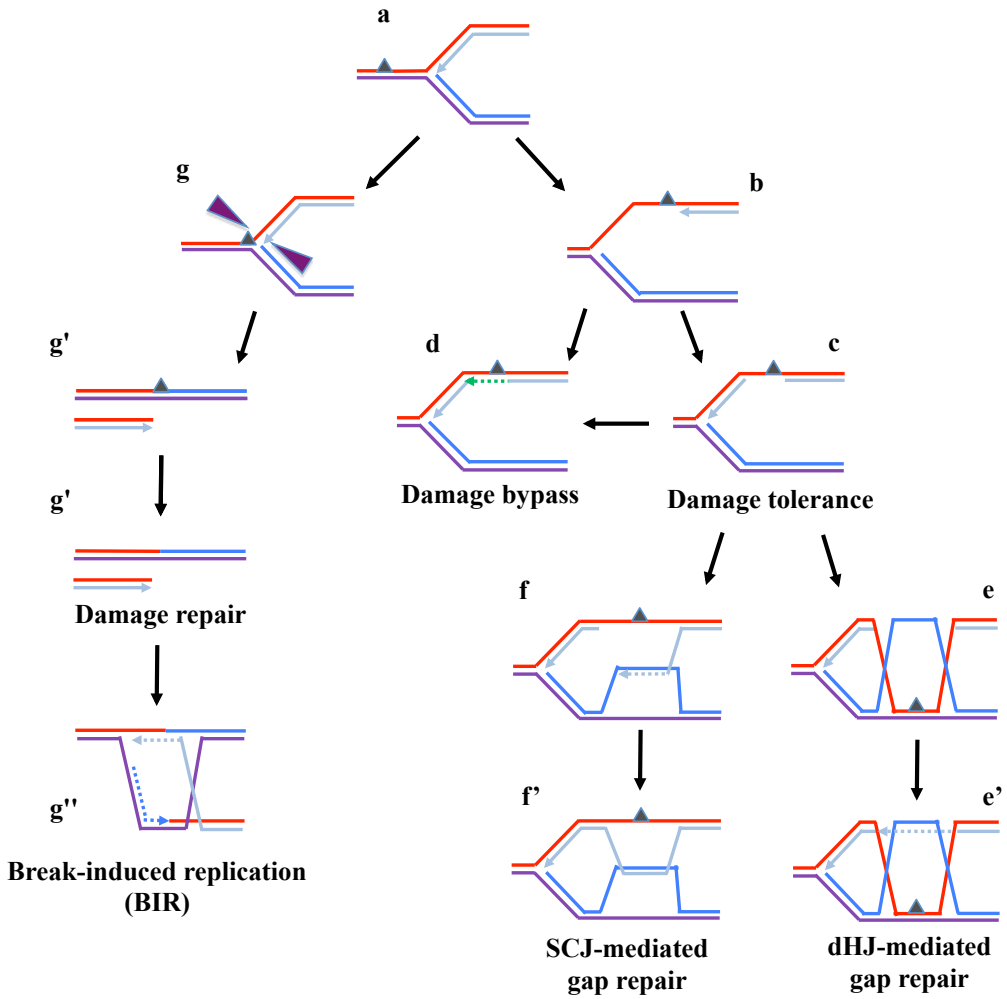

Figure 1.3. Possible pathways resolving leading strand blockage. (**a**) and (**b**) Leading strand lesions stalls polymerases but not the replicative helicase. Translesion synthesis (TLS) polymerases can lead to an error-prone lesion bypass (**d**, dashed green line). (**c**) Otherwise DNA synthesis is reinitiated downstream the lesion, resulting in a leading strand gap, which can be repaired later by HR in an error-free mechanism involving the formation of a sister chromatid junction (SCJ) (**f** and **f'**) or a double Holliday junction (dHJ) (**e** and **e'**). (**g**) Stalled replication forks can be cleaved by an endonuclease to generate a one-sided DSB. One-sided DSB repair by recombination proceeds in analogy to BIR involving DNA strand invasion and re-establishment of a functional fork (**g'** and **g''**).

1.4 Fork remodeling and reversal

Template lesions that stall the polymerase activity were suggested more than 30 years to cause replication fork reversal, where the nascent strands reanneal to form a four-way junction resembling a Holliday junction, called "chicken foot" (Figure 4a). In this way, the damaged strand is relocated into a region of duplex DNA, so that it can be repaired using the information contained in the homologous template (Figure 4b). An alternative possibility is that the lesion is simply by-passed using the nascent undamaged strand as an alternative template (Figure 4c). Otherwise, in the presence of lesions that impede replicative helicase unwinding, fork regression might represent a mean to provide the repair machinery the necessary space and time to fix the damage (Figure 4d). Finally, the reversal of the "chicken foot" structure restores a competent replication fork, likely able to resume DNA synthesis [71].

The first indication that replication forks can reverse was experimentally obtained from a study performed in 1976, where the authors demonstrated the formation of an heavy/heavy DNA upon bromodeoxyuridine pulse-labeling of human cells treated with DNA damaging agents [72]. Following this study, four-armed structures were shown to form *in vitro* in partially replicated plasmid DNA using electron microscopy (EM) [73]. Following these observations, the fork regression model has been extensively used to indirectly explain some replication or recombination mutant phenotypes, especially in the bacteria system [74, 75]. However, the formation of reversed forks *in vivo* has been clearly demonstrated only by the recent development and optimization of techniques such as neutral-neutral 2-D gel electrophoresis and, most importantly, EM on cross-linked DNA extracted from cells. First, Lopes *et al.* demonstrated through 2-D gel electrophoresis the formation of X-shaped replication structures in checkpoint-deficient *S. cerevisiae* cells upon HU treatment [76]. Successively, these observations were implemented by EM analysis that allowed the direct visualization of the replication intermediates. Checkpoint-deficient yeast cells treated with HU show two kinds of aberrant structures: the most abundant is long ssDNA stretches (up to 800 nt), arising from extensive helicase-polymerase uncoupling or nucleolytic processing on nascent DNA. The second class of intermediates is regressed forks, where the regressed arm is partially or completely single-stranded. Since these structures persist also after HU removal and correlate with fork collapse and cell death, the authors

concluded the fork regression is a "pathological" event in eukaryotic cells, rather "physiological", as it was initially suggested for bacteria [26].

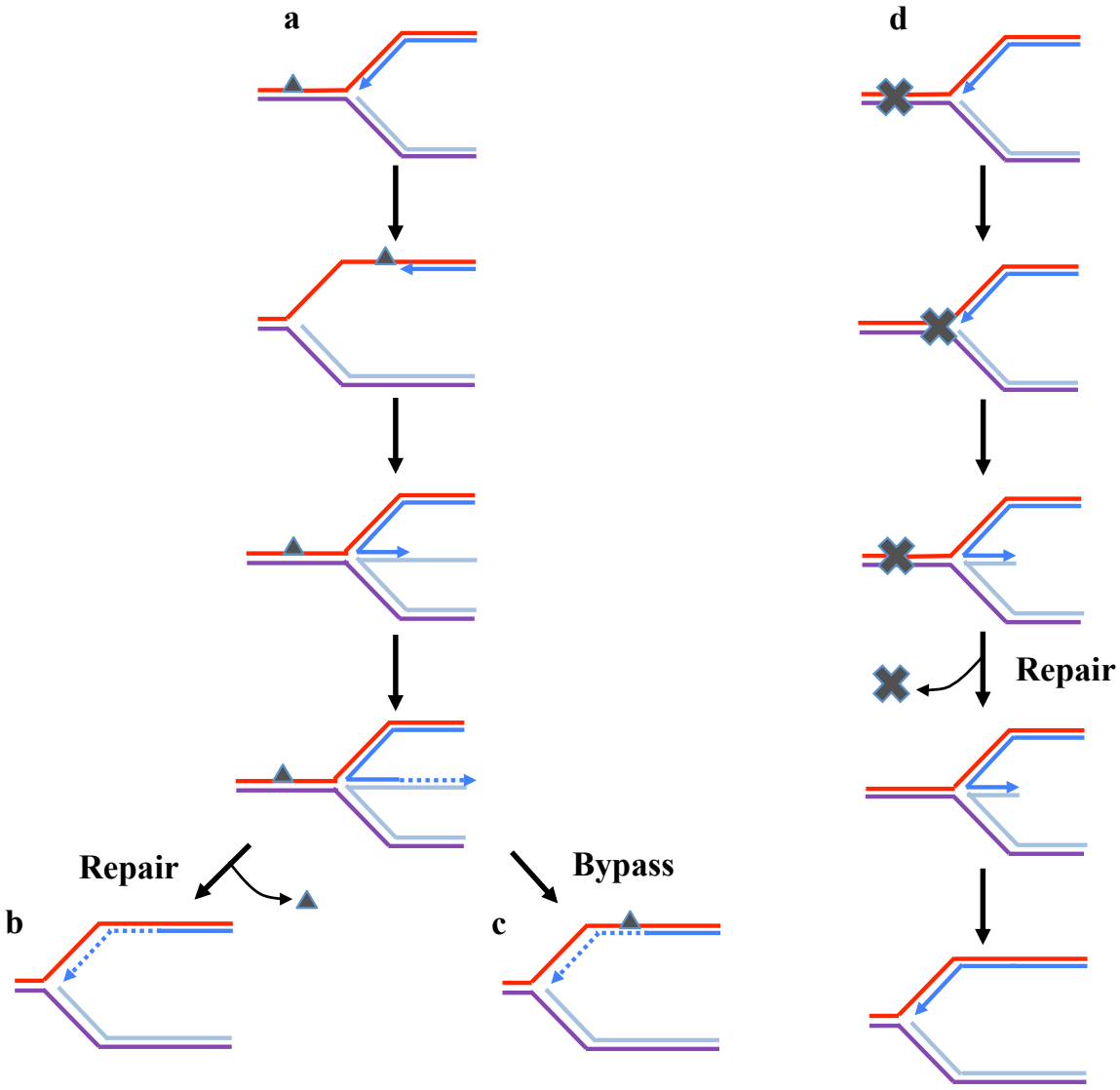

Figure 1.4. Fork regression followed by reversal. (**a**) A lesion in the leading strand template could result in the formation of a blocked fork with a gap on the leading strand. (**b**) and (**c**) Fork regression would reposition the 3′ end of the blocked leading strand so that it would be paired with the nascent lagging strand, whilst the DNA lesion would be relocated back into the reformed parental duplex. Bypass of the lesion could be effected by extension of the leading strand using the lagging strand as a template followed by reversal of fork regression. Repositioning of the lesion back into the parental duplex could also facilitate repair rather than bypass. Extension of the leading strand using the nascent lagging strand and reversal of regression would reconstitute a fork structure on to which the replication apparatus could be reloaded. (**d**) In the presence of double-strand blockages that impede further DNA unwinding replication fork reversal provides time and space for the repair machinery to fix the lesion. Once lesion gets repaired a functional replication fork is restored. Adapted from Atkinson J., 2009 [71].

Which factors drive directly fork regression is not clear yet. The formation of a four-way junction is not thermodynamically unfavorable because all the removed base pairs reanneal in the regressed arm. However, the physical presence of the replisome on the stalled forks could represent an energetic obstacle because it must dissociate in order to allow fork reversal. In addition, if leading and lagging strands synthesis is uncoupled by template lesions leading to ssDNA formation, an initial stretch of dsDNA would need to be denaturated before daughter strand annealing, thus creating a kinetic barrier to fork regression. For this reasons, it is likely that fork reversal is a specific enzyme-mediated process and indeed, an increasing number of enzymes that catalyze this transaction *in vitro* have been identified during the past 10 years. Historically the first protein shown to convert replication forks into Holliday junction structures was the bacterial DNA helicase RecG [77]. Interestingly, structural analysis of RecG bound to a forked DNA provided evidence that the helicase domains form a dsDNA traslocation motor that pulls the daughter strands into two grooves that can only accommodate ssDNA and are separated by a so-called "wedge" domain [78]. This particular structural feature allows the ATP-dependent unwinding and subsequent annealing of the nascent leading and lagging strands, which are extruded in close proximity. Other ATP-dependent DNA helicases that have been demonstrated to catalyze fork regression *in vitro* are the members of the RecQ family, whose biochemical features and biological functions are described in Section 1.7.

Recently an increasing number of ATP-dependent dsDNA translocases, members of the SWI/SNF2 family, was shown to remodel stalled replication forks in four-ways junctions despite lacking a canonical strand separation activity. Among these proteins, the *S. cerevisiae* Rad5 and its human orthologs HLTF (helics-like transcription factor), and SHPRH (SNF2 histone linker PHD RING helicase) are the most characterized in terms of biochemical and biological function [79, 80]. Rad5/HTLF can process *in vitro* model replication forks with homologous arms by generating chicken foot structures [79, 81]. Rad5, HTLF and SHPRH contain a RING finger domain that confers E3 ubiquitin ligase activity and they form a multiprotein complex with yeast and human Rad6-Rad18. Their depletion leads to gross chromosomal rearrangements, DNA damage sensitivity, elevated mutagenesis and impaired fork progression on UV or MMS damaged DNA template [82, 83, 84, 85]. Moreover, recent studies in yeast have shown that Rad5, along with the

recombinogenic factors RAD51, Rad52, Rad54, and Rad55, are required to accumulate four-way junctions, detectable by 2D-gel electrophoresis on DNA damaged replication intermediates [86]. These observations lead to the idea that Rad5/HTLF might functionally link the fork regression process with a well-conserved and defined repair pathway such as the template switching mechanism of DNA damage tolerance, under the strict control of PCNA ubiquitination signal. Moreover, these findings suggest an intimate connection between fork regression and recombination.

Rad54 is another SNF2 translocase able to migrate branched DNA structures [87], an activity that is essential during homologous recombination repair, after the RAD51-catalyzed strand invasion and D-loop formation [88]. Interestingly, Rad54 is able to overcome longer regions of heterology on branched substrates than the BLM helicase [89]. Rad54 promotes both fork regression and restoration *in vitro* and this equilibrium is shifted towards the first process in the presence of RAD51; this effect is specific for Rad54 as RAD51 does not influence the respective activity of BLM [90].

FANCM, an SNF2 component of the Fanconi Anemia (FA) complex, and its yeast orthologs Mph1 (*S. cerevisiae*) and Fml1 (*S. pombe*), was also shown to branch migrate four-ways junctions *in vitro* and catalyze the regression of a model of replication fork [30, 32, 91, 92]. Given that FA cells are especially sensitive to interstrand cross-linking agents, it has been proposed that the fork regression activity of FANCM is important for counteracting the movement of a replisome towards an interstrand cross-link, thus maintaining access of repair proteins to the lesion [93].

Finally HARP, also known as SMARCAL1, which is associated with *Human Schimke Immune-osseous Dysplasia* (SIOD), is a SNF2 family protein that possess ATP-dependent DNA rewinding activity [94]. This unique biochemical feature allows HARP to translocate backward the split-end fork and anneal the complementary DNA coated by RPA, thus limiting the amount of ssDNA formed at stalled fork [95, 96]. Moreover, HARP is characterized by ATP-dependent branch migration and fork regression activities *in vitro*, although the biological significance of these two activities is still unknown [97].

In addition to helicases and translocases, strand exchange proteins such as the bacterial RecA [98], the bacteriophage UvsX [99] and the eukaryotic RAD51 [100] has been shown to promote fork regression *in vitro,* even if at slower rate than motor proteins. Due to their

intrinsic nature that require ssDNA to allow initial binding and nucleation, they might be required to regress stalled fork with extensive ssDNA gaps at the junction [101]. On the other hand, helicases or translocases might act on stalled replication forks that have limited ssDNA. Genetic studies performed in *E. coli* have pointed to the importance of recombination proteins in promoting reversal and restart of stalled replication forks [75, 102, 103, 104]. However, it is more likely that they stabilize and protect the extruded arm of regressed forks, particularly when a ssDNA tail is present, from improper cellular processing, thus promoting their accumulation rather than directly catalyze this process.

In spite of the increasing number of protein candidates potentially able to regress arrested replication forks, we cannot rule out the possibility that this reaction can occur without the assistance of any protein. Analysis of *in vitro* partially replicated plasmid DNA treated with intercalating agents to generate overwound DNA has been used to show that replication fork reversal represents a spontaneous process aimed at dissipating the positive torsional stress accumulating ahead the advancing replisome [105]. This phenomenon has physiological relevance upon head-on collision between replication and transcription units [106] or, more generally, when replication forks are moving across chromatin domains susceptible of topological stress such as termination zones, highly transcribed regions such as rDNA, or anchored to fixed structures, such as the nuclear envelope and chromosome scaffolds [107]. Recently Bermejo *et al.* clearly demonstrated that accumulation of reversed forks in a checkpoint-defective yeast strain arises as a consequence of torsional stress generated ahead the replication forks encountering transcribed genes, gated at the nuclear envelope. In addition, the same authors demonstrated that fork reversal arises spontaneously in cells lacking Top1 and Top2 as well, underlying again the topological influence in driving spontaneously this transaction [108].

Finally, the negative supercoils accumulating behind replication forks have been suggested to trigger the formation of hemicatenate structures between sister chromatids which contribute to the establishment of sister chromatid cohesion during S-phase and assist recombination or replication bypass processes. Reversed forks can also derive from the run-off of these sister chromatid junctions (SCJs) at inactivated replication forks [109, 110].

1.5 Top1 inhibitors and replication fork reversal

In contrast to bulky lesions, double strand-related damages, such as interstrand cross-links or tightly DNA-bound nucleoprotein complexes, such as the transcriptional machinery, create a roadblock for the advancing replisome, without helicase and polymerase uncoupling. In this case, replication can only resume after block removal. Interstrand cross-link (ICL) repair, for example, is carried out by the combination of Nucleotide Exicision Repair (NER), TLS and HR pathways coordinated by the complex activities of the Fanconi Anemia (FA) proteins [93].

Replication can slow and stall if there are unresolved topological constrains ahead of the replisome generated by transcription bubbles, termination zones, another fork approaching or inhibition of topoisomerase activity. Top1 and Top2 inhibitors rely on the transient trapping of these specialized nucleases on their 3'-single-strand and 5'-double-strand DNA substrate, respectively, thus preventing the religation step [111]. Because of the high proliferation of cancer cells, drugs that target Top1 such as camptothecin, or Top2 such as etoposide, are potential chemoterapheutics and some of them have been already clinically approved for cancer treatment [112, 113]. In particular, the S-phase dependent cytotoxicity of Top1 inhibitors was thought to arise from replication run-off at Top1-DNA frozen complexes located on the leading strand, triggering to the accumulation of lethal one-side DSBs [114]. This model was recently challenged by the work of Koster *et al.* where using a combination of single-molecule and *in vivo* experiments, the authors demonstrated that Top1 inhibitors hinder the uncoiling activity of Top1, thus promoting positive supercoiling formation and replication fork slowing. They also proposed that the resulting accumulation of positive supercoils ahead of the replication machinery is the major mechanism of fork collapse and cell death upon camptothecin exposure [115, 116].

Recently, the group of Massimo Lopes in Zurich has extended this observation by demonstrating that clinical relevant doses of Top1 inhibitors are associated with replication fork slowing, without DSBs formation. By exploiting a combination of *in vivo* psoralen cross-linking and EM analysis to directly visualize replication intermediates, they were able to detect a high frequency of regressed forks upon Top1 poisoning in yeast, *Xenopus laevis* egg extract, and mammalian cells. In contrast to previous findings, they found that the replication fork slowing and reversal associated with Top1 inhibitors are not

checkpoint- or recombination-dependent. Moreover, they discovered that poly(ADP-ribose) polymerases 1 (PARP1) activity, at least in *X. laevis* egg extract and mammalian cells, is essential to slow the replication forks on CPT-damaged templates by promoting the accumulation of regressed forks. PARP1 depletion or inhibition revert this effect of Top1 poisoning, leading to the formation of DSBs likely by replication run-off at Top1-DNA covalent complexes (Top1cc) (Figure 5) [117]. PARP1 plays a critical role in mediating the cellular sensitivity to camptothecin derivatives and several clinical trials are currently investigating the potential advantages of combined therapies with PARP and Top1 inhibitors [118, 119].

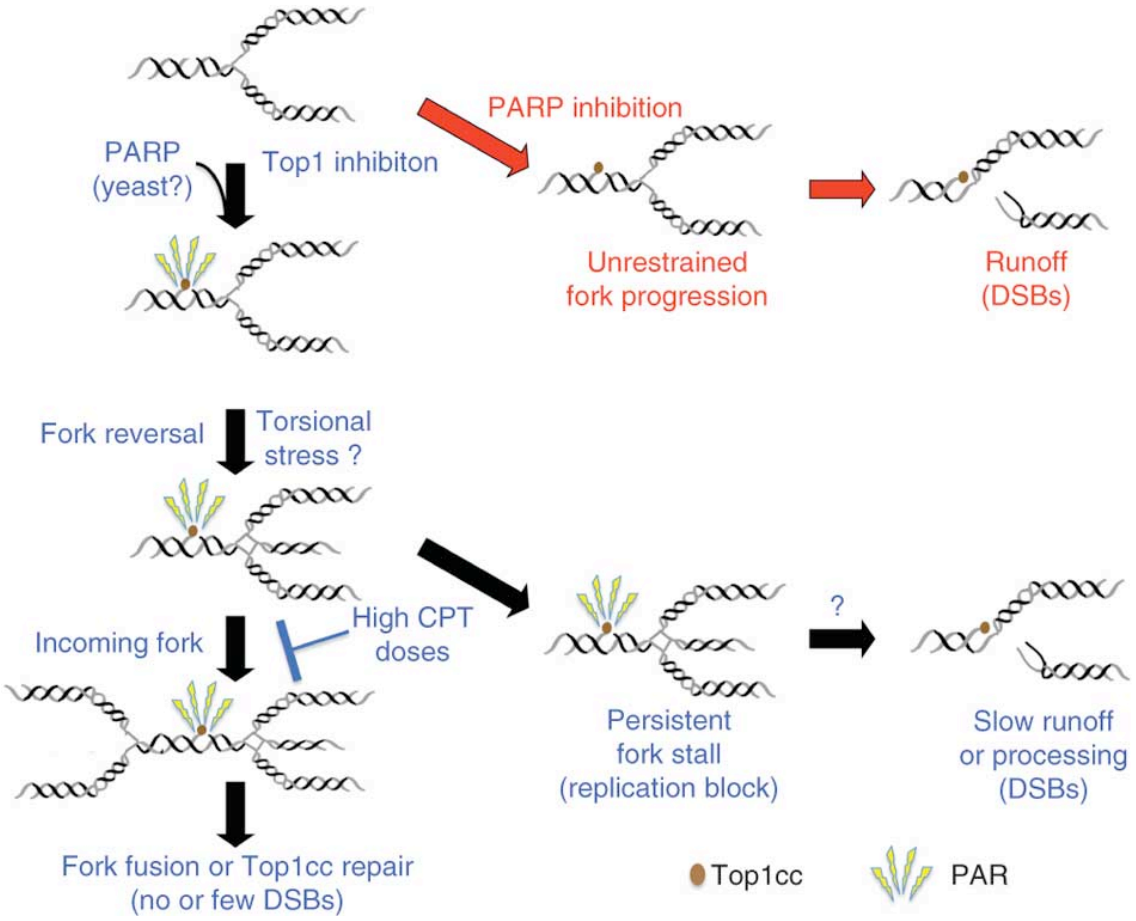

Figure 1.5. Model for replication interference by Top1 poisons and their synergistic effects with PARP inhibitors. Upon Top1 inhibition, replication forks rapidly experience slowed progression and reversal, mediated by PARP activity in higher eukaryotes (and unknown factors in yeast) and promoting Top1 covalent complex (Top1cc) repair and replication completion. PARP inactivation leads to increased DSBs, owing to unrestrained fork runoff at Top1cc. High CPT doses lead to incomplete replication and persistent fork stalling, causing DSBs by eventual fork collapse and/or processing; PAR, poly(ADP-ribose) Adapted from Ray Chaudhuri A., 2012 [117].

The results of Dr. Lopes' group provide a new rationale for the synergic effect of these inhibitors on actively proliferating cancer cells. They also point to fork reversal as a general strategy that allows the repair enzymes to fix the lesion before the replication resumes, thus avoiding replication fork collision with single, and possibly, double strand breaks. Nevertheless, this work opens several relevant biological questions: 1) since PARP1 is just a signaling molecule without motor activity, which are the factors involved in PARP-mediated fork reversal? 2) Is this PARP-mediated mechanism of fork reversal taking place also when replication is challenged with other replication inhibitors?

1.6 Replication fork restoration and restart after reversal

After regressing, replication forks must be properly restarted to complete DNA synthesis. Regressed forks might represent a highly recombinogenic substrate and, if not restarted in a timely fashion, their accumulation might lead to unscheduled HR with subsequent chromosomal rearrangements and genomic instability [26].

The simplest and probably safest mechanism of reversed fork restoration is to migrate back the branch point of the four-way junction through an enzymatic-mediated reaction (Figure 6a). Notably, most of the *in vitro* tested proteins able to perform fork reversal, have also the ability to reset the original forks, probably due to an indiscriminate branch migration activity. However, none of these enzymes has been shown to selectively perform fork restart *in vivo*.

Alternatively, the extruded arm can be degraded by nucleases or helicase/nuclease complexes to reset a proper replication fork (Figure 6b). For example, the combined activity of the *E.coli* RecQ helicase and the RecJ nuclease has been shown to degrade regressed forks formed in a RecA-dependent manner in UV-treated bacteria [103]. In addition, the *E. coli* helicase/nuclease complex RecBCD has been shown to resolve reversed forks formed in some replication mutants in a non-recombinogenic way by degrading both strands at the blunted dsDNA end of the extruded arm [74, 120]. Whilst no RecBCD homologs have been identified in eukaryotic cells, Exo1 activity is able to counteract fork reversal in checkpoint-deficient *S. cerevisiae* mutants treated with HU [110]. However, it is not clear whether Exo1 is acting directly on a four-way junction, or simply prevents its formation by

resecting newly synthesized DNA chains or resolving the sister chromatid junction that could promote fork reversal at collapsed forks.

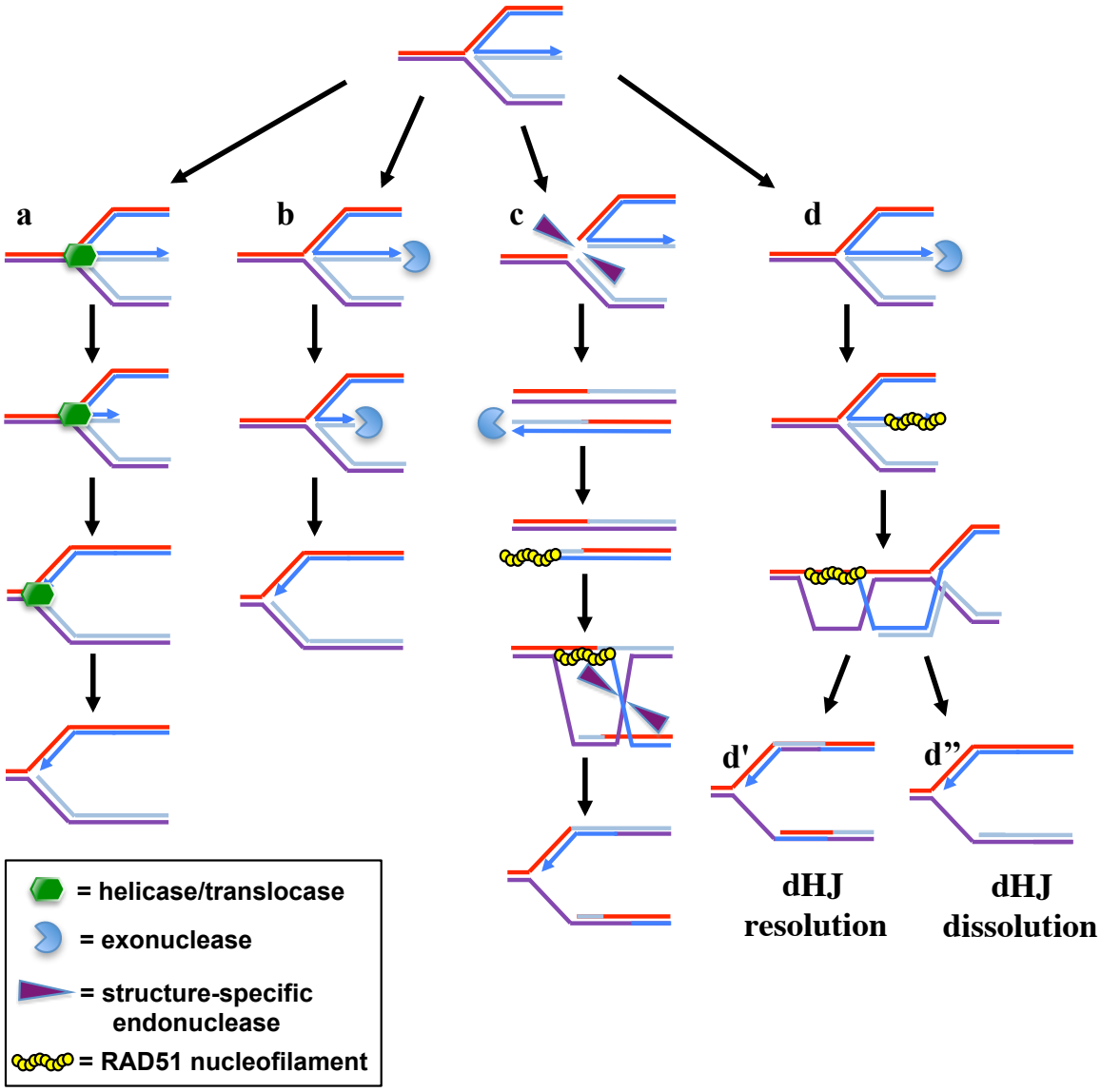

Figure 1.6. Mechanisms for replication fork restoration after reversal. (**a**) Fork restoration by forward migration of the junction by helicases/translocases. (**b**) Fork restoration by nuclease-mediated degradation of the extruded arm. (**c**) Regressed fork cleavage by structure-selective endonucleases and fork restoration by recombination. (**d**) Fork restoration by recombination of the extruded arm with the preformed parental strands ahead the junction. The resulting D-loop structure containing a double Holliday junction (dHJ) can be resolved by endonucleases (**d'**) or dissolved by the BLM-Top3α complex (**d''**).

Recent EM analysis of replication intermediates from fission yeast showed that Dna2, an enzyme with both nuclease and helicase activity, normally implicated in Okazaki fragments

processing, is able to prevent HU- or MMS-stalled forks from reversing in a checkpoint-dependent manner [121]. In the same study, the authors showed that Dna2 is able to digest the extruded arm of model regressed forks *in vitro*. However, an alternative scenario is that checkpoint-mediated phosphorylation tethers Dna2 on stalled fork to cleave nascent 3' or 5' flap DNA at the junction, thus preventing their further unwinding and fourth arm formation. Due to the redundancy of resection machineries in cells, the processes of regressed fork resolution by nucleases is quite attractive, even if it precludes the use of the lagging strand for template switching.

Regressed forks can also be resolved in a recombination-dependent manner in at least two ways. First, four-arms DNA structures are preferred substrates for some structure-selective endonucleases, such as the RuvABC complex in *E.coli* or Mus81-Eme1 in vertebrates, both of which are normally involved in dHJ resolution during the last step of the HR repair. The cleavage of the junction would generate a nicked duplex and a second duplex carrying a dsDNA end. The dsDNA end can in turn be processed to generate a 3'-tail, which will then be loaded by strand exchange proteins and invade the intact sister duplex to promote D-loop formation and HR (Figure 6c). Alternatively, upon 5'-degradation and RAD51 single-strand coating, the regressed arm might serve as invading strand in the homologous sequence of the reformed parental duplex, resulting in dHJ formation and HR (Figure 6d). The latter mechanism is theoretically less harmful because of the physical linkage between the recombining end and the donor target sequence, preventing recombination between non-identical sequences. However, since recombination is a potential threat for genome stability, cells might limit HR to a last attempt to resolve these structures in absence of non-recombinogenic mechanisms. In agreement with this conclusion, the *E.coli* Holliday junction resolvase RuvC cleaves regressed forks only in *recBC* mutants, and the chromosome breakage is repaired by HR [102, 120].

The particular structure of the stalled forks could dictate the mechanism of fork restoration. For example, a replication fork stalled by leading strand lesions or by replication inhibitors, such as HU or aphidicolin, likely presents a single-strand gap at the junction, as discussed above, and the resulting fork reversal generates a chicken foot structure with a partial single-stranded extruded arm. In the cellular environment, partially or fully single-strand arms are rapidly coated by single-strand binding proteins, which in

turn lead to the ATR-mediated checkpoint activation and/or homologous recombination. However, the 5'-tail of regressed forks arising from leading strand damage might not allow a direct restart by HR.

In contrast, in the presence of agents that block the helicase movement, such as interstrand cross-linking drugs, topoisomerase inhibitors or head-on collision with the replication machinery, the resulting regressed fork is likely to arbor a blunt-ended extruded arm. This blunt-ended arm might activate the ATM-checkpoint and would need to be processed by the resection machinery to generate a proper 3'-tail for HRR. Beside these speculations, the exact signaling pathways and cellular factors that regulate the restoration mechanism are still unknown and further studies are necessary to shed light on how reversed fork are restarted.

1.7 RecQ helicases

The RecQ DNA helicases are a subgroup of the SF2 superfamily of helicases, conserved from bacteria to humans, which play an essential role in maintaining genomic stability by acting at the interface between DNA replication, recombination and repair. Unicellular organisms contain one representative of the family, such as *E. coli* RecQ and *S. cerevisiae* Sgs1, while high eukaryotes generally express multiple RecQ enzymes (Figure 7). Mammalian cells arbor five RecQ homologs, and mutations in three of these genes (*BLM*, *WRN* and *RECQ4*) are associated with the *Bloom*, *Werner* and *Rothmund-Thomson* syndromes, respectively. Although no disease has been linked to mutations in the *RECQ5* (alias *RECQL5*) and *RECQ1* (alias *RECQL1* or *RECQL*) genes as yet, a single nucleotide polymorphism in *RECQ1* correlates with decreased survival of pancreatic cancer patients, and *RECQ5*$^{-/-}$ knockout mice display increased cancer rates [122].

All RecQ helicases have an ATP-dependent DNA helicase activity with 3'-5' polarity and, although with some differences, are able to resolve a variety of DNA structures other than standard B-form DNA duplexes.

As *bona fide* helicases, all the RecQs contain a common helicase domain formed by two 2 RecA-like domains, which functions as ATP driven motor for their 3'-5' translocation activity on ssDNA [123]. While the overall fold of the helicase domain is similar to that of other SF2 helicases, the major distinguishing feature of RecQ proteins is the region termed

RecQ-C-terminal (RQC), that is present in most RecQ helicases with the exception of RecQ4 and its orthologs (Figure 7) [124]. The RQC domain is composed of a zinc-binding module and a helix-turn-helix fold, the so-called winged-helix (WH) domain. The zinc-binding subdomain is required for protein stability as single-amino acid substitutions in the zinc domain of human BLM and *E.coli* RecQ are either insoluble or prone to degradation [125, 126].

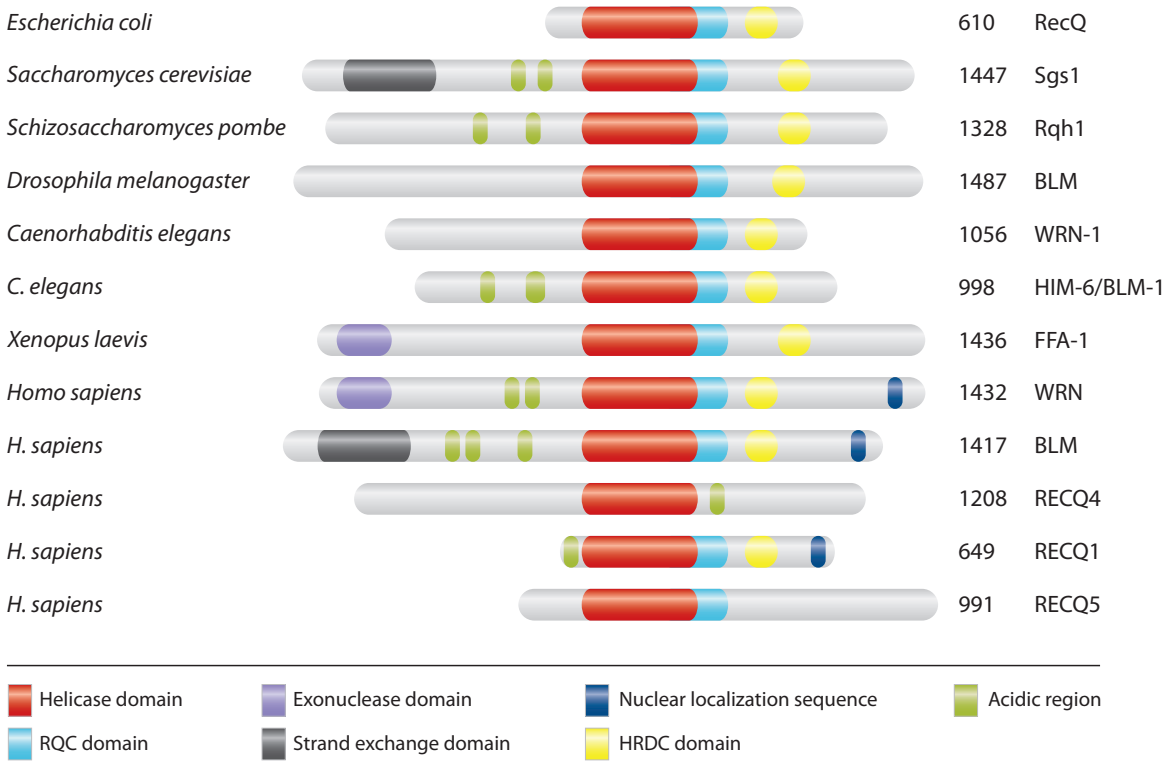

Figure 1.7. Structural features of RecQ helicases. The RecQ proteins have several structural domains that are conserved from bacteria through humans. All RecQ proteins have a core helicase domain. Most RecQ proteins also contain conserved helicase and RNAse D C-terminal (HRDC) and RecQ C-terminal (RQC) domains that are thought to mediate interactions with nucleic acid and other proteins. Many RecQ proteins have acidic regions that enable protein-protein interactions, and some of the RecQ proteins have nuclear localization sequences. WRN and FFA-1 protein are unique in that they also contain an exonuclease domain. Sgs1 and Blm are the first characterized members of this family of proteins containing a functional strand exchange domain in their N-terminus. The number of amino acids in each protein is indicated on the right. Adapted from Bernstein KA., 2010 [124].

The WH domain, despite low sequence identity, shows a structurally conserved fold among the RecQ members and it is important for DNA binding as previously demonstrated for other proteins such as the transcription factors CAP and hRFX1 or the human DNA repair

protein AGT [127]. An interesting feature of this domain is the presence of a beta-hairpin loop carrying an aromatic residue at the tip [128]. Mutagenesis studies demonstrated that the simple substitution of Tyr to Ala at the tip of the beta wing is sufficient to abrogate the helicase activity of RECQ1 [129]. Moreover, the recent crystallographic structure of the RQC domain of WRN bound to a dsDNA clearly shows that the beta-hairpin acts as a separation pin coupling the ATP-driven tracking along ssDNA tail to DNA unwinding. Interestingly, the fact that other DNA helicases such as the bacterial UvrD or the archeal Hel308 harbor a similar beta wing structure suggests a common inchworm mechanism of unwinding. However, the beta wing of these proteins is spatially located in close proximity to the ATPase domains, whereas the RecQ beta-hairpin is mobile and confers a structural separation between the translocation and the separation module. This particular feature resembles the wedge domain of the bacterial RecG and makes these proteins capable to melt non-canonical DNA molecules such as Holliday junctions, by accommodating this flexible loop at the branch point, without steric hindrance [130]. Surprisingly, given its small size and critical role in mediating DNA contacts, the RQC domain is also crucial in mediating interactions with other proteins, as already demonstrated for WRN [131].

In addition to this conserved RQC domain, some RecQ helicases have an auxiliary domain named the helicase-and-RnaseD-like-C-terminal (HRDC). Among the human RecQs, only BLM and WRN possess an HRDC domain. Structural and biochemical studies indicate that HRDC domain forms a surface for additional DNA binding. In addition, the poor sequence and structural conservation makes this domain important to confer distinct substrate specificities to the individual RecQ members [132]. For example, the HRDC domain of BLM is important for Holliday junction binding and resolution, although it has a minor effect on DNA duplex unwinding [133].

The human WRN and its orthologs also harbor a 3'-5' exonuclease domain at their N-terminus which highly resembles the structure of DnaQ exonucleases such as the 3'-5' proofreading domain of *E.coli* DNA polymerase I [134].

In addition, all the RecQ helicases have non-conserved N- or C-terminal regions that play regulatory duties, e.g. nuclear localization [127].

Notably, almost all RecQ helicases form high-order oligomers. Using a combination of size exclusion chromatography and transmission electron microscopy, our group demonstrated

that the different oligomeric states of RECQ1 result in two opposite enzymatic activities: a higher-order oligomeric form is associated with strand annealing, while a smaller form consistent with monomers or dimers is responsible to DNA unwinding. Importantly, the equilibrium between these two forms is controlled by ATP binding, which promotes oligomer dissociation [135]. Recently, a coiled-coil motif responsible for oligomerization has been identified in the N-terminus of RECQ1 and WRN [136]. Interestingly, this region was previously reported to be important for the Holliday junction resolution activity of RECQ1 [137], but not for fork unwinding, while it is required for the optimal exonuclease activity of WRN [138], probably by promoting the assembly of a hexameric ring structure where the active site of the enzyme is located in a central cavity of the appropriate size to accommodate a dsDNA. This suggests that higher-order oligomer assembly is critical for the different functions of RecQ helicases.

1.7.1 BLM

Bloom's syndrome (BS) is an extremely rare genetic disorder, characterized by a high risk to the development of a broad range of cancers, in contrast to almost all other genetically inherited cancer predispositions which are usually associated with a small subset of tumors [138]. Cells from BS patients exhibit chromosome instability with increased numbers of chromatid gaps and breaks and chromosome rearrangements. The most remarkable feature, that is used in the molecular diagnosis of BS, is an approximately tenfold increase in the frequency of sister chromatid exchanges (SCEs) and an high rate of loss of heterozygosity (LOH), which is one of the mechanisms that can lead to complete loss-of-function of tumor-suppressor genes in cancer, thus explaining the high cancer susceptibility of Bloom patients [139, 140].

BLM and its orthologs have the unique ability among the RecQ family members to "dissolve" dHJ into non-crossover products during the last step of the HRR, hence suppressing SCE formation [141]. This dissolution activity is performed by an evolutionary conserved complex formed by BLM, Top3α, RMI1 (BLAP75) and RMI2 (BLAP18), where BLM branch migrates and collapses dHJs into a hemicatenate, Top3α removes the remaining linked single strands by its strand pass activity, and RMI1 and RMI2 play a stimulatory role [142, 143, 144]. This "dissolvasome" complex has recently been shown to ensure faithful chromosome segregation by dissolution of secondary DNA structures named ultra-

fine bridges (UFBs) in anaphase cells. These UFBs arise as the result of tangled regions, such as centromeres, or from difficult-to-replicate regions, such as fragile sites or telomeres, particularly following replication stress; the BLM complex re-localizes to these structures during anaphase and catalyzes their resolution [145].

Human BLM and its yeast orthologs are also involved in DNA end resection to generated 3' ssDNA tails and promote HR [41, 42, 43, 146, 147]. *In vivo* and *in vitro* analysis have shown that after a DSB occurs, the DNA ends are recognized and partially resected by MRN complex (MRX in yeast) in collaboration with CtIP endonuclease (Sae2 in yeast), leaving a short 3' single-stranded DNA tails. Successively, these DNA ends undergo a long-range resection (up to 2-4 kb) mediated by BLM (Sgs1 in yeast) and its interacting partners RPA and Dna2, or via a parallel pathway relying on the Exo1 nuclease. In particular, BLM and RPA are needed to unwind the DSB ends and provide access for Dna2 that processes the resulting ssDNA with its 5'-3' nuclease activity. Interestingly, this process is stimulated by RMI1-Top3α and other RecQ helicases cannot substitute BLM [44]. A possible reason for explaining why cells have evolved two different and very conserved pathways is that extensive ssDNA formation is crucial to activate the DNA damage checkpoint and to ensure high-fidelity HR by preventing repair between short dispersed repeats.

As most RecQ helicase-deficient cells, BLM depleted cells are characterized by defects in replication fork progression and are sensitive to replication inhibitors or replicative damage [148]. In particular, upon HU or aphidicolin treatment, BLM is phosphorylated by ATR at T99, and is required for efficient fork restarting and for suppression of dormant origin firing [149]. Moreover BLM deficiency is associated with a strong cytidine deaminase defect, leading to pyrimidine pool imbalance; nucleotide pool normalization leads to a reduction of sister chromatid exchange frequency and it is sufficient to fully restore replication fork velocity, but not the fork restart defects [150].

In the context of HRR, BLM is also able to disrupt RAD51-ssDNA nucleofilaments and D-loops *in vitro* adding further complexity to its anti- and pro-recombination activities [151]. BLM is also able to act on a large number of non-canonical DNA substrates, which might form upon replication stress such as D-loops, G-tetraduplexes, RNA-DNA hybrids and four-way junctions [137]. In addition, BLM was shown to promote both fork regression and

fork restoration *in vitro*, but the biological function of this activity is still unknown [152, 153, 154].

1.7.2 WRN

Werner's syndrome (WS) differs from the other human RecQ helicase syndromes because of its strong premature ageing features, with death occurring at the average age of 50, mainly due to the insurgence of cancers or vascular diseases. Fibroblasts isolated from WS patients have reduced proliferative lifespan, chromosomal translocations and deletions; however, unlike BS cells, WS fibroblasts do not show an increased frequency of SCEs [155]. The pleiotropic nature of WRN and the multiplicity of its interacting partners complicate the assignment of a prominent biological function for this protein. Nevertheless, the particular ageing phenotype of WRN patients and a large number of experimental evidences suggest a crucial involvement of WRN in telomere maintenance [156, 157]. For example, the forced expression of exogenous telomerase in WS fibroblasts rescues the premature senescent phenotype of these cells and the WRN mutant mouse only recapitulates *Werner syndrome* when combined with telomerase mutant alleles [158]. Replication problems might occur at an increased frequency in telomeric regions; because of the intrinsic inability of the lagging strand DNA replication machinery to function at the very end of chromosomes, a specialized reverse transcriptase called telomerase adds a G-rich repeat sequence to the telomeric ends. WRN is required for telomere lagging strand synthesis [159] and associates with the G-rich region to unwind the G-quadruplexes [156, 160]. In addition, WRN resolves D-loops HR intermediates and telomeric T-loops *in vitro* to allow replication of the telomeric ends and suppress inappropriate recombination, in a manner regulated by the interacting telomeric proteins TRF1 and TRF2 [161].

Even if WS cells have prolonged S-phase, the involvement of WRN in DNA replication seems to be confined to difficult-to-replicate regions such as telomeres, but also fragile sites or rDNA, particularly upon replicative stress [162]. WRN depletion confers sensitivity to replication inhibitors and other fork stalling agents, and is associated with S-phase defects in cells with hyperactive c-Myc [163]. Unlike BLM, WRN depletion does not influence the ability of stalled forks to restart or the activation of dormant origins. However, WRN seems to be important for DNA replication fork progression on HU- and MMS-damaged templates, as demonstrated by DNA fiber assay [164]. One possible explanation for this role

of WRN in DNA replication relies on its interaction with the replicative polymerase Polδ, where the WRN exonucleolytic processing of 3'-terminal mismatches helps the proofreading polymerase to synthesize DNA with high fidelity upon replicative stress, hence preventing the accumulation of deleterious mutations [165]. Alternatively, WRN could be required to resolve non-B-form DNA structures that would otherwise block the polymerase processivity. In addition, WRN was shown to be required for Okazaki fragments maturation in cooperation with its interacting partner FEN1, by directly stimulating the nucleolytic activity of FEN1 on long flaps generated at blocked forks, or indirectly, by resolving hairpins or stem-loops formed at repetitive sequences [166]. In addition to Okazaki fragment processing, recent studies in human cells and *Xenopus laevis* egg extract have showed that WRN is involved with Dna2, Exo1 and RPA in the 5' resection at DSBs to promote 3' single-strand tail formation and homology-dependent repair [167, 168]. As mentioned above, BLM has also an important role in this process and it is not clear yet if these two RecQ helicases works in a redundant or complementary fashion to stimulate 5' resection. However, WRN's role in HR is not as well defined as in the case of BLM. WRN cells do not display increased SCE, but have a clear hyper-recombinogenic phenotype, particularly after DNA damage induction [169]. Moreover, WRN colocalizes with RPA upon replication inhibition and suppresses the RAD51 foci formation, probably by resolving recombinogenic structures. Finally, WRN depletion makes the repair of replicative DNA damage dependent on the Mus81-induced DSB and on the consequent HR pathway [170, 171].

Several lines of evidence point to an additional role of WRN in the DNA damage tolerance pathway. WRN binds Ubs9 and is sumoylated in mouse and human cells. WRN interacts with WRNIP1, a polyubiquitin-binding protein, that is considered a homolog of the yeast DNA damage tolerance protein Mgs1 [172]. In DT40 cells, WRN assist REV1-dependent translesion synthesis at UV-damaged templates [173]. Moreover, WRN stimulates the processivity of several TLS polymerases *in vitro* [174]. However, WRN might also have a suppressive effect on TLS, which could explain the increase of mutation rates and the constitutive ubiquitination of PCNA in WRN cells. In this context, Kobayashi *et al.* showed that WRN is recruited to replicative foci by NBS1 where it interacts with PCNA and represses its ubiquitination. Upon DNA damage, ATM/NBS1-dependent

phosphorylation of WRN triggers its degradation, making PCNA free to be modified by RAD18 and to channel the repair towards the DNA damage tolerance pathway [175].

WRN was also shown to have a role upstream and downstream of the checkpoint response. For example, WRN acts upstream of ATM and ATR to facilitate RPA foci formation and Chk1 activation upon HU exposure in *Caenorhabditis elegans* [176]. In addition, activation of ATM and its downstream checkpoint targets is impaired in WRN deficient human cells exposed to interstrand cross-link agent PUVA (psoralen plus UVA) [177]. More importantly, Patro *et al.* have recently shown that WRN is required for the S-phase checkpoint activation to prevent CPT-induced fork collapse in human cells. In particular, WRN facilitates ssDNA formation at CPT-stalled replication forks to induce a global checkpoint activation that reduces the overall fork speed and prevents further fork collision with Top1-DNA complexes [178]. Furthermore, Ammazalorso *et al.* suggested that ATR and ATM differentially regulate WRN in response to HU treatment in human cells. WRN is recruited to stalled replication forks through its interaction with Rad1, a subunit of the 9.1.1 complex, and phosphorylated by ATR to prevent DSB accumulation. Conversely, upon prolonged HU treatment and replication fork collapse, the other checkpoint kinase, ATM, phosphorylates WRN on different residues to promote its delocalization from DSB sites and to direct the repair towards the RAD51-mediated HR pathway [179, 180].

Biochemical studies showed that WRN has the ability to perform both the reversal and restoration of a regressed fork *in vitro* [153, 154, 181]. In particular, the fork regression activity of WRN is enhanced by the presence of leading strand gaps at the junction and its 3'-5' exonuclease activity might be needed to create an optimal substrate for this activity [182]. If the anti-recombinogenic function of WRN at stalled replication forks relies on its replication fork regression/restoration activity is still an open question.

Besides its role replication and in S-phase-related genome maintenance, WRN was suggested to be involved in multiple DNA repair pathways, as evicted by its interaction with a number of repair proteins [131]. For example, WRN interacts with the NHEJ core components the Ku heterodimer [183], DNA-dependent protein kinase catalytic subunit (DNA-PKcs) [184] and the XRCC4-DNA Ligase IV complex [185]. However, WRN is not an essential NHEJ factor, and it might be required only for "dirty" end processing or when NHEJ acts on sub-genomic regions, such as telomeres and rDNA.

In addition, the involvement of WRN in Base Excision Repair (BER) is supported by its functional interactions with Polβ, Apurinic/apyrimidinic endonuclease I (APE1), NEIL1 and the sensitivity of WRN to oxidative stress and methylating agents [186, 187]. In this context, WRN physically interacts with PARP1 that is also involved in BER, and WS cells are deficient in poly(ADP-ribosyl)ation activity after exposure to hydrogen peroxide and MMS [188]. In addition, unmodified PARP1 inhibits WRN helicase and exonuclease activity. However, activation and auto-poly(ADP-ribosyl)ation of PARP1 by DNA strand breaks relieves the inhibition of WRN catalytic activities, suggesting that there is a coordination between PARP1 and WRN during repair events [189]. Although PARP1 and WRN are not essential components of BER, their presence may ensure correct and efficient DNA repair. In their absence, improper and/or inefficient repair may lead to various pathologies associated with aging. In agreement with this conclusion, *PARP1*$^{-/-}$*/WRN*$^{\Delta hel/\Delta hel}$ mice have an increased frequency of cancer, and fibroblasts derived from these knockout mice display elevated levels of chromosomal breaks, fragments, and rearrangements [190]. Incomplete BER intermediates that cannot be properly repaired by the BER pathway might be shuttled to the homologous recombination pathway during replication [191]. Thus, the hyper-recombination phenotype of WS cells may also reflect the products of unrepaired SSBs during DNA replication.

1.7.3 RECQ5

In contrast to the other human RecQ homologues RECQ5 exists in three isoforms RECQ5α, RECQ5β and RECQ5γ resulting from alternative splicing. All of them contain the core helicase motifs characteristic of RecQ helicases. However, only the largest splice variants RECQ5β is nuclear, thanks to the presence of a nuclear localization signal on its C-terminal sequence and possesses helicase activity [192]. Hereafter RECQ5β will be reffered to as RECQ5. Primary mouse embryonic fibroblasts (MEF) derived from *RECQ5* knockout mice show an elevated rate of spontaneous DSBs, hypersensitivity to DNA-damaging agents and a significant increase in the frequency of SCEs comparable to that caused by *BLM* gene inactivation. However, *RECQ5* and *BLM* double depletion in mouse embryonic stem (ES) cell line leads to an even higher frequency of SCEs compared to the single mutants, indicating that these two proteins operate non-

redundantly in suppressing mitotic recombination [193, 194]. The first clue for the anti-recombinogenic role of RECQ5 comes from its ability to physically interact with RAD51, and to disrupt the RAD51 presynaptic nucleofilaments in a reaction dependent on its helicase activity [194, 195]. Furthermore, the group of Dr. Weidong Wang has recently identified a region on the RECQ5 C-terminus that is similar to the BRC repeats of BRCA2 and is essential for the interaction with RAD51 [196]. Mutations in this region recapitulate the recombinogenic phenotype of RECQ5 depleted cells. Interestingly, also the yeast Srs2 protein contains a similar functional region, suggesting that RECQ5 might be the functional homolog of Srs2 in human cells.

RECQ5 is the only RecQ member able to directly interact with RNA polymerase II (RNAPII). RNAPII is the major protein complex associated with RECQ5 *in vivo*, when purified from human chromatin under physiological conditions. RECQ5 is able to associate with both the hypo- and hyper-phosphorylated forms of RNAPII and this interaction is mediated by the RPB1 subunit of RNAPII and the C-terminal domain of RECQ5 [197]. *In vitro* transcription assays and small interfering RNA (siRNA) experiments have shown that the RECQ5-RNAPII interaction domain, named KIK domain, but not the helicase activity of RECQ5, inhibits transcriptional initiation and elongation [198]. Strikingly, the RECQ5 BRC repeat is needed for both its anti-recombination and transcription activities, which are dependent on the helicase and KIK domain, respectively, opening an interesting scenario where RECQ5 might prevent unscheduled homologous recombination arising from transcriptional perturbation of the DNA replication process.

1.7.4 RECQ4

Mutations in *RECQ4* are associated with three unrelated disorders: *Rothmund-Thompson syndrome* (RTS), *RAPADILINO syndrome* and *Baller-Gerolds syndrome* (BGS). All of them are characterized by growth retardation and radial ray defects. However, only RTS patients are predisposed to develop bone and skin cancers and show some premature aging symptoms similar to *Werner syndrome* patients [138]. In the several attempts that were made to generate mice that recapitulate these RECQ4-dependent syndromes it was discovered that deletion of the N-terminal region of RECQ4 results in embryonic lethality. Sequence analysis unmasked a limited homology of the N-terminus of RECQ4 with the yeast essential replication initiation factor Sld2 [199, 200]. Following these observations,

RECQ4 was shown to be an essential factor for replication initiation and origin firing in *Xenopus laevis* egg extract and mammalian systems [201, 202]. Moreover, immunoprecipitation experiments from native chromatin extracts of HEK 293T cells have been employed to demonstrate that RECQ4 is part of the replicative complex comprising MCM2-7, CDC45 and GINS. It specifically binds the origin of replication at the end of G1 phase in a MCM10-dependent manner and it is required for the efficient recruitment of the GINS complex prior to DNA replication initiation [203]. Even if it lacks the characteristic RQC domain, RECQ4 has a weak helicase activity in addition to a strong strand annealing activity [204]. However, the exact role of RECQ4 in replication initiation is still not well defined and whether RECQ4 is the true homolog of Sld2 in human cells is still an open question. One intriguing possibility is that RECQ4 in cooperation with MCM10 mediates the conformational transaction from the pre-replicative dsDNA-bound status of the MCM complex to the helicase processive ssDNA-encircling form of MCM during replication initiation [205].

In addition to its role in replication, RECQ4 is involved in several DNA-repair related processes including double-strand break repair (DSB), Nucleotide Excision Repair (NER) and Base Excision Repair (BER) [206]. In addition, RECQ4 interacts with and is poly(ADP-ribosyl)ated by PARP1, although the meaning of this interaction in a DNA repair context remains uncertain [207].

Finally, RECQ4 seems to be involved in all the three major mechanisms associated with aging and cellular senescence: oxidative stress, telomere maintenance and mitochondrial dysfunction. First, RTS cells are hypersensitive to oxidative damage, suggesting a modulation of the BER pathway [208]. Second, RECQ4 interacts with the telomeric components TRF1 and TRF2, and acts synergistically with WRN, but not BLM, in resolving telomeric D-loop [209]. Third, RECQ4 is the only RecQ helicase that localizes in mitochondria where it promotes p53 accumulation in unstressed condition; deletion of the mitochondria localization signal from RECQ4 N-terminus leads to mitochondrial bioenergetics defects and elevated mitochondrial DNA (mtDNA) damage [210, 211].

1.7.5 RECQ1

RECQ1 was the first RecQ helicase member to be identified in human cells, as the human homologue of the *E.coli* RecQ helicase. The cDNA cloning and FISH analysis

localized the *RECQ1* gene on the short arm of human chromosome 12 at 12p12 [212]. It encodes a 649 amino acid polypeptide with a predicted molecular weight of 73 kDa. The protein shares a high sequence similarity with *E.coli* RecQ and other human RecQ helicases. The expression of RECQ1 is significantly high in testes and in actively proliferating cells, transformed cells and tumors [213, 214].

At the cellular level, RECQ1 is found both in the cytoplasm and the nucleus, and it is ubiquitously expressed throughout the cell-cycle. Though there is no human syndrome linked to RECQ1 deficiency, mutations in the *RECQ1* gene are associated with testicular germ cell tumors [215] and recent studies have linked a single nucleotide polymorphism present in the *RECQ1* gene to a reduced survival in pancreatic cancer patients [216].

A *RECQ1* knockout mouse was created by replacing the exons of helicase domain IV and V with Neo resistance cassette. The homozygote mice did not show any particular developmental abnormalities and were viable and fertile, but prone to develop tumors, with lymphoma being the most common one [217].

Cytogenetic analysis of the embryonic fibroblasts (MEF) derived from *RECQ1* knockout mice revealed aneuploidy, suggesting a role of RECQ1 during segregation of chromosomes during mitosis. M-FISH analysis revealed increase in fragmented chromosomes, chromatid breaks, translocation events, and SCEs. These cells accumulate DNA damages, evident by the increase in γH2AX and RAD51 foci formation. In addition, RECQ1 deficient cells are hypersensitive to ionizing radiation [217].

Interestingly, acute depletion of RECQ1 in several tumor cell lines resulted in reduced cell proliferation and spontaneous DNA damage [214, 218]. Since RECQ1 is present in high copy number in cancer cells it might be considered as a suitable target for cancer therapy. Indeed Futami *et al.* showed that *RECQ1* silencing induces mitotic catastrophe in cancer cells, probably by accumulating DNA replicative damage [219]; moreover, local and systemic administration of *RECQ1*-siRNA mixed with cationic liposomes prevented cancer cell proliferation in a mouse model of cancer without detectable side effects [220, 221].

Even though RECQ1 was the first RecQ helicase to be historically discovered in human cells, it remains one of the least characterized in terms of enzymatic activity and biological function. The increased load of DNA damage and the elevated SCEs in RECQ1-deficient cells suggest that RECQ1 is involved in maintaining chromosomal stability and that might

play an anti-recombinative role by suppressing the formation of recombination intermediates that arise during replicative stress. This notion is also supported by the observation that RECQ1 promotes the dissolution of unproductive D-loop formed by a 5' single-stranded DNA invading strand *in vitro* [222]. In addition, RECQ1 has been identified as the major HJ branch migrating protein in chromatographic fractionated nuclear extracts from HEK 293T cells [223]. Genetic analysis using the chicken DT40 system demonstrated that the double mutant *RECQ1/BLM* cells were more sensitive to mitomycin C-induced SCEs compared to single mutant *BLM* cells, indicating that RECQ1 may have some non-redundant functions with the BLM helicase at the sites of DNA damage during replication fork progression [224].

The involvement of RECQ1 in replication is supported by several recent studies. Wang *et al*. employed a DNA affinity purification and mass spectrometry procedure to show that RECQ1 physically associates with the replicative lytic origin (ori-Lyt) of Kaposi's sarcoma-associated herpesvirus (KSHV) through the viral proteins K8 and RTA. Based on these observations, the authors speculated that RECQ1 is not only an integral component of the pre-replication complex, but also the so long-sought helicase that unwinds origin DNA in the initiation of KSHV lytic DNA replication [225]. Later, it was found that RECQ1 is also associated with the ori-Lyt and Zta of the Epstein–Barr virus (EBV) [226].

Chromatin immunoprecipitation (ChIP) analyses performed in our group showed that RECQ1 physically associates with replication origins in a cell-cycle-regulated fashion in unperturbed cells. In addition, genome-wide DNA fiber experiments were used to show that RECQ1 is required for efficient replication initiation and might play an additional role during replication elongation [202]. However, the exact role of RECQ1 in DNA replication remains to be determined.

A new intriguing role for RECQ1 is emerging for studies performed in *Neurospora crassa* where mutations in the gene encoding the RECQ1-like helicase QDE3, an RNA-dependent RNA polymerase (QDE1), or an Argonaute protein containing a PIWI domain (QDE2), result in a quelling defect in qiRNA (QDE1-interacting RNAs) mediated post-transcriptional gene silencing (PTGS) [227]. Consistent with the *Neurospora* genetic results, RECQ1 was found in a piRNA (PIWI-interacting RNAs) complex isolated from rat testis [228]. A number of studies suggested that piRNAs are epigenetic and translational regulators

that have the primary function of maintaining germline DNA stability, genome organization, trasposon silencing, germline determination and meiosis [229]. Moreover, overexpression of *PIWI* genes is highly correlated with cancers in humans [230] . All these data suggest a new function for RECQ1 in the generation of small RNA molecules involved in genome silencing and stabilization.

1.8 Poly(ADP-ribose) polymerase 1

Poly(ADP-ribose) polymerases (PARPs) are a heterogeneous group of ADP-ribosyl-transferase enzymes which transfer ADP-ribose groups from donor NAD molecules onto their target proteins post-traslationally. PARP1 is the most abundant and the best-characterized member of this family and plays a crucial role in regulating multiple cellular functions and DNA-related transactions such as apoptosis, transcription, chromatin remodeling and DNA repair [231]. PARP1 arbors a N-terminal DNA binding domain containing three zinc-finger motifs by which it senses alterations in the DNA secondary structure, such as single and double-strand breaks, cruciform structures and nucleosome linker DNA [232]. As revealed by a recent crystallographic report, DNA binding leads to a conformational change in PARP1 that activates its catalytic transfer of negatively charged ADP-ribose moieties from NAD^+ to acceptor proteins such as histones and p53 [233]. However, the most prominent poly(ADP-ribosyl)ated substrate of PARP1 is PARP1 itself, resulting in its dissociation from DNA due to electrostatic repulsion between the negatively charge poly(ADP-ribose) (PAR) and DNA [234]. The nature of this modification is transient and extremely short-lived because of the catabolic activity of poly(ADP-ribose) glycohydrolase (PARG) which cleaves the polymers within a matter of minutes and recycles PARP1 for subsequent steps of DNA binding/activation. The importance of a strict PAR regulation is underlined by the embryonic lethality of *PARG*-null mice [235]. Besides being a post-traslational modification, poly(ADP-ribose) (PAR) chains, which resemble the chemistry (negative charge) and the conformation (elicoidal) of nucleic acids, represent also a strong, non-covalent binding module for several proteins, regulating their enzymatic activity and cellular localization. Several years ago, Pleschke *et al.* identified a PAR binding consensus sequence built by basic residue clusters interspersed with hydrophobic amino acid and conserved in a broad range of proteins involved in DNA-

related cellular functions [236]. Moreover, in the last years three different domains have been identified as structurally specific PAR-binding modules, such as the PAR binding zinc-finger (PBZ) domain [237, 238], the macrodomain [239, 240, 241, 242], and recently the WWE domain [243]. Its temporal and structural flexibility makes the poly(ADP-ribosyl)ation axis an ideal signal mechanism for coordinating cellular pathways under stress, which require an immediate regulation. This is well-established during the DNA damage response, where PARP1 quickly senses the DNA breaks triggering the rapid poly(ADP-ribosyl)ation (PARylation) of itself or chromatin-associated proteins surrounding the lesion. Poly(ADP-ribosyl)ated chromatin acts as an interaction scaffold for the differential recruitment of a multitude of DNA repair complexes or chromatin modifying proteins [244]. The best characterized in this context is the Single-Strand Break Repair (SSBR) pathway where PARylation recruits the scaffold protein XRCC1, DNA ligase III and, depending on the complexity of the lesion, other proteins such as polynucleotide kinase (PNK) and DNA polymerase β [245].

As a consequence of poly(ADP-ribosyl)ation, the chromatin structure becomes more relaxed, thereby increasing lesion accessibility and repair efficiency. Recently, two PAR binding proteins, the chromatin remodeler ALC1 [240] and the histone chaperone APLF [246], have been shown to actively participate in the PARP1-mediated chromatin dynamics during DNA repair.

PARP1 binds and is activated by DSBs. Moreover, PARP1 directly interacts with and poly(ADP-ribosyl)ates some of NHEJ core components such as the Ku heterodimer, decreasing its DNA affinity [247], and DNA-PKcs, regulating its kinase activity [248, 249]. NHEJ preferentially works during G1, where sister chromatid are not available for HRR, and, even if it represents the major DSBR pathway in mammalian cells, it is largely error-prone leading to traslocations and genomic rearrangement. Besides canonical NHEJ (c-NHEJ), PARP1 is the central factor regulating an alternative NHEJ pathway (a-NHEJ), where, in the absence of Ku, PARP1 recruits the MRN complex and XRCC1/DNA ligase III for microhomology-mediated end-joining [250, 251, 252]. The importance of this backup NHEJ pathway is highlighted by the early embryonic lethality of *PARP1/Ku80* double null mice [253, 254].

The involvement of PARP1 in HRR is uncertain and still under debate. While PARP1 has not an effect in HRR measured by a I-SceI reporter assay [255], its depletion impairs the Mre11-dependent resection at HU-stalled replication forks and consequently RAD51 nucleofilament formation and HRR [256]. The same authors reported that PARP1 activity is actually important in protecting HU stalled forks from Mre11-mediated degradation, attributing the discrepancy with the previous result to the length of HU treatment that was much shorter in this second case compared to the previous study [257]. Indeed, long HU exposure in human cells progressively generates DSBs, which are repaired by HR. The collapsed replication forks generated by long HU exposures are unable to resume, and DNA synthesis needs to be completed by the firing of new origins. On the other hand, short HU treatments transiently stalls replication forks, which are then reactivated by a non-recombinogenic RAD51-mediated mechanism after drug removal [258].

Genetic studies showed PARP1 is an important factor in protecting the HR pathway from the toxic NHEJ engagement during S-phase DSB repair, probably by poly(ADP-ribosyl)ating Ku and decreasing in this way its affinity for double strand ends that otherwise would preclude proper DSB processing [259, 260, 261]. The importance of understanding the role of PARP during HR was highlighted few years ago by the discovery that *BRCA1*- or *BRCA2*-deficient cancer cells are exquisitely sensitive to PARP inhibitors [262, 263]. Nowadays, PARP inhibitors are in clinical trials to treat *BRCA*-mutant breast and ovarian cancers. The accepted model to explain this synthetic lethality invokes the accumulation of unrepaired SSBs upon PARP inhibition, which results into one-ended DSBs upon collision with replication forks, and cell death in a HR-deficient background. Importantly, this therapeutic strategy is not confined to *BRCA*-deficient tumors and PARP inhibitors trigger synthetic lethality in other HR-defective cancers [264, 265, 266]. In addition, the selective chemical ablation of crucial HR regulators, such as for cyclin-dependent kinase phosphorylation, can recapitulate a "BRCAness" phenotype, as demonstrated for the hypersensitivity of *BRCA*-proficient tumors to the combined CDK1/PARP inhibition [265]. Moreover, PARP1 activity is constitutively enhanced in a HR-deficient context, thereby representing a good marker for the clinical outcome of the therapy [266].

Interestingly, recent data showed that depletion of other SSBR crucial factors such as XRCC1 does not cause synthetic lethality with PARP inhibitors in *BRCA*-deficient cells,

thus challenging the SSB model of synthetic lethality. Instead, disabling the NHEJ pathway suppresses the specific killing of HR deficient cells by PARP inhibition, again suggesting a role of PARP1 in preventing the suppressive effect of NHEJ factors on HR after fork collapse [267]. Understanding the exact mechanism of PARP1/HR synthetic lethality is particularly important to prevent the primary or acquired resistance of *BRCA*-mutant cancers to this treatment. In this context, resistance to PARP inhibitors was induced in a subset of *BRCA1*-deficient breast cancers by disabling 53BP1 expression, a crucial DNA damage response protein recently demonstrated to impede DNA resection at DSBs and to promote NHEJ over HR [268, 269].

2 MATERIALS AND METHODS

2.1 Antibodies and chemicals

The antibodies used were rabbit polyclonal anti-PARP1 (ALX-210-302-R100) and mouse monoclonal anti-PAR (ALX-804-220-R100) from Enzo Life Sciences, rabbit polyclonal anti-PAR (4336-BPC-100) from Trevigen, mouse monoclonal anti-α–tubulin (T5168) and anti-FLAG M2 (F1804) from Sigma, rabbit polyclonal anti-53BP1 (NB100-304) from Novus Biologicals, mouse monoclonal anti-γH2AX (05-636) from Millipore, mouse monoclonal anti-WRN (611169) from BD laboratories, rabbit polyclonal anti-BLM (ab476) from Abcam, mouse monoclonal anti-PARP1 (sc-8007), anti-Ku70 (sc-5309), anti-Ku86 (sc-5280), anti-DNA-PKcs (sc-5282), anti-PCNA (sc-25280), rabbit polyclonal Glutation-S-Transferase (sc-459), anti-RAD51 (sc-8349), anti-TFIIH (sc-293), anti-RECQ1 raised against aa 1-110 (sc-25547) were all from Santa Cruz, and a custom made rabbit anti-RECQ1 polyclonal antibody against a synthetic peptide of a unique sequence in the last 16 aa at the C-terminus of RECQ1 [214] from Sigma.

Nucleotide analogs (EdU, CldU and IdU), camptothecin (CPT), etoposide, methyl methanesulfonate (MMS), mitomycin-C (MMC), thymidine, nocodazole, propidium iodide, NAD^+ and H_2O_2 were all from Sigma. The PARP1 inhibitors Olaparib was from Selleck Chemicals, NU1025 and 3-aminobenzamide (3-AB) were from Sigma. Protease inhibitor cocktail tablets were from Roche. All the radioactive reagents were from Perkin Helmer.

2.2 Cell culture, transfections and synchronization

Human Embryonic Kidney (HEK) 293 and 293T, human osteosarcoma (U-2 OS) and human cervical adenocarcinoma HeLa cells were grown in Dulbecco's modified Eagle's medium (DMEM, Gibco) supplemented with 10% (v/v) foetal calf serum (FCS, Life Technologies).

Cell transfections with plasmid DNA or siRNA duplexes were performed by using Nucleofector (Lonza) and HiPerFect (Qiagen), respectively, following manufacter's instruction. Cell were analyzed 48-72 hours after transfection.

U-2 OS cells were synchronized by double thymidine block and "mitotic shake-off" as previously described [270]. Briefly, cells were synchronized at G1/S transition by a 2.5 mM thymidine treatment for 16 h, release in fresh medium for 10 h and again thymidine treatment for 16 h. Subsequently the cells were released from the block in fresh medium for the indicated time. For G2/M synchronization cells were released from thymidine block for 4 hours in fresh medium and treated for 12 hours with 75 ng/ml nocodazole to trap mitotic cells; mitotic cells were collected by flask shaking-off. For G1 synchronization mitotic cells were replated and grown in fresh medium for 4 hours.

2.3 Fluorescence-activated cell sorting (FACS*)*

Cells were fixed in ice-cold 70% ethanol/PBS for 30 min. DNA was stained with 50 μg/ml propidium iodide in PBS containing 0.1% Triton X-100 and 0.5 mg/ml DNase-free RNase A (Sigma). Samples were processed on a FACSCalibur flow cytometer equipped with CellQuest software (Becton Dickinson) and cell cycle profile distributions were determined with Modfit LT 3.0 software.

2.4 Immunoblotting

Total cell extracts were obtained by sonication in Lysis buffer (25 mM Tris-HCl pH 7.5, 250 mM NaCl, 1 mM EDTA, 1 mM DTT, 20 mM NaF, 10 mM β-glycerophosphate, 0.2 mM Na3VO4, 0.5% NP-40, 10% glycerol and protease inhibitors) or by directly scraping in SDS sample buffer (0.8% SDS, 4% glycerol, 280 mM mercaptoethanol, 25 mM Tris-HCl pH 6.8, 0.005% bromophenol blue). Protein concentration was measured by BCA assay (Pierce). Proteins were resolved by SDS-PAGE, transferred onto nitrocellulose (Protran) or PVDF (GE Healthcare) membrane and probed using the appropriate primary and secondary antibodies coupled to horse-radish peroxidase (Dako, Pierce). Protein detection was done with ECL reagents (GE Healthcare).

2.5 Protein complex purification

To isolate protein complexes containing a RECQ1 bait protein, we prepared a stable, inducible HEK 293 cell line expressing a double tagged-version of the human RECQ1 helicase by Flp recombinase-mediated integration. This system allows the generation of stable mammalian cell lines exhibiting tetracycline-inducible expression of a gene of interest from a single genomic location [271]. The expression levels of the bait protein can be easily adjusted by tetracycline to levels that are comparable with corresponding endogenous protein levels. The protein complexes containing RECQ1 were isolated using a small double-affinity tag (SH-tag) consisting of a streptavidin-binding peptide and a hemagglutinin (HA) epitope tag. Following trypsin digestion, the samples were desalted and loaded directly onto a reverse-phase HPLC column coupled to a mass spectrometer. We performed three biological replicate SH-purification experiments, and analyzed each sample once by LC-MS/MS as already described [271]. To eliminate co-purifying contaminant proteins, we generated a database of proteins identified from 3 independent SH–eGFP control purifications analyzed by LC-MS/MS. Proteins identified in bait-specific experiments that were also present in the contaminant database were considered as non-specific binders and removed from the data set. Only the proteins specifically associated with the bait-RECQ1 protein in all three replicates were considered as significant.

2.6 Immunoprecipitation

HEK 293T or U-2 OS cells were treated as indicated, washed with ice-cold PBS and resuspended in cytoplasmic extraction buffer (10 mM Tris-HCl pH 7.9, 0.34 M sucrose, 3 mM $CaCl_2$, 2 mM magnesium acetate, 0.1 mM EDTA, 1 mM DTT, 20 mM NaF, 10 mM β-glycerophosphate, 0.2 mM Na_3VO_4, 0.5% Nonidet P-40 and protease inhibitors) for 10 min at 4°C. Intact nuclei were pelleted by low-speed centrifugation, washed with cytoplasmic lysis buffer (without Nonidet P-40), lysed in nuclear lysis buffer (20 mM HEPES-KOH pH 7.9, 150 mM KCl, 1.5 mM $MgCl_2$, 20 mM NaF, 10 mM β-glycerophosphate, 0.2 mM Na_3VO_4, 10% glycerol, 0.5% Nonidet P-40 and protease inhibitors) by homogenization. DNA and RNA in the suspension were digested with 50 U/µl Benzonase (Sigma) at 4°C for 1 hour. In some experiments 50 µg/ml Ethidium bromide was added to nuclear lysate.

The nuclear soluble extract was clarified from insoluble material by centrifugation at 20,000 × g at 4°C for 20 min, precleared with 50 µl protein A beads slurry (Santa Cruz) at 4°C for 1 hour and incubated overnight with anti-RECQ1 (Sigma), anti-PARP1 (ALX-210-302), or a control IgG rabbit polyclonal antibody (Santa Cruz) at 4°C. The immunocomplexes were captured by adding 50 µl of protein A beads slurry for 2 hours at 4°C. After extensive washing with nuclear lysis buffer, proteins were eluted from beads with 2X SDS sample buffer at 95°C for 5 min, separated by SDS-PAGE and detected by immunoblotting with the appropriate antibodies.

2.7 GST pull-down experiments

Glutathione S-transferase (GST) and GST-fused wild-type and truncated RECQ1 proteins were expressed in bacteria and purified according to a previously described procedure [272]. Briefly, bacterial cultures harboring GST fused proteins were induced with 1 mM isopropyl-β-D-thiogalactopyranoside (IPTG) overnight at room temperature. The pellets were resuspended in lysis buffer (50 mM Tris-HCl pH 8.0, 250 mM NaCl, 5% glycerol, 5 mM EDTA, 2 mM DTT, 1 mM PMSF and protease inhibitor) and sonicated. The cleared lysates were then loaded onto glutathione agarose beads (Sigma) and incubated for 1 h at 4ºC. Following incubation and extensive washing with lysis buffer, proteins immobilized on beads were resuspended at 50% (v/v) in the same buffer and kept frozen until use.

We produced [^{35}S]-labeled RECQ1 and [^{35}S]-labeled PARP1 for in vitro binding assays by the TNT Reticulocyte Lysate System (Promega), using the corresponding pIRES FLAG-Hemagglutinin (FH)-RECQ1 or PARP1 vector as template.

Pull-down assays with GST-RECQ1 fragments were performed as previously described. Briefly, immobilized GST-fused RECQ1 fragments were pretreated with DNase I and RNase A for 30 min at 25ºC to remove bacterial nucleic acids. The beads were then washed twice with high salt solution (1 M NaCl) and equilibrated in binding buffer TNEN (20 mM Tris-HCl pH 7.5, 150 mM NaCl, 1 mM EDTA, 1 mM DTT, 1 mM PMSF and 0.5 % NP-40) supplemented with 0.1 mg/ml of ethidium bromide. ^{35}S-methionine-labeled, in vitro-translated PARP1 was incubated with GST-fusion RECQ1 fragments bound to 10 µl of glutathione–Sepharose beads (Amersham) in binding buffer TNEN (20 mM Tris–HCl pH

7.5, 150 mM NaCl, 1 mM EDTA, 1 mM DTT, 1 mM PMSF and 0.5 % NP-40) supplemented with 0.1 mg/ml ethidium bromide for 2 hours at 4°C. The beads were subsequently washed two times in ethidium bromide-supplemented TNEN buffer, and three times with TNEN buffer. Bound proteins were eluted with SDS sample buffer, resolved by gel electrophoresis, and visualized by direct autoradiography (Cyclon, GE Healthcare).

For the production of GST-PARP1 fragments, HeLa cells (2×10^6 cells) were transfected by calcium-phosphate co-precipitation with 10 μg of recombinant DNA. Cells were lysed 48 h later in lysis buffer (50 mM Tris–HCl pH 8.0, 250 mM NaCl, 0.5% NP-40, 0.5 mM PMSF and protease inhibitors). Lysates were cleared by centrifugation and incubated for 2 hours with glutathione sepharose beads. Beads were washed 3 times with lysis buffer, 2 times with lysis buffer adjusted to 1M NaCl and resuspended in GST binding buffer. Pull-down experiments with the purified GST-PARP1 fragments and the ^{35}S-methionine-labeled, in vitro-translated RECQ1 was performed as described above.

GST-pulldown experiments with GST-RECQ1 and purified recombinant PARP1 was performed as described above with some modification. Briefly, unmodified recombinant PARP1 (1 μg) or PARylated PARP1 (1 μg) were incubated with GST-RECQ1 (1 μg) or GST alone (1 μg), as a control. 100 μM NU1025 or 200 mM NAD^+ were added as indicated. After incubation in binding buffer, the beads were washed with TNEN buffer containing 150 or 500 mM NaCl, as indicated. Bound proteins were eluted with SDS sample buffer, resolved by gel electrophoresis, and visualized by western blot with the appropriate antibodies.

2.8 Purification of recombinant proteins

Recombinant full-length RECQ1, RECQ1-ATPase mutants and PARP1 were expressed and purified from baculovirus/Sf9 cells as previously described in our laboratory [135]. The RECQ1-K119R and RECQ1-E220Q constructs were generated with the QuickChange XL site-directed mutagenesis kit (Strategene). The constructs of full length proteins and ATPase mutants were prepared in pFastBac LIC-Bse vectors, all of them with an N-terminal histidine tag. The recombinant bacmids were produced according to the manufacturer's instructions using the modified pFastBac LIC-Bse transfer vector

(Invitrogen). SF9 cells were subsequently transfected with the recombinant bacmid DNA in order to produce the recombinant baculovirus expressing His6-tagged proteins. The baculovirus was used to infect Sf9 cells cultured in suspension on 27˚C. Three days after infection, cells were harvested by centrifugation, washed in cold PBS and then resuspended in lysis buffer (20 mM Tris-HCl pH 7.4, 400 mM KCl, 5 mM β-mercaptoethanol and protease inhibitor). For PARP1 purification 2 mM 3-AB was added to the lysis and wash buffer to prevent PARP1 activation during the purification procedure. The lysate was cleared by centrifugation (15000 r.p.m. at 4°C) and then incubated with TALON metal affinity resin (Clontech) (1 ml resin/5 mg protein) for 2 hours at 4°C. The resin was washed first with high salt buffer (20 mM Tris–HCl pH 7.4, 500 mM KCl, 5 mM β-mercaptoethanol, 12.5 mM imidazole) for three times, and then equilibrated with low salt buffer (20 mM Tris–HCl pH 7.4, 100 mM KCl, 5 mM β-mercaptoethanol, 12.5 mM imidazole). The polyhistidine-tagged RECQ1 was eluted in buffer (20 mM Tris-HCl pH 7.5, 100 mM NaCl, 5 mM β-mercaptoethanol, 120 mM imidazole). The purity of the protein was verified by SDS–PAGE.

Recombinant E84A-WRN protein was kindly provided by Dr. Orren DK.

2.9 In vitro poly(ADP-ribosyl)ation of PARP1 and GST-RECQ1 fragments

Recombinant PARP1 (500 ng) was incubated in 20 µl of activity buffer (50 mM Tris-HCl pH 7.5, 4 mM MgCl2, 50 mM NaCl, 200 µM DTT, 0.1 µg/µl BSA, 4 ng/µl DNaseI-activated calf thymus DNA, and 400 µM NAD^+) for 20 min at 37°C and the reaction was stopped by 100 µM NU1025 or 2 mM 3-AB.

To test RECQ1 poly(ADP-ribosyl)ation, GST fusion proteins were incubated with 100 ng of recombinant PARP1 in activity buffer. After 10 min at 37°C, reactions were stopped by dilution in GST binding buffer supplemented with PARP inhibitor and washed extensively with the same buffer supplemented by 1M NaCl. The (ADP-ribosyl)ated products were resolved by gel electrophoresis and transferred to nitrocellulose membrane for visualization by western blot using an anti-PAR antibody.

2.10 Purified PAR production and PAR-binding assay

PAR polymer was produced and purified as previously described [239]. Briefly poly(ADP-ribosyl)ation reaction was set up as above and DNA digested for 30 min at 37°C by adding 10 U/ml of DNAseI (Fermentas) to the reaction. Next, 50 U/ml of proteinase K (Roche) and 1% SDS was added, followed by incubation for 1.5 hour at 55°C. After phenol–chloroform extraction, the water-soluble polymer was washed twice with diethyl ether, precipitated with ethanol, air-dried and dissolved in TBS (Tris-HCl pH 7.5, 150 mM NaCl). PAR concentration was determined spetrophotometrically using the following equation: $[PAR] = (A_{258})\ cm^{-1}/13{,}500\ cm^{-1}\ M^{-1}$

To perform PAR-binding assay, 2 pmol of recombinant proteins were spotted on a 0.2 μm pore size nitrocellulose membrane (Whatman) and air-dried. After extensively washing with TBS-T (TBS supplemented with 0.1% Tween-20) the membranes were incubated with 100 nM PAR dissolved in 10 ml TBS-T for 1 hour at room temperature. Afterwards, the membranes were washed twice for 10 min with 10 ml TBS-T and three times for 10 min with TBS-T containing 1 M NaCl. The membranes were then blocked in TBS-T supplemented with 5% skim milk and developed by blotting with PAR antibody. Alternatively, $[^{32}P]NAD^+$ was used as substrate in the poly(ADP-ribosyl)ation reaction and the membranes were developed by autoradiography (Cyclon, GE Healthcare).

2.11 Isolation of proteins on nascent DNA (iPOND)

iPOND assays were performed as recently described [273]. Briefly 1 x 10^8 HEK 293T cells were pulse-labeled with 10 μM EdU for 20 min and treated as indicated. After cross-linking with 1% Formaldehyde/PBS for 10 min at room temperature, cells are collected by scraping and washed twice with cold PBS. Collected cell pellets were frozen at -80°C, then resuspended in 0.25% Triton-X100/PBS and permeabilized for 30 min at room temperature. Pellets were washed twice with cold PBS and incubated at room temperature in click reaction buffer containing 10 μM biotin-azide, 10 mM sodium ascorbate and 2 mM $CuSO_4$ in PBS, for 2 hours at a concentration of 1 x 10^7 cells per milliliter of click reaction buffer. DMSO was added instead of biotin-azide to the negative control samples (marked as *no click*). Cell pellets were washed twice with cold PBS, resuspended in lysis buffer

containing 50 mM Tris-HCl pH 8.0, 1% SDS, 1 μg/ml leupeptin and 1 μg/ml aprotinin, and sonicated by a Bioruptor sonicator (Diagenode) to generate DNA fragment sized ranged between 100-300 bp. Samples were centrifuged at 13,200 r.p.m. for 10 min and diluted 1:1 (v/v) with PBS containing 1 μg/ml leupeptin and 1 μg/ml aprotinin. 50 μl streptavidin-agarose beads (Novagen) were incubated with the samples overnight at 4°C in the dark. The beads were washed once with lysis buffer, once with 1M NaCl, and again twice with lysis buffer. Captured proteins were eluted and cross-links reversed in SDS sample buffer by incubating for 25 min at 95°C. Proteins were resolved on SDS-PAGE and detected by immunoblotting with the appropriate antibodies.

2.12 Cell competition assays

To study the response of RECQ1-depleted cells to specific genotoxic agents, we utilized a quantitative multicolor cell completion assay where RECQ1- or Luciferase (Luc)-depleted cells were mixed in equal amount with U-2 OS cells expressing dsRed following a previously described procedure [274]. The mixed cells are treated with the specific DNA replication inhibitor or damaging agent, or left untreated. The relative sensitivity of the RECQ1-downregulated cells was then monitored by flow cytometric analysis of the ratio of uncolored RECQ1- downregulated cells to red fluorescence protein-positive (RFP^+) cells from three different experiments.

2.13 Clonogenic assays

Colony forming assays were conducted as already described [275]. Briefly, Luc-siRNA or RECQ1-siRNA transfected U-2 OS cells were seeded at a dilution of 800 cells per well in six-well plates the day before treatment with the indicated drugs. Colonies formed after at least one week of growth were fixed with glutaraldehyde (6.0% v/v), stained with crystal violet (0.5% w/v) and counted using VersaDoc 4000 imaging system (BioRad). Colony forming efficiency was calculated following a procedure already published [275] from three different experiments.

2.14 DNA substrates

All oligonucleotides were chemically synthesized and purified by reverse-phase high-pressure liquid chromatography (RP-HPLC) (Intergrated DNA Tecnologies). Each nucleotide was then resuspended in Tris-EDTA (TE) buffer (10 mM Tris-HCl pH 7.5, 1 mM EDTA). Oligonucleotide sequences used in branch migration and EMSA assays are reported in Table 2.1. For each substrate, a single oligonucleotide was 5'-end-labeled with [γ-^{32}P]ATP using T4 polynucleotide kinase (New England Biolabs). The kinase reaction was performed in PNK buffer (70 mM Tris-HCl pH 7.6, 10 mM $MgCl_2$, 5 mM DTT) at 37°C for 45 min and stopped by incubating at 70°C for 10 min for enzyme denaturation. For forked DNA intermediates, the [γ-^{32}P]ATP-labeled or unlabeled oligonucleotides were respectively annealed to a 1.6-fold excess or an equal amount of the unlabeled complementary strands in annealing buffer (10 mM Tris-HCl pH 7.5, 50 mM NaCl) by heating at 95 °C for 8 min and then cooling slowly to room temperature. The purification of the forked duplex substrates was performed using Micro Bio-Spin columns (Bio-Rad), and analyzed on a 10% non-denaturing polyacrylamide gel run in TBE buffer (89 mM Tris-borate pH 8.0, 2 mM EDTA).

To prepare the branch migration substrates, [γ-^{32}P]ATP-labeled and a 1.5-fold excess of unlabeled fork DNA intermediates were incubated in annealing buffer supplemented with 5 mM $MgCl_2$ for 30 min at 37^{o}C, and then for an additional 30 min at room temperature.

Holliday junction substrates were prepared by annealing the [γ-^{32}P]ATP-labeled oligonucleotide to a 1.5 fold excess of the unlabeled three complementary strands in annealing buffer supplemented with 5 mM $MgCl_2$ by heating at 95°C for 8 min and then slowly cooling to room temperature and purified by 5 ml of sepharose 4B column in TEN buffer (10 mM Tris HCl pH 8.0, 1 mM EDTA and 100 mM NaCl). Various fractions were then eluted and analyzed on a 10% non-denaturing polyacrylamide gel run in TBE buffer. The fractions were selected based on the purity of the substrates.

Name	Length (nt)	Sequence 5' → 3'
A	81	CTT TAG CTG CAT ATT TAC AAC ATG TTG ACC TTC AGT A/isodC/A ATC TGC TCT GAT GCC GCA TAG TGT CAT GCC AGA GCT TTG TAC
B	81	CGG GTG TCG GGG CGC ATG ACA CTA TGC GGC ATC AGA GCA GAT T**G**T ACT GAA GGT CAA CAT GTT GTA AAT ATG CAG CTA AAG
C	50	TCA GTA CAA TCT GCT CTG ATG CCG CAT AGT ATC ATG CGC CCC GAC ACC CG
D	43	GTA CAA AGC TCT GGC ATG ATA CTA TGC GGC ATC AGA GCA GAT T
E	49	GTA CAA AGC TCT GGC ATG ATA CTA TGC GGC ATC AGA GCA GAT TGT ACT G
F	60	CCT GCA TAC AGA TGT TGA CCC AGC ACT GAC TAC TGT CGT CAA TCA TCG TGC ATC ACA GTG
G	60	CAC TGT GAT GCA CGA TGA TTG ACG ACA GTA GTC AGT GCT GCA GTG GTC AGG TGT CAT CAC
H	60	CAC TGT GAT GCA CGA TGA T**C**G ACG ACA GTA GTC AGT GCT GGG TCA ACA TCT GTA TGC AGG
I	60	GTG ATG ACA CCT GAC CAC TGC AGC ACT GAC TAC TGT CGT C**G**A TCA TCG TGC ATC ACA GTG
J	60	CAC TGT GAT GCA CGA TGA T**CA GT**G ACA GTA GTC AGT GCT GGG TCA ACA TCT GTA TGC AGG
K	60	GTG ATG ACA CCT GAC CAC TGC AGC ACT GAC TAC TGT C**AC TG**A TCA TCG TGC ATC ACA GTG
L	50	GAC GCT GCC GAA TTC TGG CTT GCT AGG ACA TCT TTG CCC ACG TTG ACC CG
M	50	CGG GTC AAC GTG GGC AAA GAT GTC CTA GCA ATG TAA TCG TCT ATG ACG TC
N	50	GAC GTC ATA GAC GAT TAC ATT GCT AGG ACA TGC TGT CTA GAG ACT ATC GC
O	50	GCG ATA GTC TCT AGA CAG CAT GTC CTA GCA AGC CAG AAT TCG GCA GCG TC

Table 2.1 Sequences of the oligonucleotides used for substrate preparation. Bold red letters indicate the nucleotides that form mismatched pairs in the branch migration products.

2.15 Electrophoretic mobility shift assay (EMSA)

Purified proteins were incubated with 0.5 nM DNA in binding buffer containing 20 mM Hepes-KOH pH 7.6, 75 mM KCl, 2 mM $MgCl_2$, 2 mM ATPγS, 1 mM DTT, 0.25 mM EDTA, 20 μg/ml BSA, 5% glycerol, 0.1% NP-40 for 30 minutes at room temperature. When indicated 200 μM NAD^+, 10 μM Olaparib and 100 nM PAR were added. Protein-DNA complexes were resolved by electrophoresis on a 5% non-denaturing polyacrylamide gels in 0.5x TBE buffer for 3 hours at 4°C. Labeled DNA fragments were detected by autoradiography (Cyclon, GE Healthcare) and quantified as described previously [276].

2.16 In vitro fork regression and restart assays

Reactions were performed in a 20 μl of reaction mixture containing the indicated protein concentrations and 2 nM DNA substrate in branch migration buffer (35 mM Tris-HCl pH 7.5, 20 mM KCl, 5 mM $MgCl_2$, 0.1 mg/ml BSA, 2 mM DTT, 15 mM phosphocreatine, 30 U/ml creatine phosphokinase, 5% glycerol) at 37°C for the indicated times. The reaction was started by the addition of 2 mM ATP. For the poly(ADP-ribosyl)ation experiments, the indicated concentrations of PARP1 and 200 μM NAD^+, or 100 nM purified PAR, were added to the reaction mixture without ATP and preincubated together with RECQ1 and the substrate at 37°C for 10 min. The reaction was then started by the addition of 2 mM ATP. DNA substrates were deproteinized by adding 3X stop reaction (1.2% SDS, 30% glycerol supplemented with proteinase K (3mg/ml)) and incubating at room temperature for 10 min prior to being resolved on an 8% non-denaturing polyacrylamide gel run in TBE buffer at 4°C. Labeled DNA fragments were detected by autoradiography (Cyclon, GE Healthcare) and quantified as described previously [276].

2.17 RECQ1, WRN and BLM downregulation, and RECQ1 complementation assays

siRNA-mediated transient downregulation of RECQ1 was achieved using 50 nM siRNA SMART pool against human RECQ1 (NM_032941, Dharmacon) in U-2 OS cells and a previously described protocol in which we established the specificity of the siRNA

pool [202, 214]. siRNA-mediated transient depletion of WRN and BLM was achieved using the following siRNAs from Microsynth: siWRN (5'-UAGAGGGAAACUUGGCAAAdTdT-3') and siBLM (5'-CCGAAUCUCAAUGUACAUAGAdTdT-3'). shRNA-mediated downregulation was achieved by cloning the sequence targeting RECQ1 (5'-GAGCTTATGTTACCAGTTA-3') into the pLKO.1 lentiviral shRNA expression vector. Virus was generated by transient co-transfection of pLKO.1 and the packaging plasmids psPAX2 and pM2D.G into HEK 293T cells. Viral supernatants were filtered through a 45-μM filter and transduced on U-2 OS cells for 24 hours, followed by selection with puromycin (8μg/ml) for 3 days. Control transductions were performed using the pLKO.1 vector expressing a shRNA targeting Luciferase (5'-ACGCTGAGTACTTCGAAATGT-3'). The level of depletion was verified by western blot analysis. For the complementation assays we used a locally constructed RECQ1 RNAi-resistant open reading frame cloned into a pIRES vector under the control of the CMV promoter. Specifically, the nucleotides targeted by the RNAi (5'-GAGCTTATGTTACCAGTTA-3') were partially substituted without changing the amino acidic sequence (5'-GTCACTATGCTATCAATTA-3') by site-directed mutagenesis. Lentiviral depletion of endogenous RECQ1 was achieved using the protocol described above, and the resulting RECQ1-depleted cells were then nucleofected with a shRNA-resistant RECQ1 expression vector. Expression of the RNAi-resistant, FLAG-tagged RECQ1 and K119R mutant was verified in control and RECQ1-depleted cells by western blot analysis 48 hours after transfection.

2.18 Microfluidic–assisted DNA fiber stretching and replication fork progression analysis

Asynchronous U-2 OS cells were transiently transfected for 72 hours with siRNA SMART pools (or specific shRNA) against RECQ1 or Luciferase as reported earlier [202, 214]. RECQ1- or Luciferase-depleted U-2 OS cells were labeled for 30 min each with 50μM CldU followed by 50 μM IdU. Cells were collected by trypsinization, and high molecular weight DNA from cells embedded in agarose plugs was isolated and stretched using a microfluidic platform as described earlier [277]. For immunostaining, stretched DNA fibers were denatured with 2.5 N HCl for 45 min, neutralized in 0.1 M Na borate pH 8.0 and PBS, and blocked with 5% BSA/0.5% Tween-20/PBS for 30 min. Rat anti-CldU/BrdU

(ab6326, Abcam), goat anti-rat Alexa 594 (A11007, Invitrogen), mouse anti- IdU/BrdU (347580, BD Biosciences), and goat anti-mouse Alexa 488 (A11001, Invitrogen) antibodies were used to reveal CldU and IdU labeled tracts, respectively. A Leica SP5X confocal microscope was used to visualize the labeled tracts, and tract lengths were measured using the Image J software. Statistical analysis of the tract length was performed using Graphpad Prism.

2.19 DSB detection by PFGE

DSB detection by PFGE was performed in Massimo Lopes's lab as previously described with minor modifications [278]. Asynchronous subconfluent cultures of U-2 OS cells were harvested by trypsinization, and agarose plugs of 5 x 10^5 cells were prepared in a disposable plug mold (BioRad). Plugs were then incubated in lysis buffer (100 mM EDTA, 1% (w/v) sodium lauryl sarcosyl, 0.2% (w/v) sodium deoxycholate, 1mg/ml proteinase K) at 37°C for 72 hours and washed four times in 20 mM Tris-HCl pH 8.0, 50 mM EDTA before loading onto an agarose gel. Electrophoresis was performed for 23 hours at 14°C in 0.9% (w/v) Pulse Field Certified Agarose (BioRad) containing TBE buffer in a BioRad CHEF DR III apparatus, according to the following protocol (Block I: 9 hours, 120° included angle, 5.5 V/cm, 30- 18s switch; Block II: 6 hours, 117° included angle, 4.5 V/cm, 18-9s switch; Block III: 6 hours, 112° included angle, 4.0 V/cm, 9-5s switch). The gel was then stained with ethidium bromide and analyzed using an Alpha Innotech Imaging system. DSB quantification was performed using ImageJ software, normalizing DSB signals to unsaturated signals of DNA trapped in the well (loading control). For each treatment, relative DSB levels were obtained comparing each treatment to the background DSB signals observed in untreated (NT) conditions. Mean and standard error of the mean (s.e.m.) values were obtained from three biological replicates of the same experiment.

2.20 Immunofluorescence staining and analyses

U-2 OS cells were grown on coverslips, fixed in 3.7% paraformaldehyde, permeabilized in 0.5% Triton X-100/PBS and blocked in 3% BSA/PBS. Coverslips were then stained with anti-53BP1 and anti-γH2AX primary antibodies and detected by

appropriate Alexa 488- and Alexa 594-conjugated secondary antibodies (Molecular probes). Toto3 Iodide (Life Technologies) was used as a nuclear counterstain. For RAD51 and γH2AX double immunofluorescence, cells were extracted with cytoskeleton (CSK) buffer (10 mM Hepes-KOH pH 7.5, 300 mM sucrose, 100 mM NaCl, 3 mM $MgCl_2$ and 0.2% Triton X-100) for 5 min at 4°C to remove non-chromatin bound proteins and subsequently washed with cold PBS before fixation and staining with the appropriate antibodies. Cells were imaged using a Zeiss LSM 510 Meta confocal microscope. Images were acquired using the LSM 5 software. Foci were counted with ImageJ "Analyze particles" function or by direct visualization and "JACoP" plugin was used to calculate colocalization. The average number of foci was obtained from 3 independent experiments analyzing at least 60 (for 53BP1/ γH2AX) or 200 (for RAD51/ γH2AX) cells per sample.

2.21 EM analysis of genomic DNA in mammalian cells

In vivo psoralen cross-linking, isolation of total genomic DNA, and enrichment of the RIs from mammalian cells were performed in Massimo Lopes's lab as previously described [279].

3 RESULTS

3.1 RECQ1 interactome

Recent studies point to an important, but yet not clearly defined, role of the human RECQ1 helicase in DNA replication and repair that is distinct from that of the other four human RecQ proteins [202]. In order to better define the role of human RECQ1 helicase in DNA replication and repair, we first determined the composition of protein complexes containing RECQ1, using a new integrated proteomic approach [271].

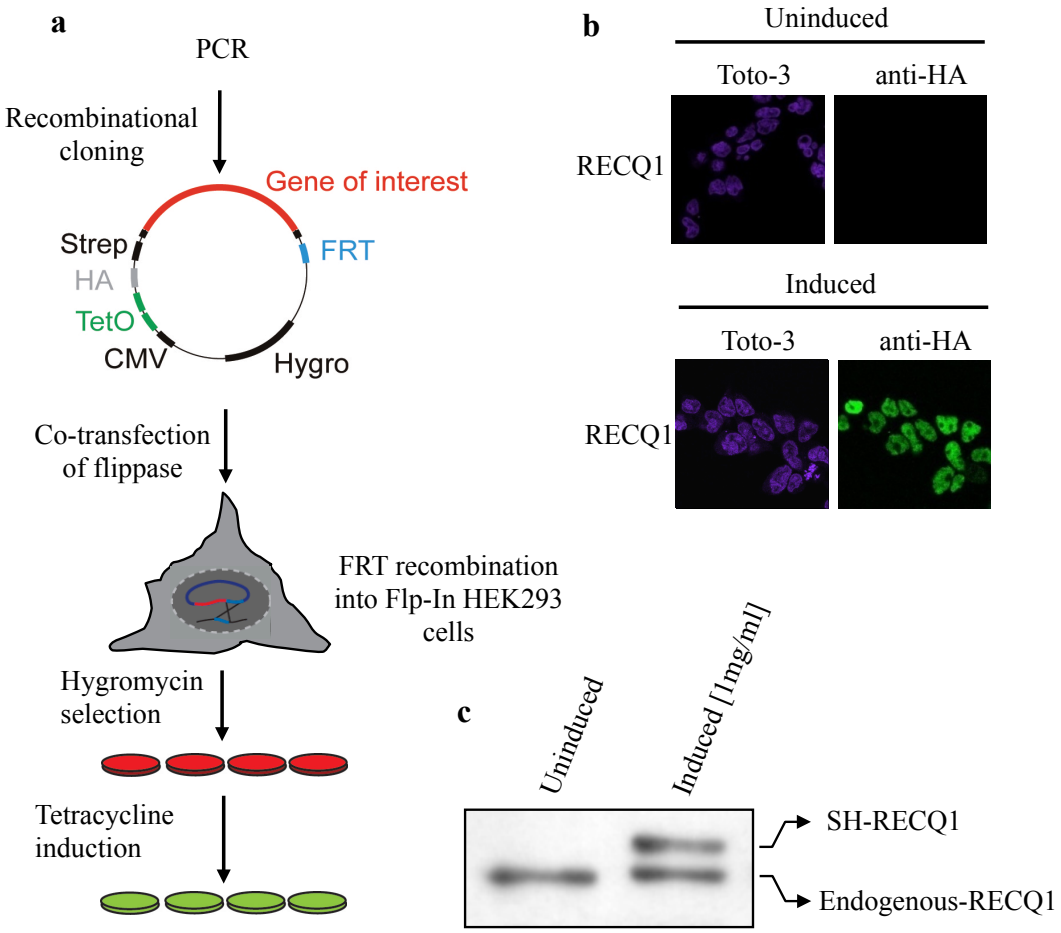

Figure 3.1. Expression of SH-tagged RECQ1 in HEK293T cells. (**a**) Schematic representation of the procedure followed for the generation of the inducible cell lines expressing a double-tagged version of human RECQ1. Isogenic cell lines were generated using Flp-recombinase-mediated integration into a single FRT site in Flp-in 293T-Rex cells that contain the genomic Flp-In site and a tet repressor (Invitrogen). (**b**) Isogenic bait protein expression in the presence and absence of 1μg/ml tetracycline was visualized by indirect fluorescence microscopy with an anti-HA antibody. (**c**) Bait protein expression monitored by immunoblotting using an anti-HA antibody.

a

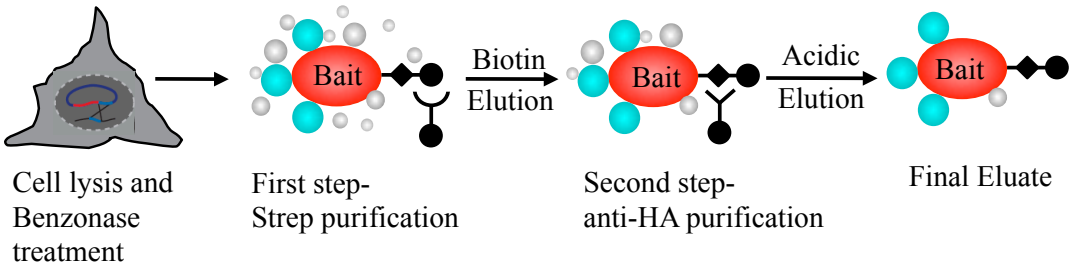

b

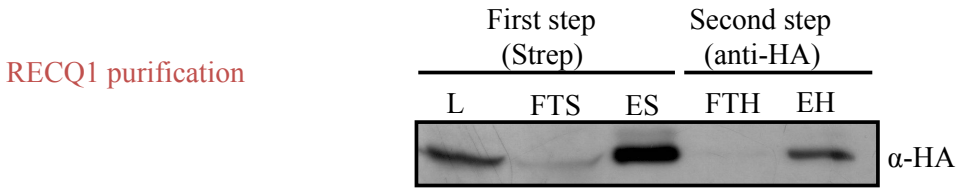

c

Protein ID (Gene Symbol)	Total number of peptides		
	Replicate 1	Replicate 2	Replicate 3
RECQ1 (RECQL)	291	289	275
PARP1 (PARP1)	18	13	12
Ku70 (XRCC6)	26	28	18
Ku80 (XRCC5)	28	19	14
Histone H2A type 1-A (HIST1H2AA)	7	3	6
Histone H2A type 2-A (HIST2H2AA4)	5	4	4
Histone H2B type 1-L (HIST1H2BL)	9	8	9
Histone 3.2 (HIST2H3A)	2	2	2

Figure 3.2. Purification of SH-tagged RECQ1 from HEK293 cells and mass spectrometry analysis of the RECQ1 complex. (**a**) Schematic representation of the purification procedure. (**b**) Western blot analysis of the SH-purification steps monitored using the anti-HA antibody. L: lysate; FTS: flow-through after streptavidin purification; ES: elution from streptavidin sepharose; FTH: flow-through after anti-HA purification; EH: elution form the anti-HA agarose (final eluate). (**c**) RECQ1 interacting proteins identified by mass spectrometry. We performed three biological replicate SH-purification experiments and analyzed each sample by LC-MS/MS. Only the proteins specifically associated with the bait-RECQ1 protein in all three replicates were considered as significant interacting proteins.

We generated a stable, inducible HEK 293 cell line expressing a doubly tagged-version of RECQ1, consisting of a streptavidin-binding peptide and a hemagglutinin tag, then isolated the protein complexes containing RECQ1 by affinity purification (Figure 3.1, 3.2a, 3.2b). The resulting protein complexes were then characterized by mass spectrometry profiling to identify RECQ1-associated proteins. Among the most abundant co-purified proteins were PARP1, Ku70 and Ku80, two key components of the DNA NHEJ repair pathway and several histone components (Figure 3.2c). In light of recent reports that suggest a role for PARP1 in the replication stress response [256], we decided to focus our next experiments on defining the role of the interaction between RECQ1 and PARP1.

The RECQ1 interaction with PARP1 was confirmed by co-immunoprecipitation (Co-IP) experiments using nuclease-solubilized nuclear extracts from U-2 OS and HEK 293T cell lines, and an anti-RECQ1 antibody recognizing the last 16 aa at the C-terminus of RECQ1 (aa 633-648). The same results were obtained using a different anti-RECQ1 antibody recognizing the first 110 aa at the N-terminus of the protein (data not shown). We also confirmed this interaction by parallel co-IPs using an anti-PARP1 antibody (Figure 3.3a). All co-IPs were performed in the presence of EtBr or Benzonase to make sure that the protein interaction was not DNA-mediated. Similar results were obtained using nuclear extracts from several additional cell lines, indicating that the association between RECQ1 and PARP1 is not cell type-specific (data not shown). Moreover, we showed that RECQ1 binds directly PARP1 by Far Western blot using the recombinant proteins, thus ruling out the possibility that other factors mediate this interaction in cells (Figure 3.3b). Our observation of a physical interaction between PARP1 and RECQ1 is also in agreement with previously published work that reported RECQ1 and PARP1 interact at viral replication origins [225], and with a study published while this work was in progress reporting an interaction between RECQ1 and PARP1 in human cells [280].

Given the important role of RECQ1 during DNA replication, we decided to check whether this interaction is cell-cycle regulated. U-2 OS cells were synchronized at G1/S border by a double thymidine block, or at the beginning of mitosis by nocodazole treatment plus mitotic “shake-off”, and then released and collected at different time points. FACS analysis was employed to verify the synchronization procedure and the cell-cycle progression upon release (Figure 3.4c). Immunoprecipitation experiments performed on nuclear extracts

prepared collecting cells at different cell-cycle stages showed that the RECQ1-PARP1 interaction in conserved throughout the cell-cycle and it is slightly increased at G1/S border (Figure 3.4b).

Next, we performed new co-immunoprecipitation experiments treating cells with different DNA damaging agents. The results showed that the RECQ1-PARP1 interaction is markedly increased, particularly when using drugs that activate PARP1 such as CPT, MMS and H_2O_2 (Figure 3.5a and 3.8).

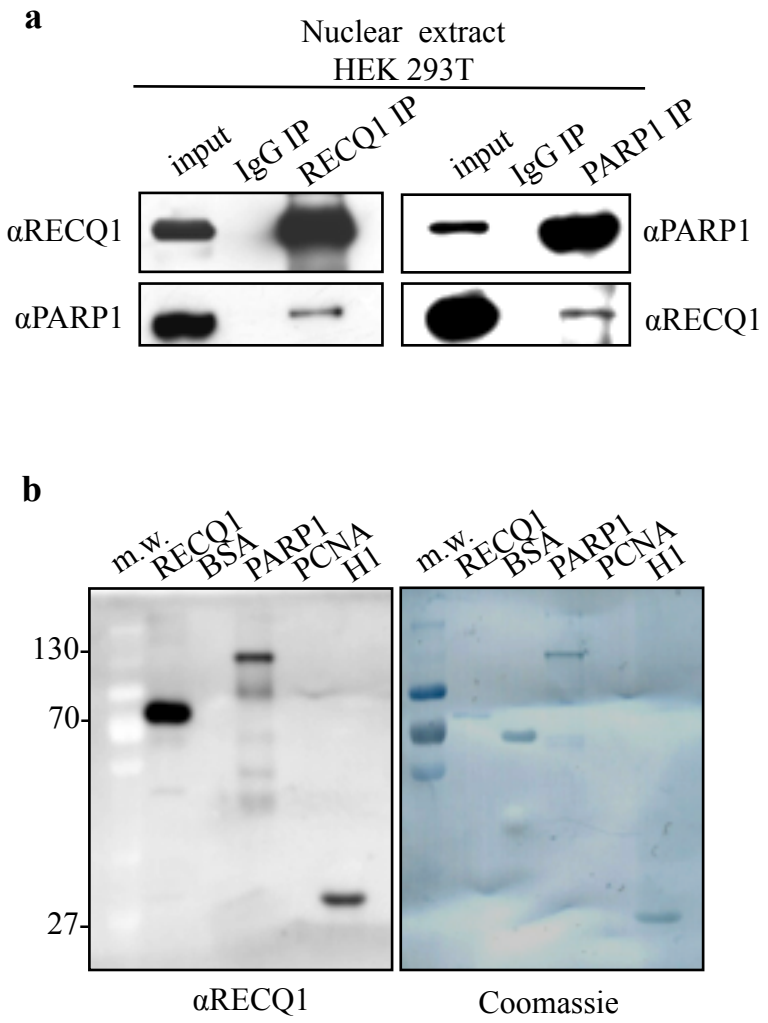

Figure 3.3. RECQ1 interacts with PARP1. (**a**) IPs from HEK 293T cells using the anti-RECQ1 or the anti-PARP1 antibody. Rabbit IgG IP served as a negative control. (**b**) Far Western analysis of the RECQ1-PARP1 interaction using purified recombinant proteins. Bovine Serum Albumin (BSA) and Proliferating Cell Nuclear Antigen (PCNA) were used as a negative control.

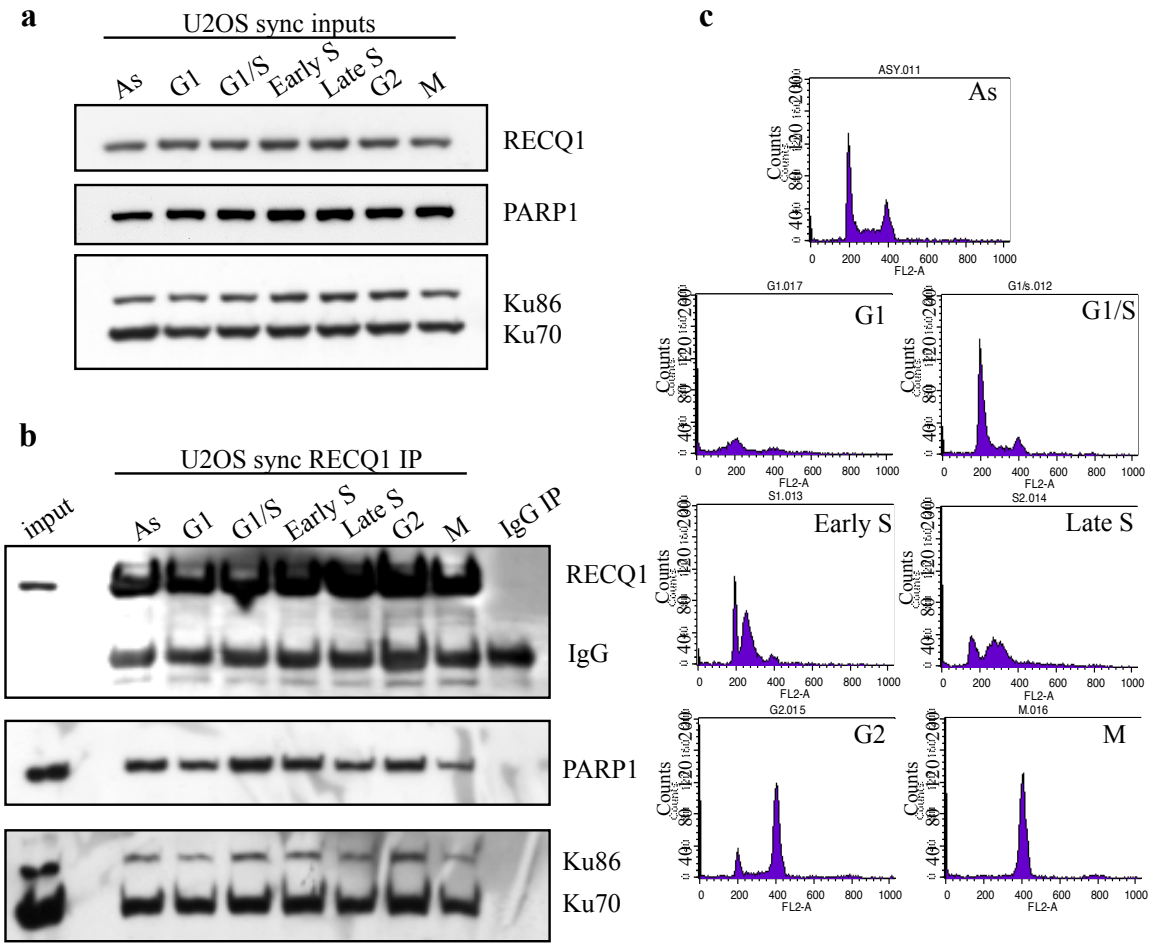

Figure 3.4. Cell-cycle dependence of RECQ1-PARP1 interaction. (**a**) and (**b**) Inpunts and IPs from double thymidine and "mitotic shake-off" synchronized U-2 OS cells. Rabbit IgG IP served as a negative control. (**c**) FACS analysis confirms enrichment of cell-cycle-specific stages.

There is growing evidences that the activity of PARP1 is important to build poly(ADP-ribose) scaffolds on the chromatin surrounding a DNA lesion to allow the differential recruitment of protein complexes in the proximity of the damaged area [244]. Thus, we decided to test if the RECQ1-PARP1 interaction is affected by the poly(ADP-ribosyl)ation of PARP1. By pretreating the cells with the specific PARP inhibitor NU1025 we were able to verify that the co-association of the two proteins is sharply reduced not only under normal conditions, but also upon DNA damage, suggesting that the poly(ADP-ribose) moieties synthetized by PARP1 on itself and on the damaged chromatin regulate the interaction with RECQ1, as previously demonstrated for other PARP1 binding partners (Figure 3.5a and 3.8).

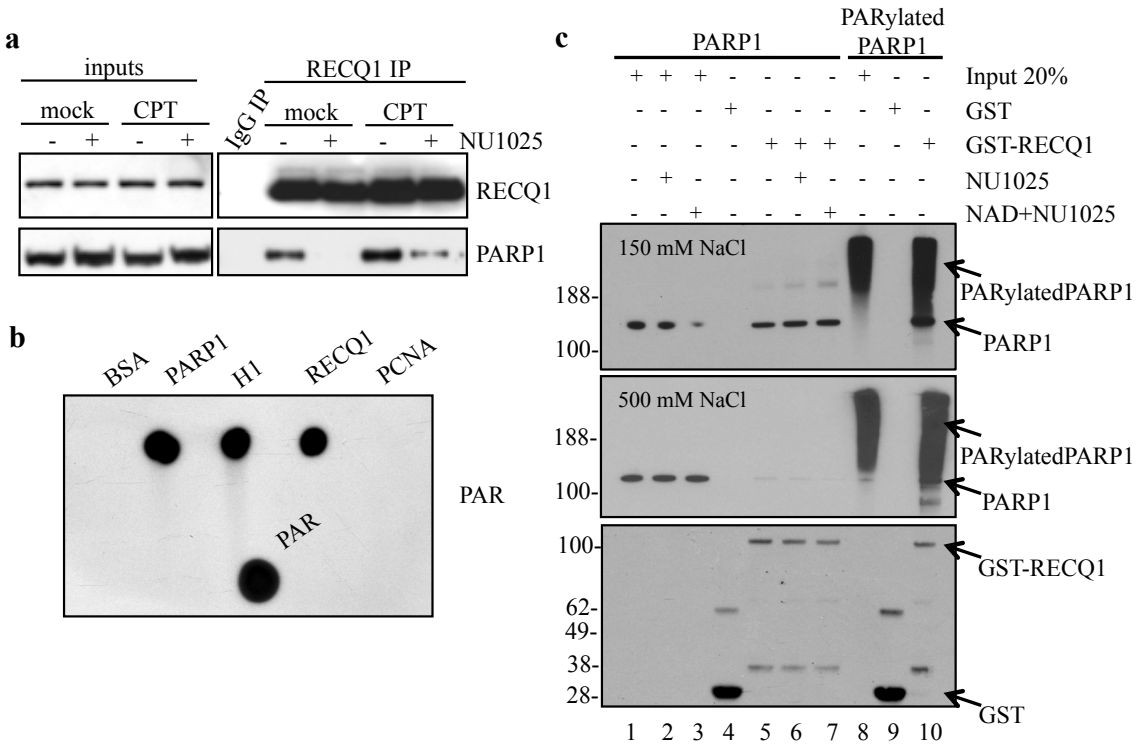

Figure 3.5. RECQ1 interacts with poly(ADP-ribosyl)ated PARP1. (**a**) IPs from U-2 OS cells using the anti-RECQ1 antibody +/- PARP inhibitor (50 µM NU1025) and +/- DNA damage (100 nM CPT for 2 hours). (**b**) Analysis of RECQ1-PAR binding *in vitro*. Proteins (2 pmol) were dot-blotted onto a nitrocellulose membrane and incubated with ^{32}P-labeled PAR, as described in the Material and Methods. BSA and PCNA were used as negative controls, while PARP1 and histone H1 were used as positive controls. (**c**) GST-pulldown experiments with unmodified recombinant PARP1 (1 µg) or PARylated PARP1 (1 µg) incubated with GST-RECQ1 (1 µg) or GST alone (1 µg), as a control. 100 mM NU1025 or 200 mM NAD^+ and 100 mM NU1025 were added as indicated. The interaction between RECQ1 and PARP1 is not affected by NU1025. However, the interaction of GST-RECQ1 with PARP1 is significantly decreased when the salt concentration in the washing buffer is increased from 150 to 500 mM, whereas the interaction with PARylated PARP1 is resistant to the washes with 500 mM NaCl. Bound proteins were resolved by gel electrophoresis, and visualized by western blot with anti-PAR, anti-PARP1 and anti-GST antibodies. The arrows point to the right signal for the indicated proteins.

This notion was further supported by additional experiments using purified poly(ADP-ribose) (PAR) in a dot-blot polymer assay. Recombinant proteins were dotted onto a nitrocellulose membrane, and their ability to bind ^{32}P-radiolabeled PAR was measured (Figure 3.5b). The results showed that RECQ1 and the positive control Histone H1 specifically interact with PAR despite bioinformatic analysis did not reveal any known PAR binding motif [281] or domain [244] in the RECQ1 sequence (data not shown). We next validated these observations using recombinant, purified PARP1 and GST-RECQ1. GST *in*

vitro pull-down confirmed that the interaction was direct, and significantly stronger when using a poly(ADP-ribosyl)ated form of PARP1 (Figure 3.5c). As a control, we also demonstrated that the interaction between recombinant RECQ1 and PARP1 was not affected by the addition of NU1025 indicating that the reduced RECQ1-PARP1 interaction detected in our co-IPs in the presence of NU1025 is due to the inhibition of PARP1 poly(ADP-ribosyl)ation activity rather than to an effect of NU1025 on its conformation. Moreover, RECQ1 interaction with poly(ADP-ribosyl)ated PARP1 is resistant to high salt washing, while RECQ1-PARP1 binding is disrupted, supporting our conclusion that the PAR modification of PARP1 is important for strengthening the interaction with RECQ1 (Figure 3.5c).

We next mapped the domains of RECQ1 that interact with PARP1 and PAR using a series of GST-tagged RECQ1 fragments. These experiments showed that the same domain of RECQ1 involved in PARP1 recognition interacts with the PAR polymer. In particular, both PARP1 and PAR interact with the C-terminal fragment of RECQ1 (amino acids 391-649) containing the Zn-binding and Winged Helix (WH) domains that form the so-called RQC domain, but not with the fragment 391-473 containing the Zn-binding domain alone. The fragment consisting of residues 474-649 that encompasses the WH domain is also able to interact with PARP1, although more weakly compared to fragment 391-649 (Figure 3.6c and 3.6e). This suggests that the deletion of residues 391-473 might affect the stability and/or conformation of the WH domain. *In vitro* poly(ADP-ribosyl)ation experiment also showed the same domain of RECQ1 involved in PARP1 and PAR binding is poly(ADP-ribosyl)ated by PARP1 (Figure 3.7), although the biological relevance of this observation is limited by the fact that RECQ1 does not seem to be poly(ADP-ribosyl)ated *in vivo* (data not shown and as recently reported [280]).

To determine the region(s) of PARP1 involved in RECQ1 recognition, we generated corresponding GST-fusion proteins expressing truncated versions of PARP1 by overexpression and purification of each fragment from HeLa cells. Only the fragments 1-371 and 384-524 were able to efficiently interact with RECQ1 by *in vitro* GST pull-down experiments. The fact that the fragment 174-366 did not pull-down RECQ1 indicates that the interaction is mediated by the first 173 N-terminal residues of PARP1 containing the DNA binding domain, and by residues 384-524 containing the BRCT domain of PARP1,

which is the automodification domain (Figure 3.5d). These two PARP1 domains are involved both in homodimerization [232], and in the binding of several partners including the human WRN helicase [189].

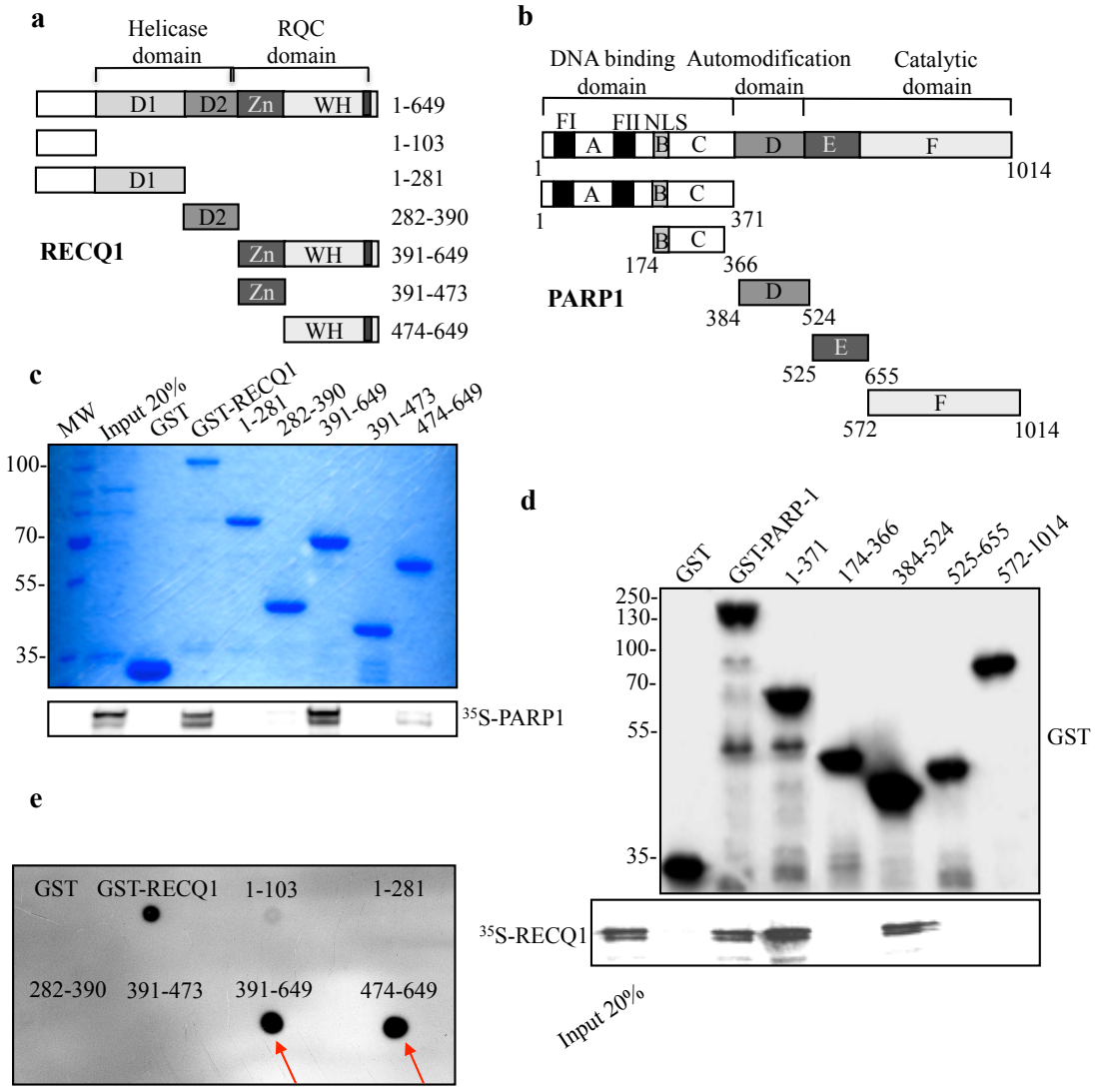

Figure 3.6. Structural determinants for the RECQ1-PARP1 interacion (**a**) and (**b**) Schematic representation of the domain structure of RECQ1 (D1 and D2, RecA-like domains; Zn, zinc-binding domain; WH, winged-helix domain) and PARP1 (A, DNA binding domain; B, nuclear localization signal (NLS); D, BRCT automodification domain; E, contains a WGR motif; F, catalytic domain; FI and FII, zinc-finger motifs. A third zinc-finger motif has been recently been identified in domain C [282, 283]). (**c**) Pulldown assays with GST-tagged RECQ1 fragments. Top: Coomassie stained gel of GST-tagged RECQ1 fragments. Bottom: autoradiography of *in vitro* GST pull-down assay using ^{35}S-labeled *in vitro*-translated PARP1 protein. MW, molecular weight (kDa). (**d**) Pulldown assays with GST-tagged PARP1 fragments. Bound proteins were revealed by autoradiography (bottom panel). Purified GST or GST–PARP1 proteins were detected with an anti-GST antibody (top panel). (**e**) Analysis of PAR binding to GST-RECQ1 fragments (2 pmol) dot-blotted onto a nitrocellulose membrane. The arrows indicate the two RECQ1 fragments that interact with ^{32}P-labeled PAR.

Altogether, these results show that RECQ1 binds PARP1 and poly-ADP-ribose, and that the ADP-ribosylation activity of PARP1 regulates this interaction.

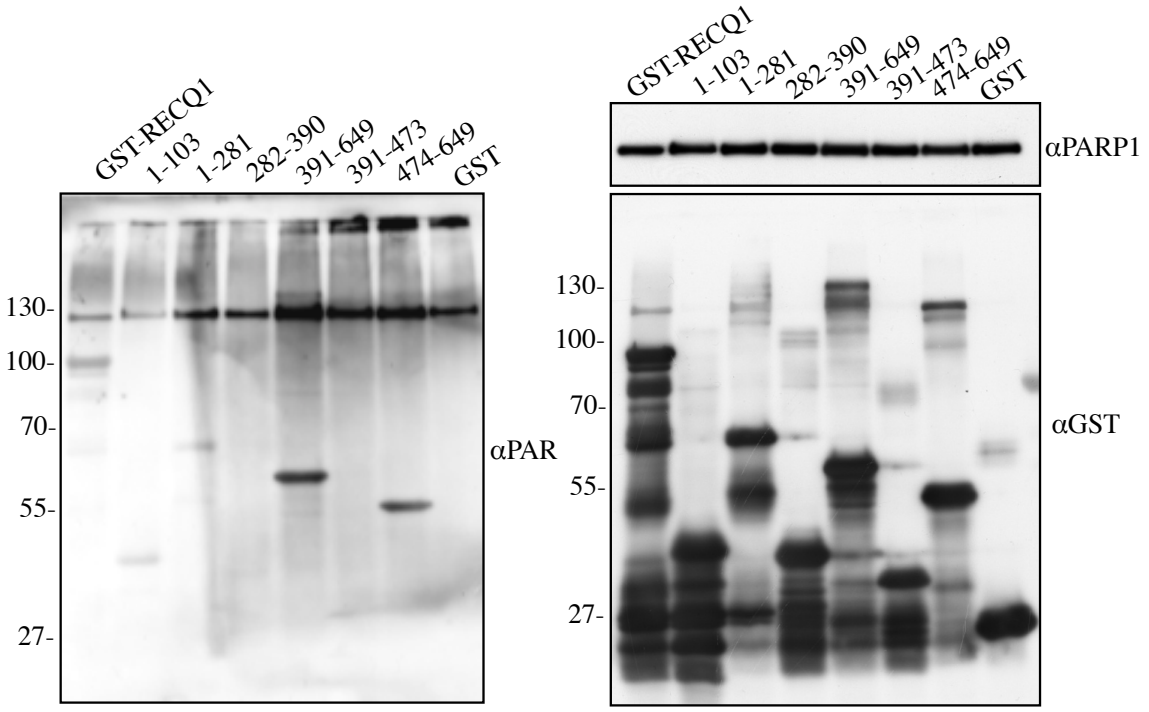

Figure 3.7. RECQ1 is poly(ADP-ribosyl)ated *in vitro*. *In vitro* analysis of RECQ1 poly(ADPribosyl)ation. GST-tagged RECQ1 fragments were incubated with PARP1 (1 μM) and 200 μM of NAD^+, and the presence of the PAR polymer was verified by Western analysis. The amount of PARP and GST-tagged RECQ1 fragments used in each experiment was also confirmed by Western analysis using anti-PARP1 and anti-GST antibodies, respectively.

3.2 RECQ1-PARP1 interaction at damaged replication forks

Our previous finding that RECQ1 associates with DNA replication origins in a cell-cycle-regulated fashion pointed to a role for RECQ1 in DNA replication [202]. Thus, we decided to investigate if RECQ1 associates with replicative factors by co-IP experiments. In addition to the previously identified interacting partners, we found that RECQ1 interacts with several MCM complex components in a DNA damage-dependent fashion, suggesting a possible involvement of RECQ1 at damaged replication forks. Again these interactions are lost upon PARP inhibition (Figure 3.8). The fact that these RECQ1-associated proteins were not detected by the mass spectrometry-coupled affinity purification could be due to the different procedure employed for the cellular extract preparation, or to a competition between the bait RECQ1 and the endogenous protein for binding to low abundant proteins.

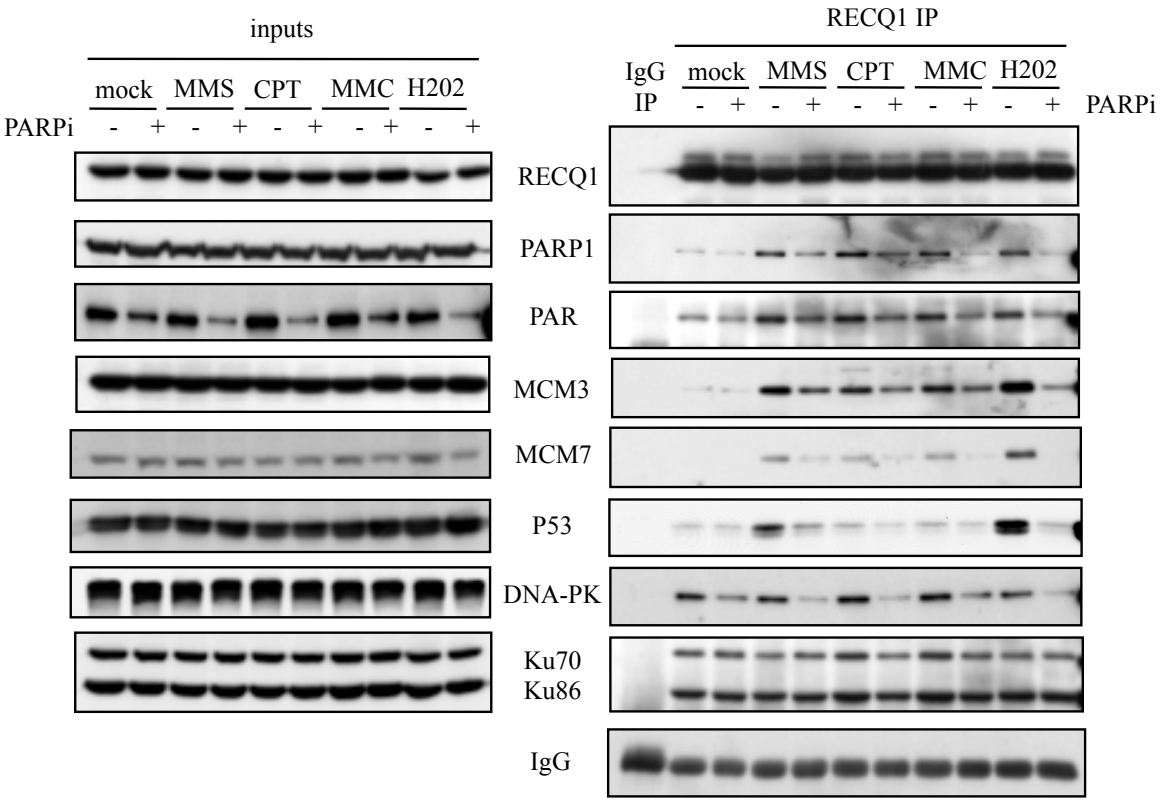

Figure 3.8. RECQ1 interactome upon different DNA damage and PARP inhibition. IPs from U-2 OS cells using the anti-RECQ1 antibody ± PARP inhibitor (50 μM NU1025) and ± DNA damage (2 mM MMS for 30 min, 100 nM CPT for 2 hrs; 2 μM MMC for 2 hrs; or 5 mM H_2O_2 for 30 min).

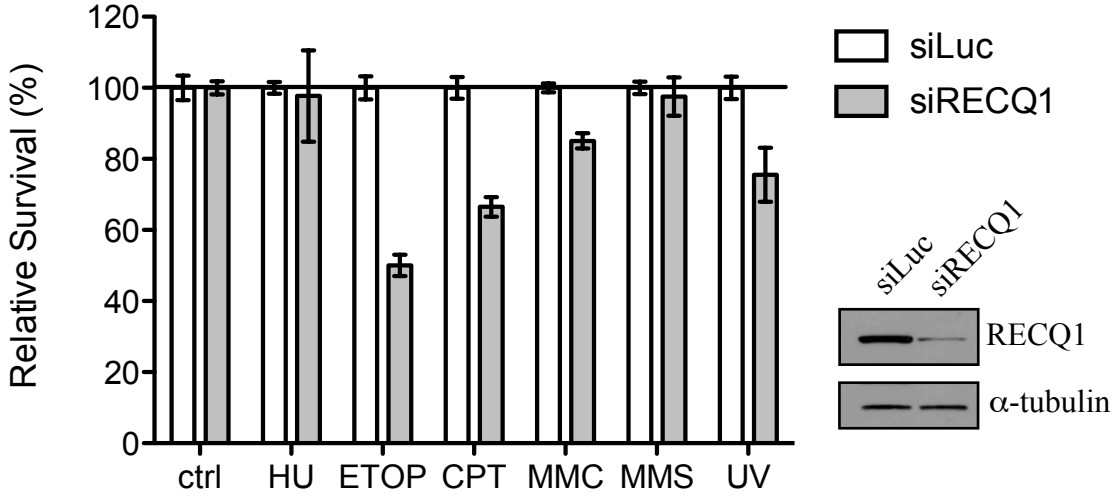

Figure 3.9. DNA damage sensitivity of RECQ1 depleted cells. The Y-axis shows the relative survival of U-2 OS cells expressing a RECQ1 shRNA or Luc shRNA relative to dsRed-expressing U-2 OS cells, following treatment with HU (2 mM, 16 hrs), etoposide (ETOP, 1 μM, 16 hrs), CPT (10 nM, 24 hrs), MMC (750 nM, 1 hrs), MMS (1 mM, 1 hrs) and UV (20 J/m^2).

Based on the recent discovery that PARP1 plays an important role in the reversal of replication forks after CPT treatment [117], we decided to investigate whether RECQ1 is also required for the cellular response to Top1 inhibition. First, we confirmed the previous observation that human cells depleted of RECQ1 have increased sensitivity to CPT [218]. Cell competition analysis showed that RECQ1-depleted cells are only mildly sensitive to most replication inhibitors or DNA damaging agents apart from CPT and etoposide (ETOP) (Figure 3.9). Second, we exploited a new chromatin immunoprecipitation (ChIP) method to isolate proteins on nascent DNA (iPOND), in order to study the RECQ1-PARP1 interaction in the context of ongoing DNA replication [273]. Briefly, replicating HEK 293T cells were pulse-labeled (20 min) with the nucleotide analog EdU , CPT-treated and cross-linked, as indicated in Figure 3.10a. After lysis and sonication, replicative chromatin was precipitated following biotin conjugation to EdU-labeled DNA by click chemistry, and a single-step of purification using streptavidin beads. Western blot analysis of recovered elutes confirmed that RECQ1 travels with the replisome under normal condition, expanding our previous finding that RECQ1 interacts with replication origins. Moreover, the RECQ1 binding on nascent DNA is significantly increased upon treatment with CPT, while the amount of the clamp loader PCNA is significantly decreased, in agreement with previous studies [284]. More importantly, RECQ1 association with nascent DNA is sharply decreased by PARP inhibition (Figure 3.10b). We noticed that also PARP1 associates with nascent DNA in a poly(ADP-ribosyl)ation-dependent fashion, as we observed for RECQ1 and in contrast to previous findings [256]. This phenomenon might be explained by the biochemical nature of this protein whose activation decreases its DNA affinity, but, at the same time it is required to recruit other PARP1 molecules through interaction between the newly synthesized poly(ADP-ribose) chains and the BRTC domain of PARP, thus creating a positive feedback for PARP1 accumulation at DNA damage sites, as previously demonstrated in locally irradiated cells [285]. Next, we confirmed these observation using a similar, but technically different, strategy where CldU-labeled replicative chromatin was isolated by a specific antibody to halogenated nucleoside analogs [256] (data not shown). Collectively, these results suggest that PARP1 activity is important for RECQ1 accumulation at replication forks, particularly after DNA damage.

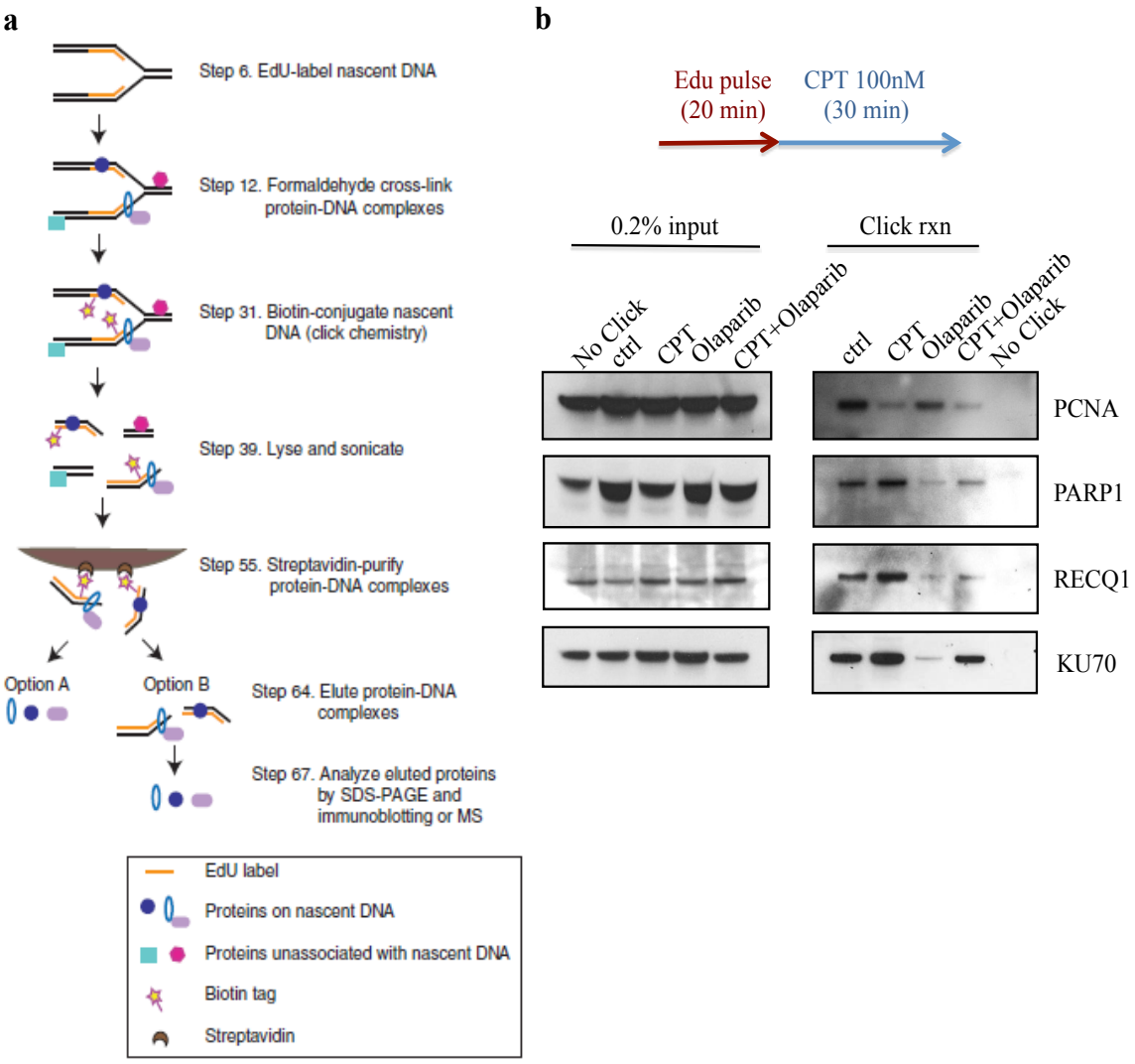

Figure 3.10. RECQ1 associates with nascent DNA in a PARylation-dependent manner. (**a**) Schematic overview of the iPOND (isolation of protein on nascent DNA) procedure. Adapted from Sirbu BM., 2012 [273]. (**b**) iPOND analysis of proteins associated with CPT-damaged replication forks and PARylation dependence. U-2 OS cells were pulsed with EdU for 20 min and then collected or incubated with 100 nM CPT for 30 min. Olaparib was added 1 hrs before EdU labeling and maintained throughout the experiment where indicated. iPOND was performed as described in the Materials and Methods. The "No click" sample was treated with EdU only, but no biotin-azide was added during the click reaction.

3.3 RECQ1 catalyzes restoration of model replication forks in vitro

Next, we tested whether recombinant RECQ1 mediates replication fork regression and/or restoration on synthetic DNA substrates. To measure these RECQ1 activities *in vitro*, we used a set of four oligonucleotides that can be annealed into two alternative ways that mimic model replication fork and "chicken-foot" structures, as previously described (Figure 3.11a) [90]. The two terminal regions of the vertical arms contained different, complementary but mutually exclusive sequences to ensure that the "chicken foot" (or HJ structure) structure is converted to a replication fork structure and prevent complete separation of the two strands. In addition, we inserted a single isocytosine (iso-C) residue in the oligonucleotide that represents a replication fork leading strand and two mismatches on the substrate vertical arms to prevent spontaneous fork regression and restoration. These substrates allowed us to follow the branch migration activity of RECQ1 on a synthetic replication fork substrate, and to understand how the interaction of RECQ1 with PARP1 affects the equilibrium between fork regression and restoration. Branch migration reactions were started by the addition of RECQ1, and performed as a function of time and protein concentration to investigate the kinetic and protein concentration dependence of the reaction. We found that RECQ1 promotes model replication fork restoration very efficiently and in a concentration-dependent fashion: more than 75 % of the chicken foot structure was converted into the model replication fork at 50 nM RECQ1 after 20 min (Figure 3.11b and 3.11c). In contrast, RECQ1 was unable to catalyze the opposite reaction, fork regression even at the highest RECQ1 concentration. Identical results were obtained using a variant of the same substrate that lacks the 6 nt ssDNA gap on the leading strand template, thus ruling out the possibility that RECQ1 is unable to promote fork regression because of the presence of this single-stranded region at the junction (Figure 3.12a and 3.12b). We observed that the poorly hydrolysable ATP analog ATPγS, or the non-hydrolysable analog AMP-PNP, strongly inhibited the reaction, confirming that the ATPase activity of RECQ1 is essential to promote branch migration of the chicken foot structure and restoration of the active replication fork. The requirement for ATPase activity was also supported by the observation that two previously characterized ATPase-deficient RECQ1 mutants, K119R and E220Q [135], were unable to promote fork restoration (Figure 3.13).

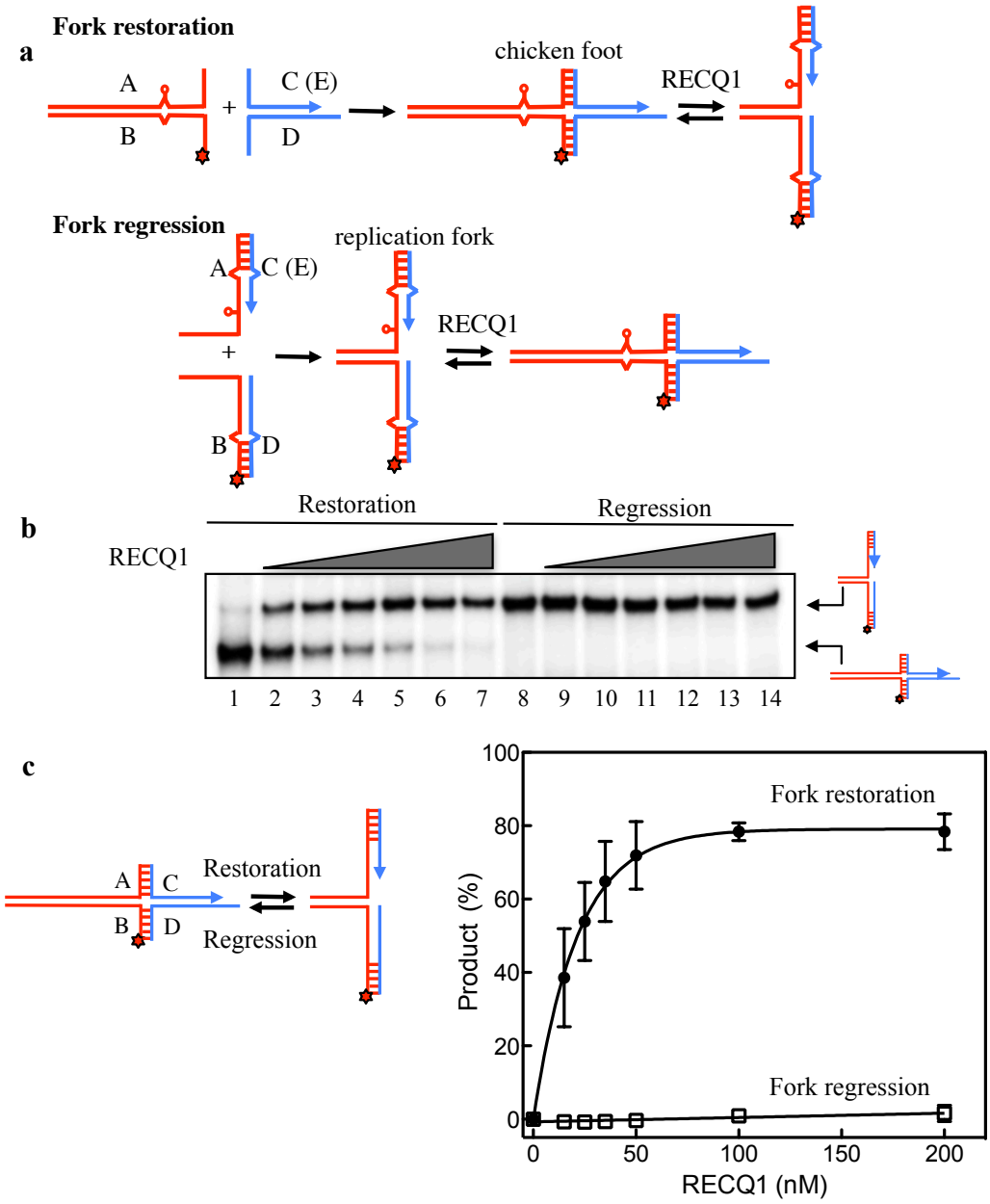

Figure 3.11. RECQ1 promotes *in vitro* fork restoration but not regression on synthetic DNA substrate. (a) Schematic of the procedure used for substrate preparation. Lined regions indicate heterologous sequences included in the vertical arms to prevent complete strand separation. In addition, a single isocytosine (iso-C) residue (denoted with a circle) and two mismatches (shown by carets) were introduced to prevent spontaneous substrate conversion. Oligonucleotide B was end-labeled with [γ-^{32}P]ATP (shown by a star). The sequence of all the oligonucleotides are reported in Table 2.1. **(b)** Fork restoration assays (lane 1-7) and fork regression assay (lane 8-14) performed using increasing RECQ1 concentrations (0, 15, 25, 35, 50, 100, and 200 nM) and a fixed concentration of the chicken foot substrate (2 nM, for restoration assay) or the replication fork structure (2 nM, for regression assay). All the reactions were stopped after 20 min. **(c)** Left, schematic of the reaction products. Right, percentage of the fork restoration and regression products plotted as a function of protein concentration. The data points represent the mean of three independent experiments. Error bars indicate s.e.m.

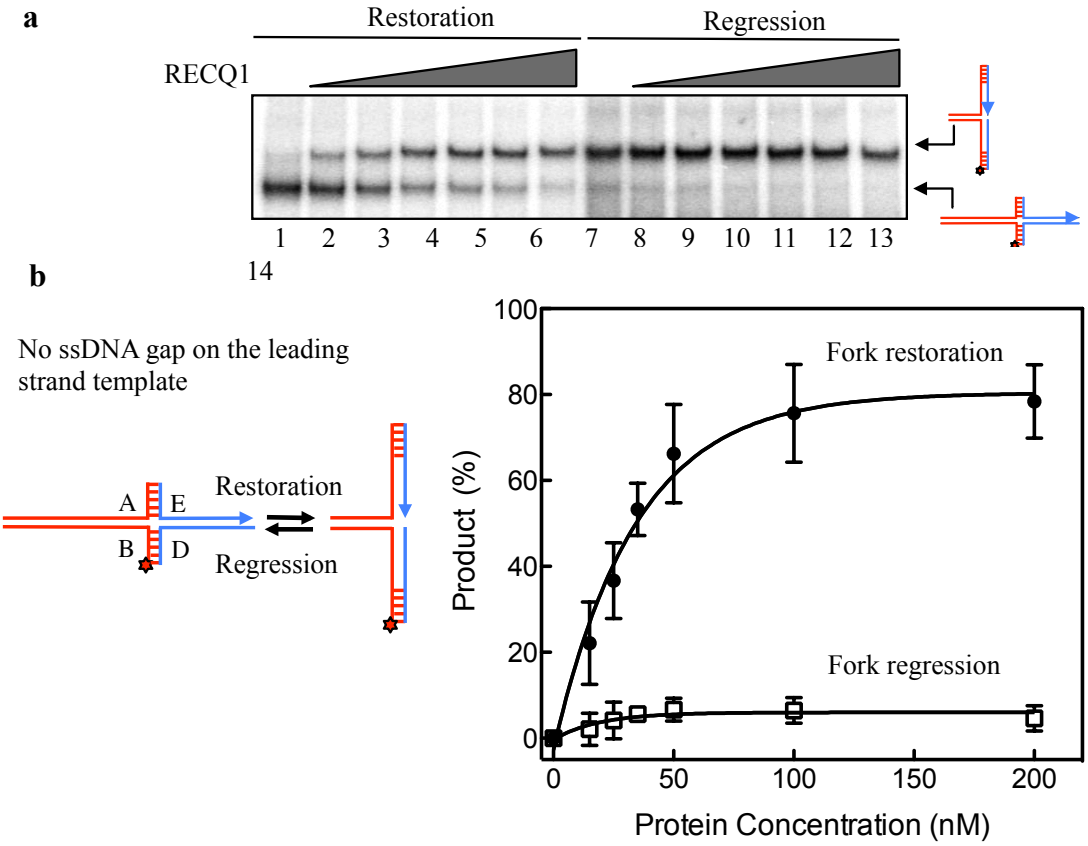

Figure 3.12. Fork restoration and regression assays using a DNA substrate that lacks a ssDNA gap on the leading strand template. (**a**) Fork restoration assays (lane 1-7) and fork regression assay (lane 8-14) performed using increasing RECQ1 concentrations (0, 15, 25, 35, 50, 100, and 200 nM) and a fixed concentration of the chicken foot substrate (2 nM, for restoration assay) or the replication fork structure (2 nM, for regression assay). All the reactions were stopped after 20 min. (**b**) Left, schematic of the reaction products. Right, percentage of the fork restoration and regression products plotted as a function of protein concentration. The data points represent the mean of three independent experiments. Error bars indicate s.e.m.

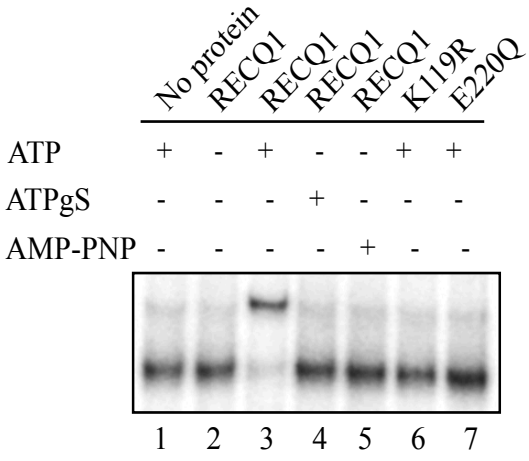

Figure 3.13. Fork restoration and regression assays using non-hydrolysable ATP analogs or ATPase deficient RECQ1 mutants. Fork restoration and regression assays were performed in the presence of ATP or different ATP analogs using wild-type RECQ1 (lanes 2-5) or the ATPase deficient RECQ1 mutant, K119R (lane 6) and E220Q (lane 7). The protein concentration was 50 nM for all the experiments. All the reactions were stopped after 20 min.

On the basis of our results that RECQ1 interacts with PARylated PARP1 and the previous observations that the poly(ADP-ribosyl)ation activity of PARP plays a key role in mediating the accumulation of regressed forks after DNA damage [117], we examined the effect of PARylated PARP1 on the RECQ1 fork restoration activity. We found that PARylated PARP1 strongly inhibited fork restoration rates of RECQ1: approximately 80 % of the chicken foot structure was converted within 20 min into a replication fork structure using 40 nM RECQ1. This fraction of restored fork structures was reduced to <30% by an equimolar concentration of PARylated PARP1 (Figure 3.14). Experiments performed at increasing PARylated PARP1 concentrations showed that the maximal inhibition was already achieved at equimolar concentrations since no further inhibition was observed by using a 2-fold excess of PARylated PARP1 (Figure 3.15).

Additional experiments using other four-ways junction substrates with heterology regions of 1 and 4 bases (Figure 3.16a), confirmed that RECQ1 has a strong branch migration activity and that its helicase activity may be used to bypass regions of heterology. However, we observed a 3-4-fold decrease in the formation of the branch migration product when the heterology region was increased from 1 to 4 bases (Figure 3.15b, 3.15d). PARylated PARP1 inhibited RECQ1 branch migration activity on these substrates, as previously observed with the replication fork substrates (Figure 3.15c, 3.15e).

Importantly, this conclusion was also supported by additional fork restoration assays performed using purified poly(ADP-ribose) (PAR), instead of PARylated PARP1, confirming that the interaction of RECQ1 with PAR is responsible for the inhibition of the fork restoration activity (Figure 3.14).

In agreement with previous findings [234], EMSA experiments using no-moveable HJ as a probe confirmed that PARylated PARP1 binds DNA with very low affinity because of the electrostatic repulsion between DNA and highly negative charged PAR, ruling out the possibility that the inhibitory effect of PARylated PARP1 on RECQ1 activity is due to a competition for DNA binding (Figure 3.17). Furthermore, to gain more insight into the mechanism for PAR-mediated RECQ1 inhibition, we tested whether PARylated PARP1 and PAR influence the ability of RECQ1 to bind DNA. Our results showed that poly(ADP-ribosyl)ated PARP1 and PAR inhibit RECQ1 affinity for HJ in a concentration–dependent manner, and again this effect is not related to a competition for DNA (Figure 3.18).

Interestingly, this inhibitory effect is more evident on high-order molecular species of RECQ1 bound to the DNA, thus suggesting that PAR might prevent the binding of RECQ1 oligomers on branched DNA structures. However, PAR does not seem to inhibit the ATPase activity of RECQ1 in the presence of ssDNA, HJ, and fork substrates (data not shown).

The ability of RECQ1 to promote fork restoration is not unique for this helicase. Previous studies using the same substrate showed that the human BLM helicase and RAD54, a member of the SNF2 family of DNA-dependent ATPases, catalyze both fork restoration and regression, with a bias toward fork restoration [90].

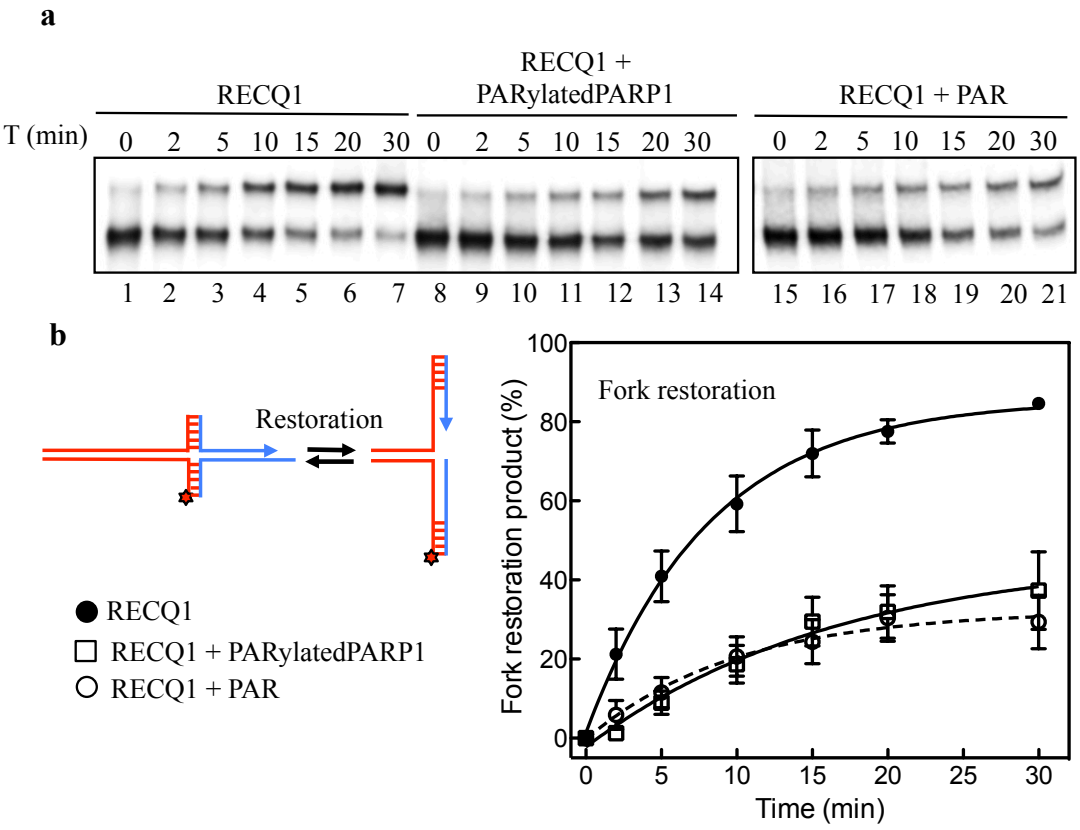

Figure 3.14. Inhibition of *in vitro* fork restoration activity of RECQ1 by PARylated PARP1 and PAR. (a) Kinetic experiments using RECQ1 (40 nM) and the chicken foot substrate (2 nM), visualized by gel electrophoresis and autoradiography. Lanes 1-7, RECQ1 alone; lanes 8-14, RECQ1 in the presence of PARylated PARP1 (40 nM); lanes 15-21, RECQ1 in the presence of PAR (100 nM). (**b**) Left, schematic of the reaction products. Right, percentage of the fork restoration products for RECQ1 alone and RECQ1 in the presence of PARylated PARP1 or PAR plotted as a function of time (min). The data points represent the mean of three independent experiments. Error bars indicate s.e.m.

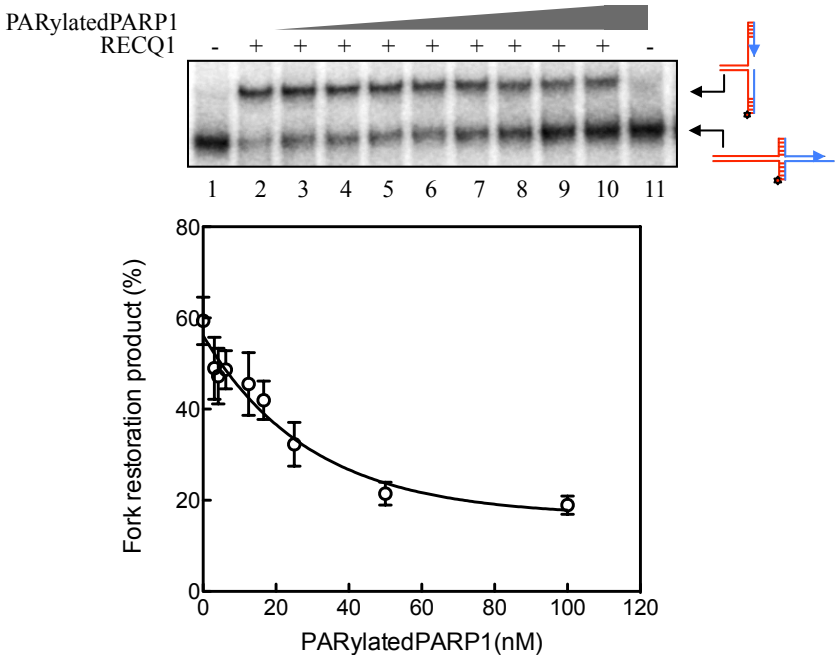

Figure 3.15. Inhibition of the *in vitro* fork restoration activity of RECQ1 by increasing concentrations of PARylated PARP1. Top, fork regression assay using a fixed concentration of chicken foot substrate (2 nM) and visualized by gel electrophoresis and autoradiography. Lanes 1, substrate alone; lane 2, RECQ1 alone (50 nM); lanes 3-10, fork restoration assays performed using increasing PARylated PARP1 concentrations (3.125, 4.16, 6.25, 12.5, 16.6, 25, 50 and 100 nM) and a fixed concentration of RECQ1 (50 nM); lane 11, PARylated PARP1 alone (100 nM). All the reactions were stopped after 20 min. Bottom, percentage of the fork restoration products plotted as a function of PARylated PARP1 concentration. The data points represent the mean of three independent experiments. Error bars indicate s.e.m.

This equilibrium was dramatically shifted by RAD51 that inhibits the fork restoration and stimulates fork regression activity of RAD54, but not of BLM. In addition, the human WRN helicase was previously shown to promote both regression and re-establishment of model replication forks *in vitro* [153, 182]. These results were confirmed by our experiments using the exonuclease-deficient WRN-E84A mutant that allows following the branch migration reaction without possible complications arising from the substrate digestion. WRN-E84A was able to promote both reactions with similar efficiency, with a slight bias toward fork restoration (Figure 3.19a). Furthermore, the fork restoration activity of WRN-E84A was not inhibited by the presence of PARylated PARP1, in agreement with previous studies performed using a different set of substrates [189] (Figure 3.19c). Collectively, these results show that although other helicases or translocases are able to promote fork restoration and regression, RECQ1 has a striking preference to promote fork restoration *versus* regression, and its activity is uniquely regulated by PARylated PARP1.

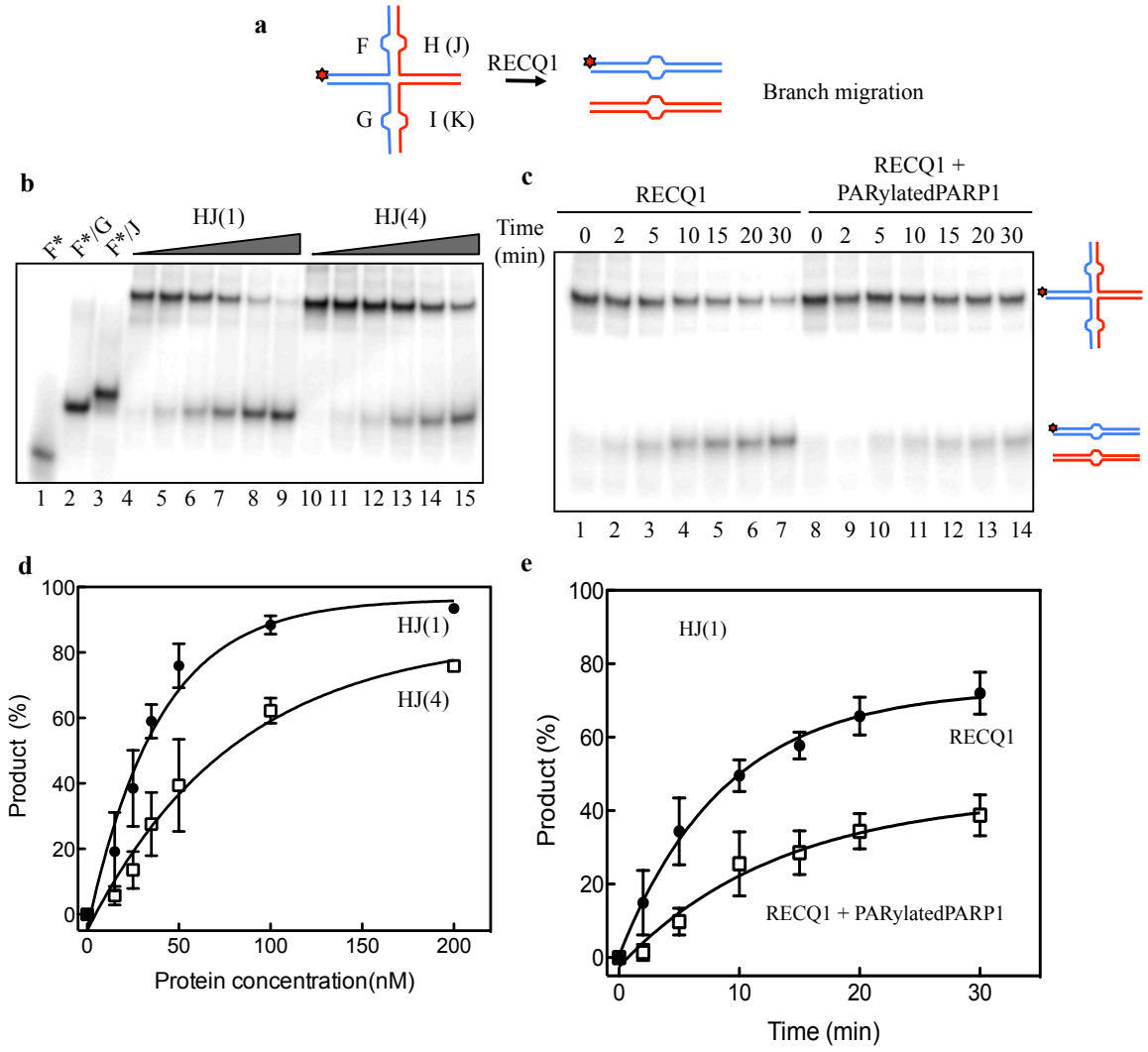

Figure 3.16. Effect of PARylated PARP1 on RECQ1 branch migration activity using the HJ substrate. (**a**) Schematic representation of the Holliday junction (X-junction) substrates used for the branch migration assays; HJ(1) and HJ(4) contain 1 or 4 base of heterology (shown by carets), respectively. The sequence of all the oligonucleotides are reported in Table 2.1. (**b**) Lanes 1-3, DNA migration markers; lanes 4-9, branch migration assays performed using increasing RECQ1 concentrations (0, 25, 35, 50, 100, and 200 nM) and a fixed concentration of HJ(1) substrate (2 nM); lanes 10-15, branch migration assays using increasing RECQ1 concentrations (0, 25, 35, 50, 100, and 200 nM) and a fixed concentration of the HJ(4) (2 nM). (**d**) Percentage of the branch migration products plotted as a function of protein concentration. The data points represent the mean of three independent experiments. Error bars indicate s.e.m. (**c**) Lanes 1-7, kinetic experiments performed using 50 nM RECQ1 and a fixed concentration of HJ(1) substrate (2 nM); lanes 8-14, kinetic experiments performed in the presence of 50 nM RECQ1, PARylated PARP1 (50 nM) and a fixed concentration of HJ(1) substrate (2 nM). (**e**) Percentage of the branch migration products for RECQ1 alone and RECQ1 in the presence of PARylated PARP1 plotted as a function of time (min). The data points represent the mean of three independent experiments with the standard deviation indicated by error bars.

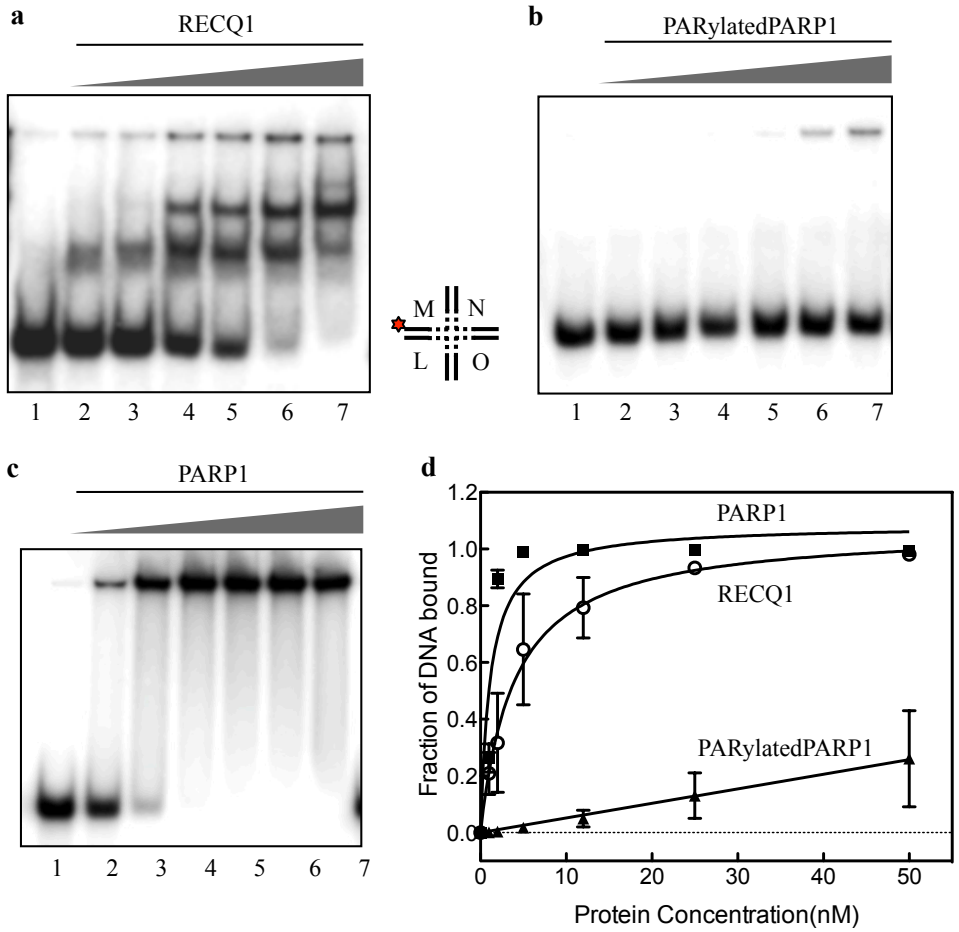

Figure 3.17. DNA binding assays at increasing protein concentrations using the HJ probe. EMSA experiments performed using a "non-moveable" HJ substrate with a 12-bp homologous core (0.5 nM). Lane 1, substrate alone; lanes 2-7, experiments at increasing RECQ1 (**a**), PARylated PARP1 (**b**), and PARP1 (**c**) concentrations (1, 2, 5, 12, 25, 50 nM). (**d**) The plots are the average of three independent experiments. Error bars indicate s.e.m.

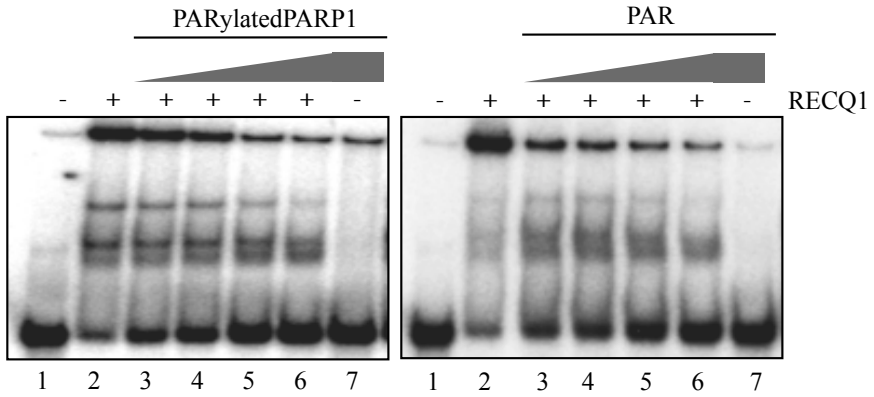

Figure 3.18. PARylated PARP1 or PAR inhibition of RECQ1 binding to DNA. EMSA experiments performed using a "non-moveable" HJ substrate with a 12-bp homologous core (0.5 nM). Lane 1, substrate alone; lane 3, 20 nM RECQ1 alone; lanes 3-7, experiments at increasing PARylated PARP1 (5, 12, 25, 50 nM) and PAR (25, 50, 100, 200 nM) concentrations.

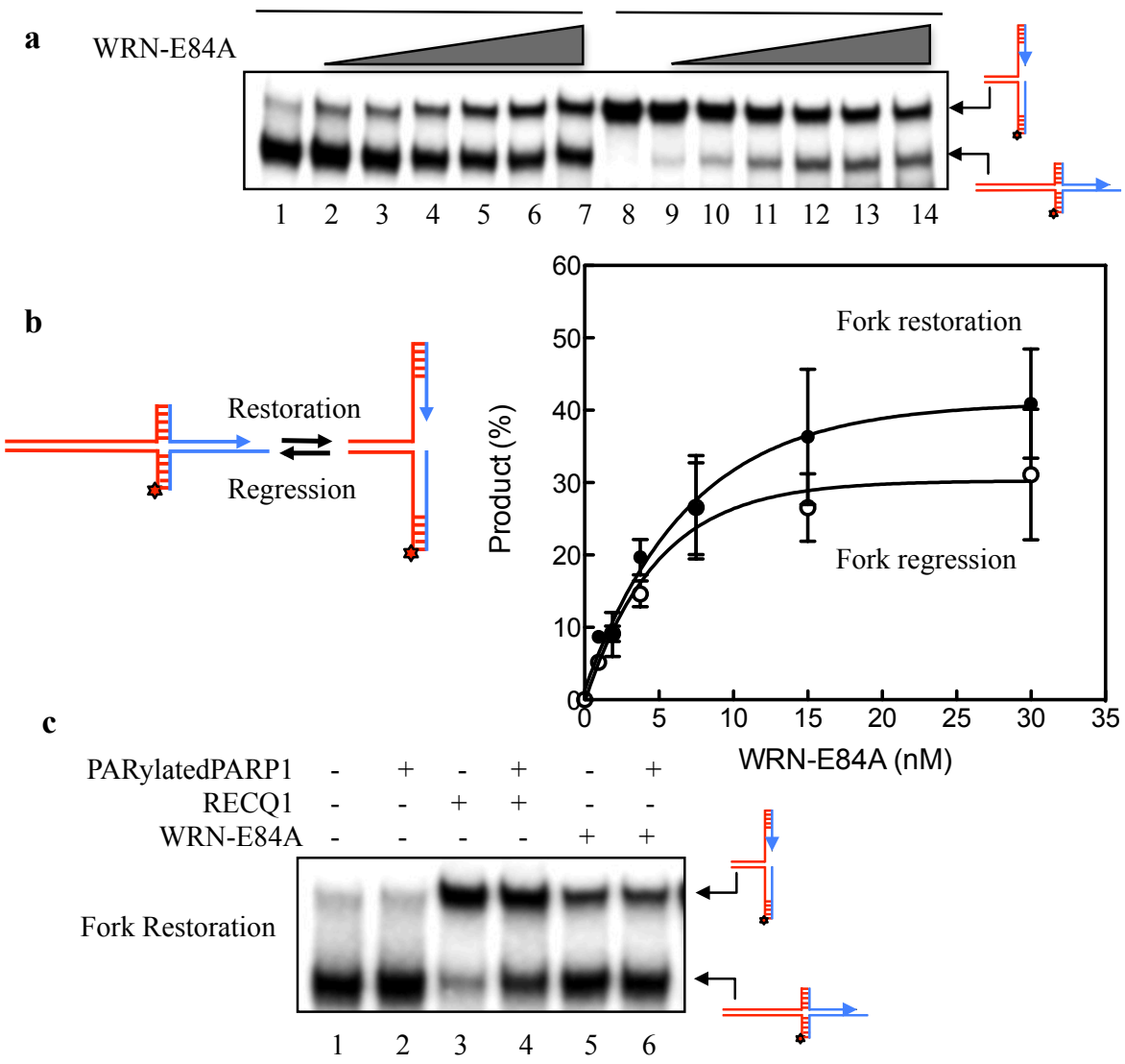

Figure 3.19. Fork restoration and regression assays using human WRN. (**a**) These experiments were performed using exonuclease-deficient WRN-E84A mutant that allows following the branch migration reaction without possible complications arising form the substrate digestion. Lanes 1-7, fork restoration assays performed at increasing WRN-E84A concentrations (0, 0.9375, 1.875, 3.75, 7.5, 15, and 30 nM) and a fixed concentration of the chicken foot substrate (2 nM); lanes 8-14, fork regression assays at increasing WRN-E84A concentrations (0, 0.9375, 1.875, 3.75, 7.5, 15, and 30 nM) and a fixed concentration of the replication fork structure (2 nM). All the reactions were stopped for 20 min. (**b**) Left, schematic of the reaction products. Right, percentage of the fork restoration and regression products plotted as a function of protein concentration. The data points represent the mean of three independent experiments. Error bars indicate s.e.m. (**c**) Fork restoration assays performed in the presence (lanes 2, 4, 6) and absence (lanes 1, 3, 5) of PARylated PARP1 (50 nM) using wild-type RECQ1 (50 nM; lanes 3, 4) or WRN-E84A (20 nM; lane 5, 6). All the reactions were stopped for 20 min.

3.4 RECQ1 depletion makes PARP activity dispensable to promote CPT-induced replication fork slowing and prevent DSB accumulation

Next, we decided to test if RECQ1 depletion affects the rates of replication fork progression upon Top1 inhibition in a cellular context using genome-wide single-molecule DNA replication assays. We pulse-labeled U-2 OS cells with the thymidine analog CIdU (red label) for 30 min, then treated cells with 50 nM CPT and concomitantly labeled them with the second thymidine analog, ldU (green label), for an additional 30 min (Figure 3.20a). The IdU tract length distributions were then analyzed after CPT treatment with or without PARP inhibition. Using this approach, we initially confirmed the previous findings that replication forks rapidly slow upon treatment with low CPT doses (50 nM), and that this effect requires the action of the poly(ADP-ribose) polymerase 1 (PARP1) [117]. This is consistent with the notion that PARP inactivation does not perturb normal fork progression, but prevents fork slowing after Top1 inhibition. Next, we looked at the rates of fork progression in RECQ1-depleted cells treated with CPT and the clinically useful PARP inhibitor Olaparib. Our results showed that PARP inhibition did not rescue CPT-induced fork slowing in RECQ1-deficient cells (Figure 3.20b and 3.20c).

These results identify an essential role of RECQ1 in the control of fork progression upon Top1 inhibition. Analogous results were obtained using a U-2 OS cell line where endogenous RECQ1 is efficiently downregulated by lentiviral expression of a *RECQ1* shRNA with a different RNAi sequence (figure 3.21b), confirming that the observed effect is specifically associated with RECQ1 loss, and not simply due to an unspecific RNAi outcome (Figure 3.21c). This notion was further validated by complementation assays in RECQ1-depleted cells rescued with an shRNA-resistant version of the RECQ1 protein (Figure 3.22b). The complementation of RECQ1-depleted U-2 OS cells with shRNA-resistant wild type RECQ1 abrogated the effect of RECQ1 depletion on replication fork progression upon Top1 inhibition. Moreover, the complementation of RECQ1-depleted cells with the ATPase deficient RECQ1 mutant (K119R) confirmed that the ATPase/helicase activity of RECQ1 is essential for its role in replication fork progression upon Top1 inhibition, as already inferred from the biochemical studies (Figure 3.21c and 3.21d). Additional DNA fiber experiments with BLM- and WRN-depleted cells showed

that, in contrast to the results obtained with RECQ1-depleted cells, PARP inhibition was still able to abrogate CPT-induced fork slowing in the absence of these two helicases (Figure 3.22). These results strongly support the notion that the identified role of RECQ1 in the control of fork progression upon Top1 inhibition reflects a specific function of RECQ1 and not a more general role of the RecQ helicase family members.

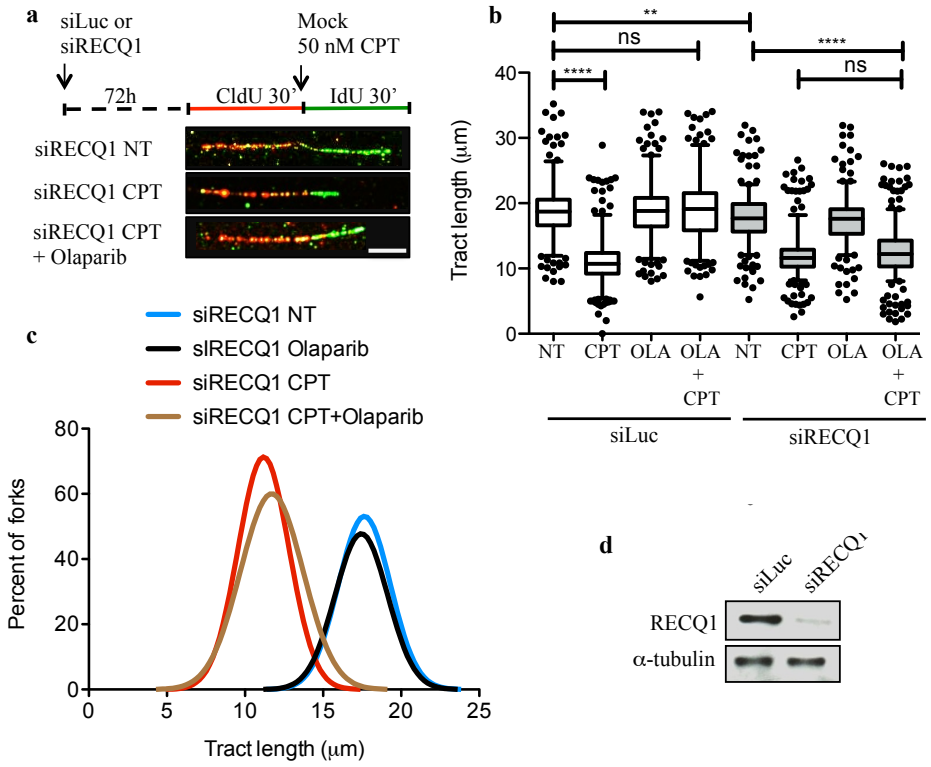

Figure 3.20. Restoration of normal replication fork progression after Top1 and PARP inhibition is impaired in RECQ1-depleted U-2 OS cells. (**a**) Top, schematic of single DNA fiber replication track analysis. U-2 OS cells were transfected with siRNA against Luciferase (siLuc) or RECQ1 (siRECQ1) before CldU or IdU labeling, as indicated. Red and green denote CldU- and IdU-containing tracts, respectively. CPT (50 nM) was added concomitantly with the second label. Bottom, representative DNA fiber tracts from Microfluidic-assisted replication tract analysis of RECQ1 depleted U-2 OS cells upon Top1 and/or PARP inhibition. Scale bar, 12.5 µm. (**b**) Statistical analysis of IdU tract-length measurements from Luc- or RECQ1-depleted cells. Relative length of IdU tracts synthesized after mock (NT) or CPT treatment (50 nM). At least 175 tracts were scored for each dataset. Olaparib (OLA, 10 µM) was optionally added 2 hours before CldU labeling and maintained during labeling. Whiskers indicate the 10th and 90th percentiles. *ns*, not significant; **p<0.006, **** p<0.0001 (Mann-Whitney test). (**c**) Smoothed histogram of IdU tract-length distribution after Top1 and/or PARP inhibition in RECQ1-depleted cells. (**d**) RECQ1 expression after siRNA knockdown, detected by western blot. α-tubulin was detected as loading control.

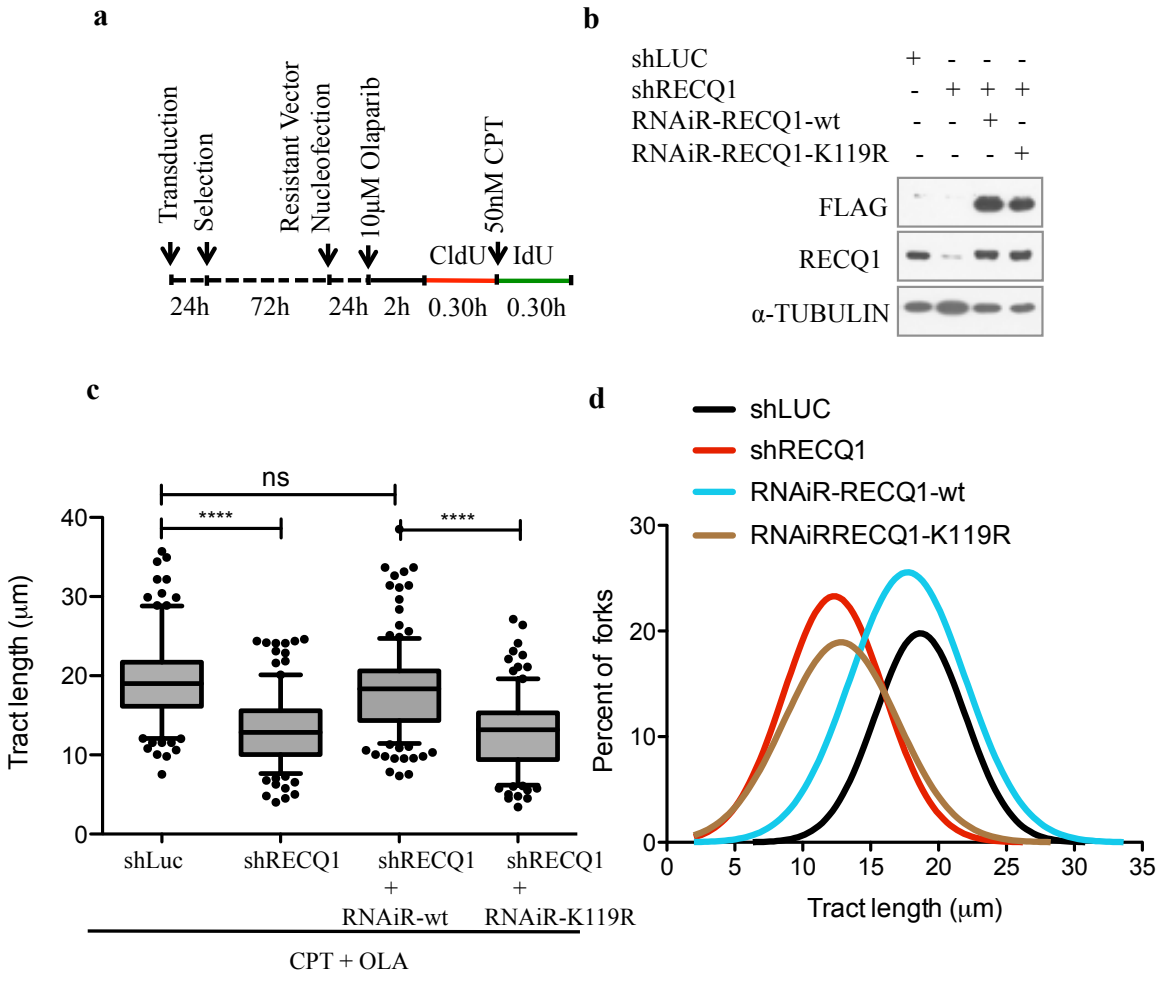

Figure 3.21. Genetic complementation of RECQ1-depleted cells with wild-type RECQ1, but not with the ATP-deficient K119R mutant, rescues the fork progression phenotype observed in RECQ1-depleted U-2 OS cells. (**a**) Experimental scheme for genetic knockdown-rescue experiments. U-2 OS cells were transduced with lentivirus to Luciferase (shLuc) or RECQ1 (shRECQ1). RECQ1-depleted cells were nucleofected to express RNAi resistant wild-type (RNAiR-wt) and ATPase-deficient (RNAiR-K119R) RECQ1 before CldU labeling. (**b**) Western blot analysis of RECQ1-depleted cells (shRECQ1) complemented with the shRNA resistant wild type RECQ1 or K119R mutant (both proteins are FLAG-tagged). Tubulin was detected as a loading control (**c**) Statistical analysis of IdU tract length measurements from **a**. Relative length of IdU tracts synthesized after CPT treatment (50 nM). At least 175 tracts were scored for each dataset. Olaparib (OLA, 10 μM) was optionally added 2 hours before CldU labeling and maintained during labeling. Whiskers indicate the 10^{th} and 90^{th} percentiles. *ns*, not significant; **p<0.006, **** p<0.0001 (Mann-Whitney test). (**d**) Smoothened histogram of IdU tract-length after Top1 and PARP inhibition in RECQ1-depleted cells alone and genetically complemented with RNAiR-wt or RNAiR-K119R RECQ1.

Interestingly, there was a minor, but statistically significant, difference between the mean length of the replication tracts measured in the untreated RECQ1-depleted cells relative to the untreated control cells (siLuc). This is in line with our previous studies where we observed that the replication tracts were slightly shorter in RECQ1-depleted cells versus controls in the absence of DNA damage [202]. These data suggest that RECQ1 may play an additional role in replication fork progression in unperturbed cells.

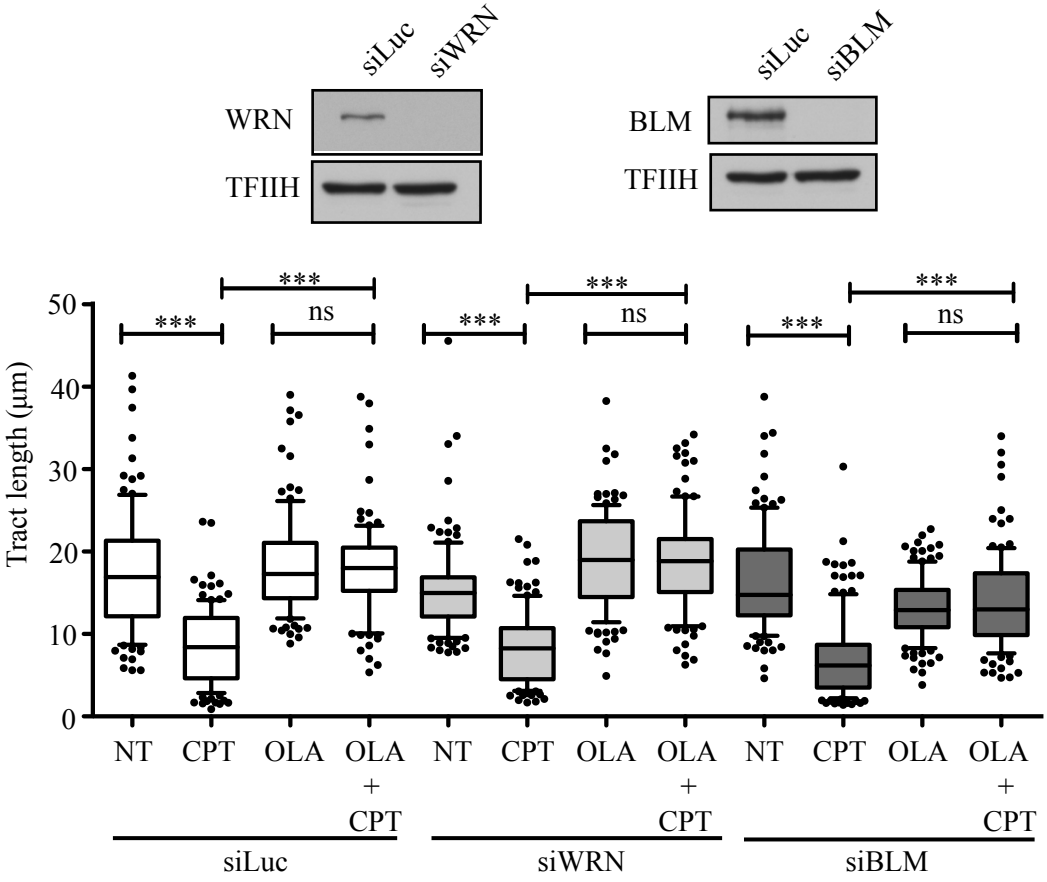

Figure 3.22. Restoration of normal replication fork progression after Top1 and PARP inhibition is not impaired in WRN- or BLM-depleted U-2 OS cells. Top, WRN and BLM expression after siRNA knockdown, detected by western blotting. Transcription factor II H (TFIIH) was detected as loading control. Bottom, statistical analysis of IdU tract-length measurements from siLuc-, WRN- and BLM-depleted cells. Relative length of IdU tracts synthesized after mock (NT) or CPT treatment (50 nM). At least 175 tracts were scored for each dataset. Olaparib (OLA, 10 µM) was optionally added 2 hours before CldU labeling and maintained during labeling. Whiskers indicate the 10th and 90th percentiles. *ns*, not significant; **p<0.006, **** p<0.0001 (Mann-Whitney test).

PARP inhibition prevents CPT-induced fork slowing, and results in detectable chromosomal breakage at low CPT doses [117]. Thus, we decided to determine whether RECQ1 depletion also influences DSB accumulation after CPT using a recently optimized Pulsed Field Gel Electrophoresis (PFGE) protocol [117]. Our PFGE analysis confirmed that PARP inhibition in U-2 OS cells leads to the induction of high levels of DSBs after CPT treatment (100nM) (Figure 3.23a and 3.23b). These results are consistent with the notion that PARP-inhibited or defective cells do not slow or accumulate reversed forks after CPT treatment, leading to replication run-off at Topoisomerase I cleavage complexes (Top1cc) and DSB formation even at low CPT doses [117]. RECQ1 depletion, on other hand, had the opposite effect: fork slowing after CPT is not rescued by PARP1 inhibition, and DSB induction by PARP inhibitors is suppressed in RECQ1-depleted cells (Figure 3.23a and 3.23b).

As an alternative method to monitor DSB formation, we looked at γH2AX and 53BP1 foci colocalization under the same conditions used for the PFGE experiments.

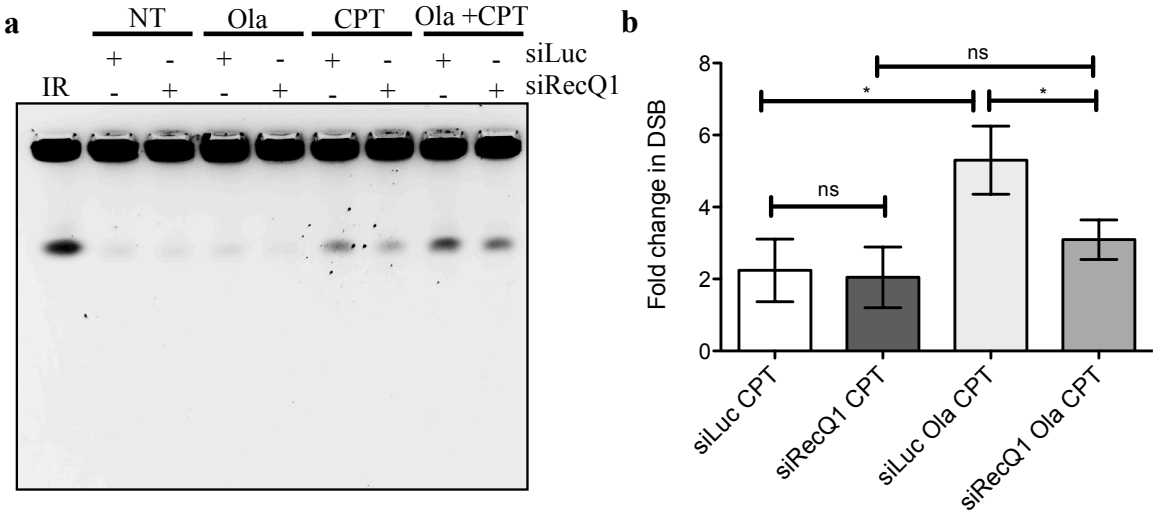

Figure 3.23. PARP inactivation leads to DSB formation at low CPT doses in the presence but not in the absence of RECQ1. (**a**) PFGE of U-2 OS cells transfected with siLuc or siRECQ1, untreated (NT) or treated with CPT (100 nM) and/or Olaparib (OLA, 10 μM). Ionizing radiation (IR)-treated cells was used as positive control. (**b**) DSB signals quantified by ImageJ and normalized to unsaturated signals of DNA retained in the wells. Values obtained from each treatments were then normalized against their respective untreated controls to obtain the fold change in DSBs upon treatment with CPT. Results from three independent experiments; *p<0.05 (paired *t*-test); ns, not significant.

In agreement with previous findings, we found that only a minor fraction of γH2AX foci colocalized with 53BP1 upon 100 nM CPT treatment and that PARP inhibition led to a considerably higher degree of colocalization of γH2AX and 53BP1 [117] (Figure 3.24a and 3.24b). However, RECQ1 depletion reduced the fraction of colocalizing foci in the presence of Olaparib, supporting the notion that DSB induction by PARP inhibitors is suppressed in RECQ1-depleted cells. Collectively, these data indicate that RECQ1 regulates the rate of replication fork progression and that RECQ1 depletion makes PARP activity dispensable to prevent DSB accumulation after Top1 inhibition.

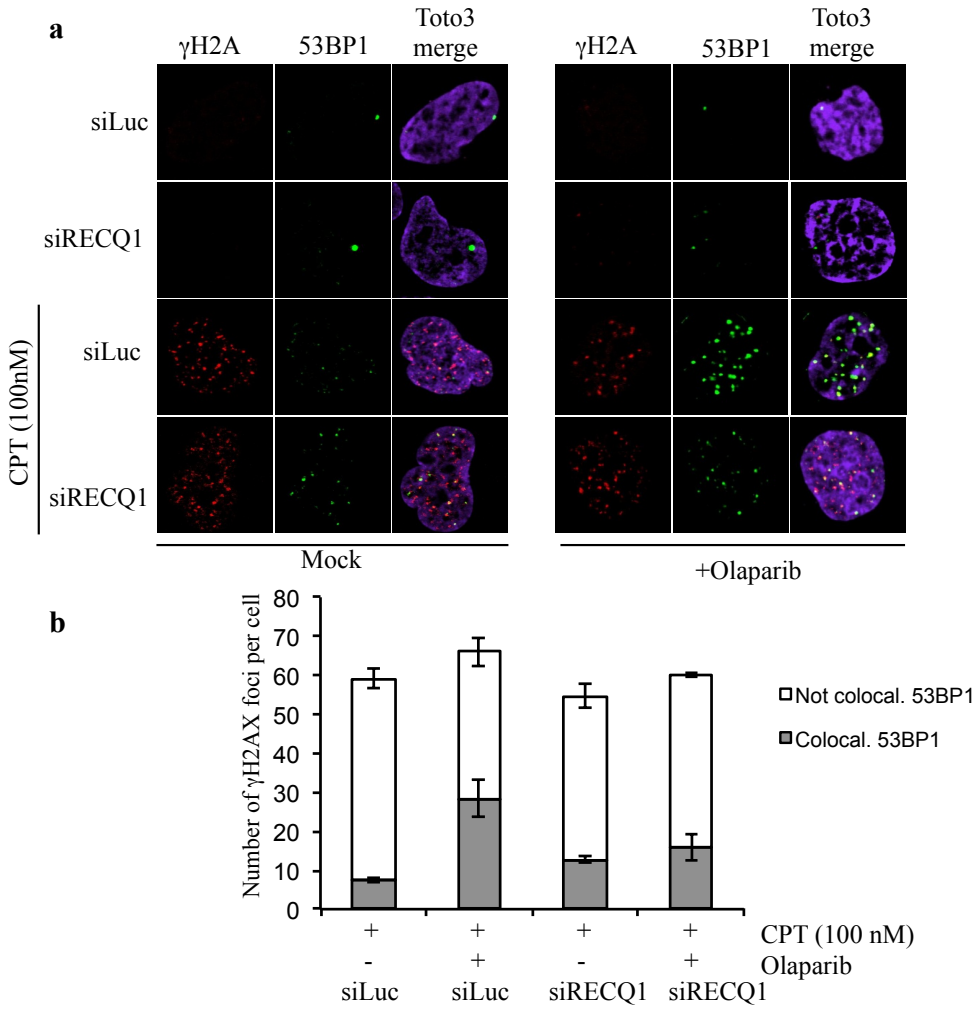

Figure 3.24. PARP inactivation leads to DSB0 formation at low CPT doses in the presence, but not in the absence of RECQ1. (**a**) Representative images of immunofluorescence in U-2 OS cells transfected with siLuc or siRECQ1, untreated or treated with CPT (100 nM) and/or Olaparib (10 μM), and stained for γH2AX and 53BP1. Nuclei were stained with Toto3 and merged fluorescence images are shown (**b**) Average number of γH2AX foci per cell and the average fraction (shaded) of γH2AX foci colocalizing with 53BP1. At least 35 cells were scored for each dataset. Error bars, s.e.m.

3.5 RECQ1 is essential for fork restart upon Top1 poisoning

The fact that RECQ1 loss makes PARP activity dispensable to prevent fork slowing and DSB formation in CPT-treated cells suggests that there may be accumulation of regressed forks in RECQ1-depleted cells [117]. This is in agreement with our biochemical results that suggest a role for RECQ1 in regressed fork restart. In order to provide more direct evidence for this idea we used electron microscopy (EM), one of the most powerful techniques to visualize the fine architecture of *in vivo* replication intermediates [279]. Previous EM analysis of replication intermediates showed that replication forks undergo rapid fork reversal upon Top1 inhibition [117]. Furthermore, PARP1 activity has been shown to be required for effective fork reversal, possibly by promoting the accumulation/stabilization of regressed replication forks and thus preventing fork collision with a CPT-induced lesion to generate a DSB. To test the hypothesis that there might be an accumulation of reversed forks in RECQ1-depleted CPT-treated cells, we performed EM experiments using RECQ1-depleted CPT-treated U-2 OS cells with or without PARP inhibition (Figure 3.25a and 3.25b). Consistent with previous findings, we observed a high frequency of fork reversal (approximately 30% of molecules analyzed) in U-2 OS cells transfected with a control (siRNA-Luc) siRNA and treated with 25 nM CPT. The same experiments performed in the presence of Olaparib confirmed that PARP inhibition in control cells markedly decreased the fraction of reversed forks from 30% to less than 10%. RECQ1 depletion upon CPT treatment resulted in a higher frequency of fork reversal events (approximately 44%) than in control cells. Most importantly, PARP inactivation in RECQ1-depleted cells did not result in a marked reduction in the fraction of regressed forks, suggesting that regressed forks are not restarted in the absence of PARP activity upon RECQ1 inactivation. To test this hypothesis directly, we performed recovery experiments and measured reversed fork frequency after CPT removal. While in control cells drug removal resulted in a marked decrease in the frequency of fork reversal (from 30 to 10%), RECQ1-depleted cells maintained a high frequency of reversed forks (approximately 33%) 3 hours after CPT withdrawal. These data strongly suggest that RECQ1 is needed to restart reversed forks and indicate that PARP requirement to observe CPT-induced reversed forks uniquely reflects its role in limiting RECQ1-mediated fork reactivation.

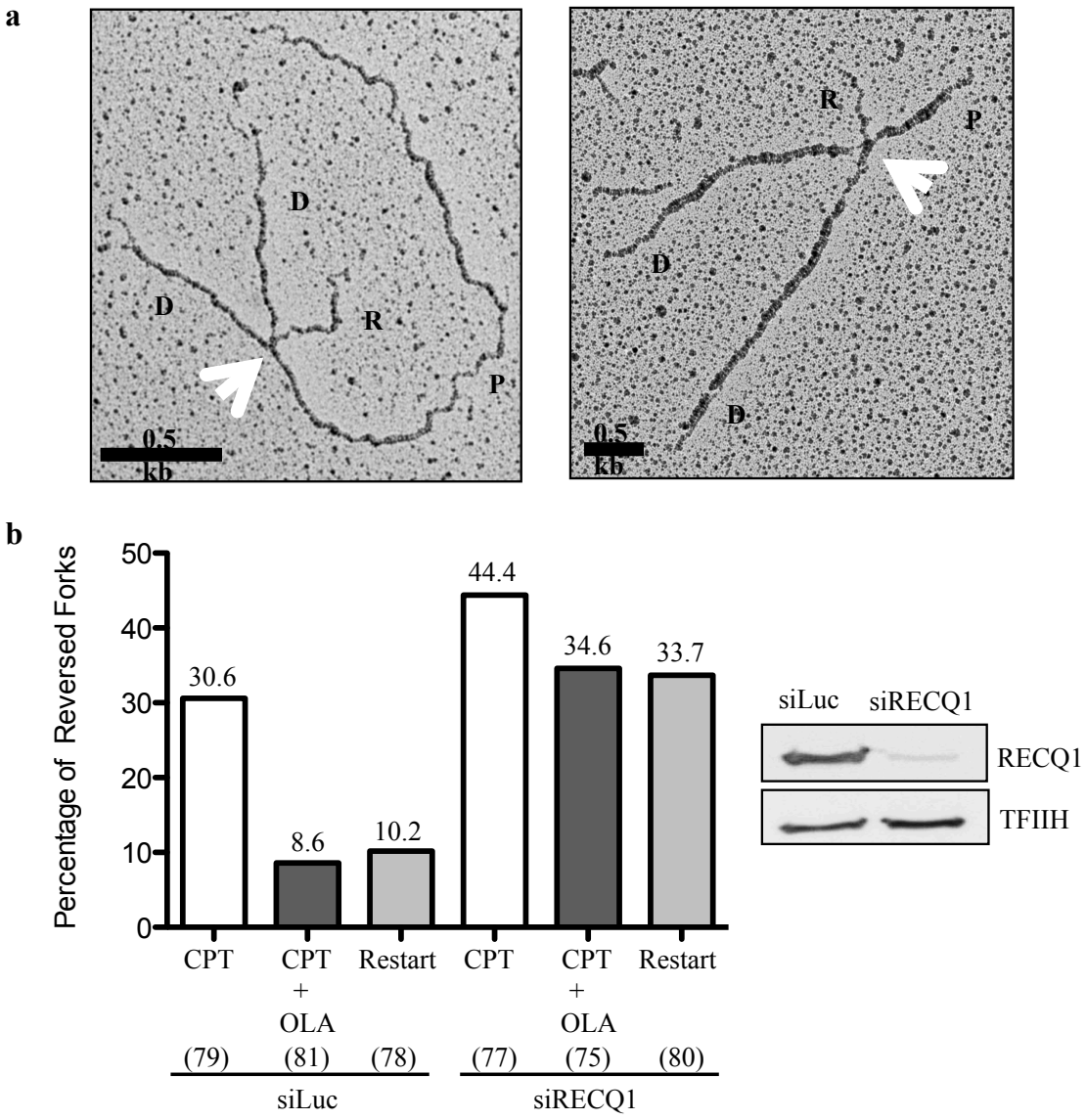

Figure 3.25. Reversed forks accumulate and are unable to restart in RECQ1-depleted cells after CPT treatment. (**a**) Representative electron micrograph of a reversed fork observed on genomic DNA from U-2 OS cells transfected with siRECQ1 and treated with CPT (25 nM) and Olaparib (10 μM). The white arrow points to the four-way junction at the replication fork. D = Daughter strand, P = Parental strand, R = Reversed arm. (**b**) Left, frequency of fork reversal in U-2 OS cells transfected either with siLuc or siRECQ1 and treated with CPT and/or Olaparib (OLA). Restart experiments measuring the frequency of fork reversal were performed 3 hours after CPT removal. Numbers above bars indicate proportion of reversed forks as a percentage of total number of molecules (bottom, parentheses). Right, RECQ1 expression after siRNA knockdown detected by western blotting. TFIIH was detected as loading control.

3.6 Role of Homologous Recombination in the restart of CPT-damaged replication forks upon RECQ1 depletion and/or PARP1 inhibition

DSBs are the major cellular events leading to cell death following DNA replication stress. On the basis of our discovery that PARP1 activation prevents DSB formation upon CPT treatment by limiting RECQ1-mediated fork restart, we would predict that RECQ1 depletion should partially rescue the cellular hypersensitivity to combined Top1 and PARP inhibition. Unexpectedly, PARP inhibition results in an increased CPT sensitivity of RECQ1-depleted U-2 OS cells relative to the control measured by colony forming assays (Figure 3.26).

In order to better understand the molecular basis of this result, we first analyzed the formations of RAD51 foci on γH2AX-positive cells by indirect immunofluorescence. Homologous recombination is the elective pathway that cells use to deal with replicative damage, and HR-defective cells are extremely sensitive to Top1 inhibition [286]. The formation of long RAD51 nucleofilaments (several kilobases) during the first step of HRR results in chromatin-associated foci that can be cytologically detected and quantified as read-out of ongoing recombination repair [287]. On the other hand, DSB-independent assembly of RAD51 on DNA, as in the case of stalled replication fork protection, does not trigger visible foci formation, perhaps because of the shorter nature of the RAD51-ssDNA filament (less than 1 kilobase) [258]. Our immunofluorescence analysis showed that the short treatment (1 hour) with low doses of CPT (25 nM and 100 nM) used in this study trigger only a moderate increase of RAD51 foci in siLuc-transfected U-2 OS cells, confirming again the notion that there is a low level of DSBs generated by clinical relevant CPT doses under normal conditions. In contrast, RECQ1 depletion leads to a significant increase in RAD51 foci (Figure 3.27a), particularly in the experiment performed 3 hours after removal of CPT (Figure 3.27b). These evidences challenge the dogma that RAD51 foci are strictly associated with DSB repair centers during S-phase (see Discussion).

On the other hand, CPT-induced RAD51 foci markedly decreased both in wild type and RECQ1-depleted cells upon PARP inhibition. Interestingly, PARP1 is known to be implicated in Mre11-mediated DNA resection and RPA/RAD51 foci formation upon DSB formation induced by long HU exposure (12-24 hours) [256]. Collectively, these findings indicate that RECQ1 is important to restart CPT-induced regressed forks in a non-

recombinogenic way, whereas its depletion leads to RAD51-mediated processing of these replicative structures. The role of PARP1 in this process is more intricate: in a first attempt, its PARylation activity coordinates the processes of fork reversal to avoid DSB formation by controlling the non-recombinogenic RECQ1-mediated restart of CPT-damaged forks; if this mechanism fails (as in the absence of RECQ1), PARP1 might be required for the proper establishment of HR-mediated replication fork repair/restart. Intriguingly, PARP1 activity is enhanced in RECQ1 depleted cells both under genotoxic stress and normal conditions (data not shown). Further experiments will be necessary to elucidate the role of PARP1 in this context and clarify the molecular basis of the synergistic toxicity of PARP inhibitors with Top1 poisons.

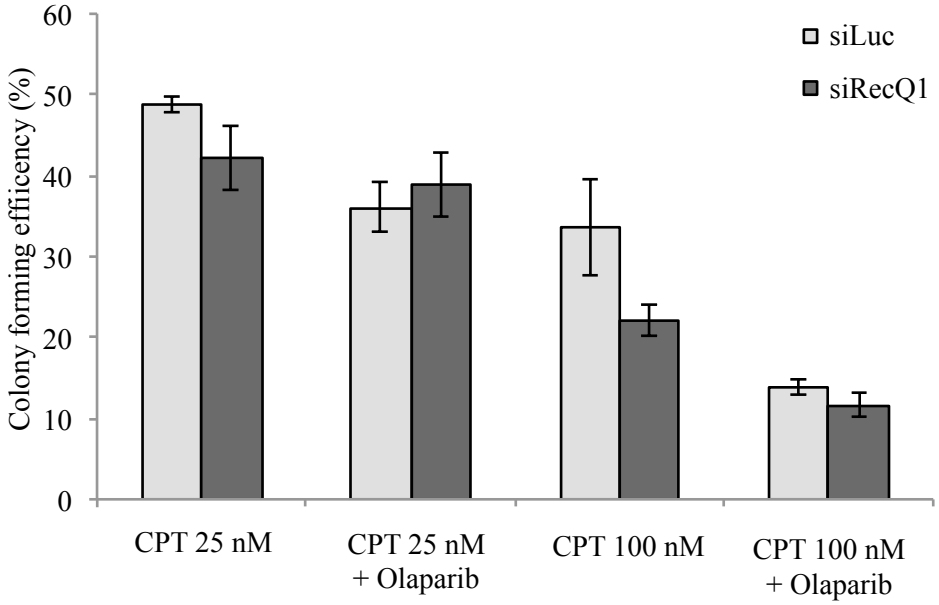

Figure 3.26. CPT sensitivity of RECQ1 depleted and/or PARP1 inhibited U-2 OS cells. The Y-axis shows colony formation efficiency (percentage) of U-2 OS cells expressing a RECQ1 shRNA or Luc shRNA relative to untreated control following treatment with CPT (25 or 100 nM, 16 hrs) and 10 uM Olaparib. Results from three independent experiments. Error bars, s.e.m.

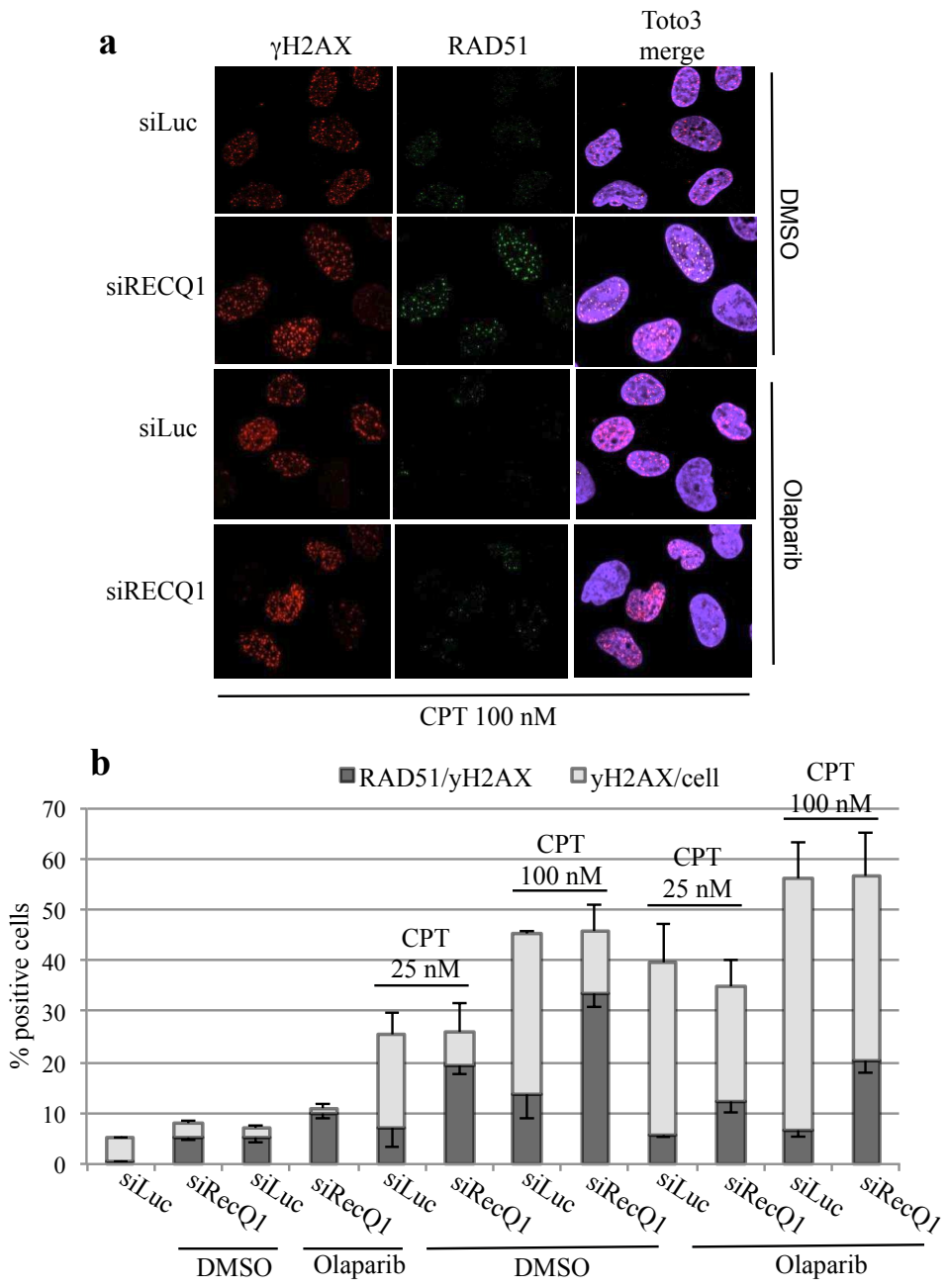

Figure 3.27. RAD51 and γH2AX colocalization at CPT-damaged replication forks upon RECQ1 depletion and/or PARP1 inhibition. (**a**) Representative images of immunofluorescence in U-2 OS cells transfected with siLuc or siRECQ1, untreated or treated with 25 (not shown) or 100 nM CPT for 1 hour, with 10 μM Olaparib or DMSO and stained for chromatin-bound γH2AX and RAD51 after detergent extraction and fixation. Nuclei were stained with Toto3 and merged fluorescence images are showed. (**b**) Results show the percentage of γH2AX positive cells and the RAD51/γH2AX double-positive cells (shaded). Cells with > 9 foci were counted as positive. At least 200 nuclei were scored per treatment in each experiment. Results from three independent experiments. Error bars, s.e.m.

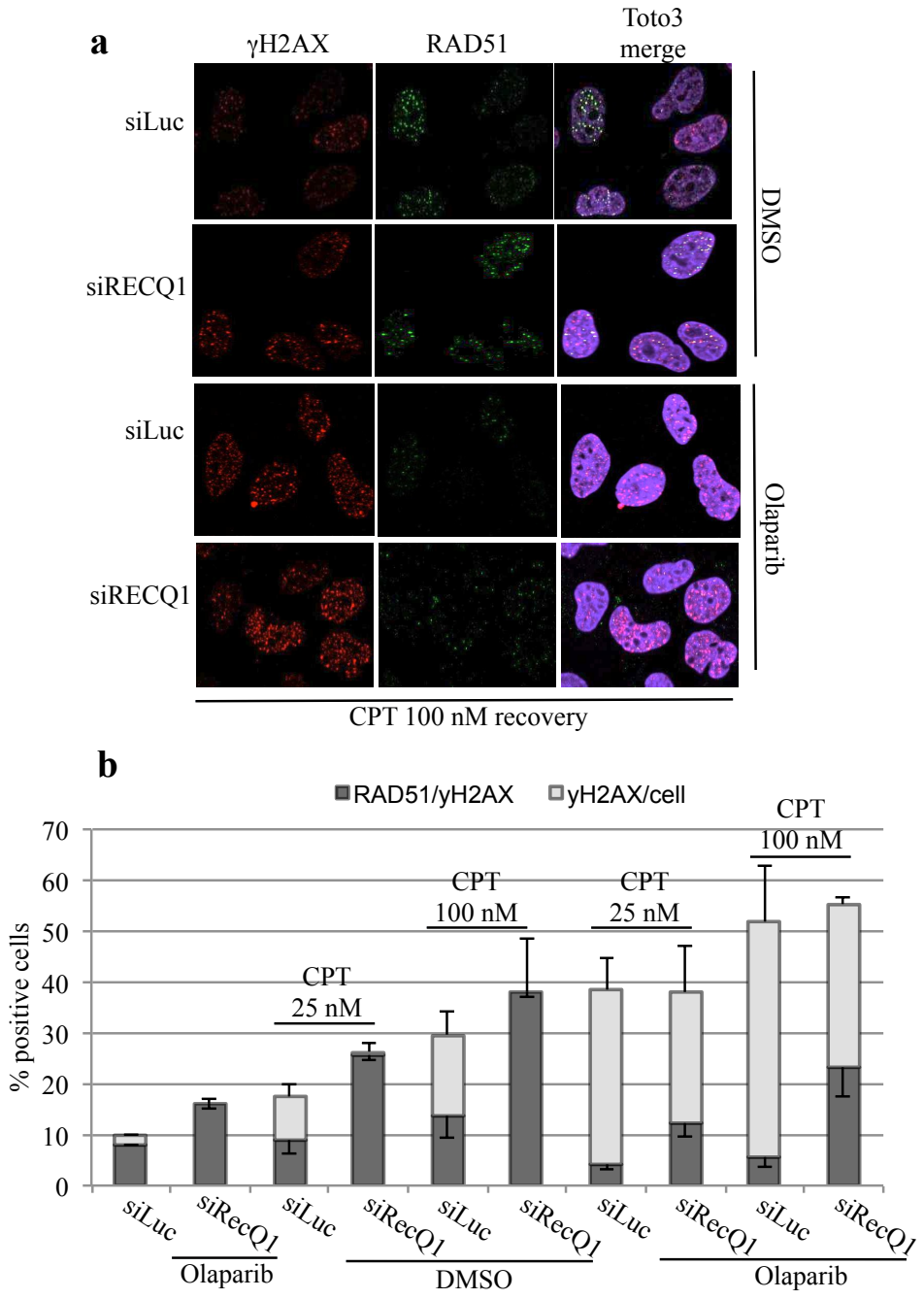

Figure 3.28. RAD51 and γH2AX colocalization at CPT-damaged replication forks upon RECQ1 depletion and/or PARP1 inhibition. (**a**) Representative images of immunofluorescence in U-2 OS cells transfected with siLuc or siRECQ1, untreated or treated with 25 (not shown) or 100 nM CPT for 1 hour, with 10 μM Olaparib or DMSO and stained for chromatin-bound γH2AX and RAD51 after 3 hrs release in fresh medium containing Olaparib or DMSO, detergent extraction and fixation. Nuclei were stained with Toto3 and merged fluorescence images are showed. (**b**) Results show the percentage of γH2AX positive cells and the RAD51/γH2AX double-positive cells (shaded). Cells with > 9 foci were counted as positive. At least 200 nuclei were scored per treatment in each experiment. Results from three independent experiments. Error bars, s.e.m.

4 DISCUSSION

Replication fork regression is rapidly emerging as a pivotal mechanism of replication stress response. Preliminary studies performed in bacteria have underlined the importance of this process for the restart of damaged DNA replication forks more than 30 years ago [73]. Conceptually, the mechanism of fork regression and restart has been suggested to aid the cells overcoming replication stress in at least three ways. First, pairing of the nascent strands allows error free bypass of template damage by repositioning the lesion in a double-stranded DNA structure that will facilitate its repair. Second, the lesion is simply skipped and DNA synthesis primed ahead. Third, the backward migration of the branch point of a replication fork impedes the collision with breaks and/or roadblocks, providing the necessary room and time for the repair machinery to be recruited on and to fix the lesions. Despite these speculations, EM analysis of replication intermediates performed in *S. cerevisiae* have shown that regressed forks, along with aberrant structures such as gaps and partially replicated molecules, accumulate upon HU treatment only in a checkpoint-deficient background. The authors interpreted the formation of regressed forks as the pathological destabilization of stalled replication forks in absence of a functional checkpoint. Under these conditions, the reversed forks collapsed and were unable to restart, leading to chromosome aberrations and cell death [26]. Moreover, recent studies demonstrated that HU-induced fork reversal is counteracted by the Dna2 nuclease activity in *S. pombe*, which, under the checkpoint-mediated phosphorylation control, cleaves single-strand flaps that dissociate from the nascent strand to form a reversed fork [121]. These notions lead to the idea that regressed forks merely represent pathological structures in yeast arising from destabilization of stalled forks. On the other hand, recent studies showed that Top1 inhibition induces replication fork slowing and reversal in a process that prevents double-strand break formation at clinically relevant CPT doses [117]. This is the first evidence that fork reversal occurs also in mammalian cells and, more importantly, it represents a physiological controlled process that contribute to maintain genomic integrity upon fork blockage. A crucial cellular mediator required to accumulate/stabilize regressed forks upon Top1 poisoning is PARP1. PARP1 itself is a target for anticancer therapies, most conspicuously in *BRCA*-mutant breast and ovarian cancers [118]. Moreover, PARP inhibition

leads to increased sensitivity to a broad range of chemotherapeutics, such as alkylating agents or different camptothecin derivatives, and combinatorial therapies are under clinical trials [288]. PARP activation at CPT-damaged replication forks promotes the accumulation of regressed forks in a checkpoint- and recombination-independent manner [117]. However, the mechanism by which PARP activity promotes fork reversal is still unknown, and the requirements for the restart of reversed forks have not been defined.

The work reported in this thesis provides answers to all these questions. First, our results show that regressed forks can restart *in vivo* and identify a key role for human RECQ1 in promoting efficient replication fork restart after Top1 inhibition by virtue of its helicase/branch migration activities. Importantly, our results also show that this is a specific function of RECQ1 not shared by other helicases, such as BLM and WRN. Furthermore, our results provide new insight into the molecular role of PARP in fork reversal by showing that the poly(ADP-ribosyl)ation activity of PARP is important to regulate RECQ1 activity on replication forks after CPT treatment.

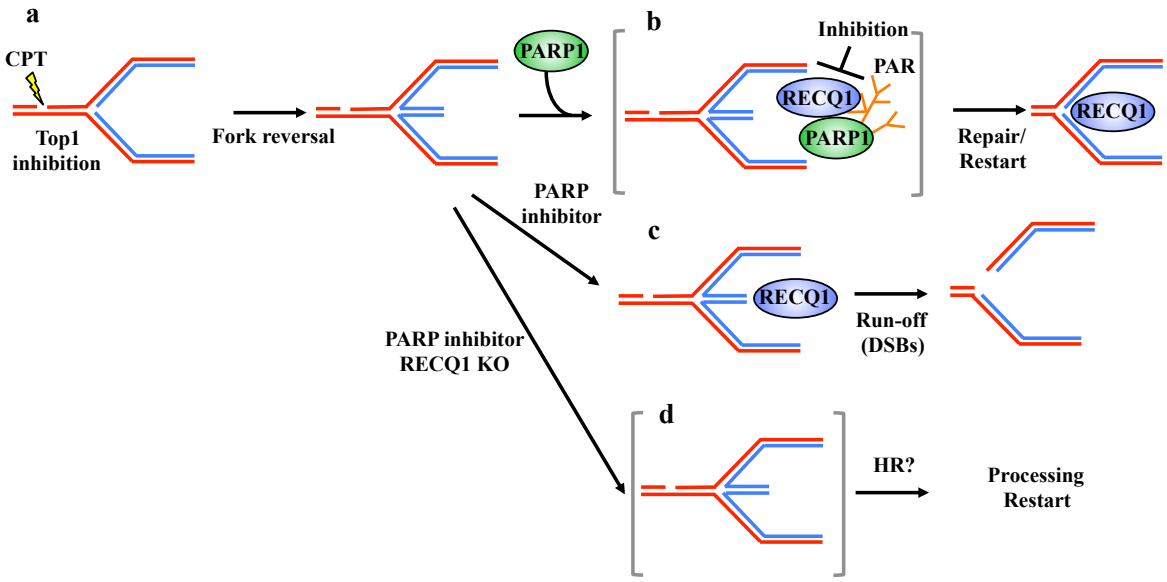

Figure 4.1. Schematic model of the combined roles of PARP1 and RECQ1 in response to Top1 inhibition. (**a**), (**b**) PARP poly(ADPribosyl)ation activity is not required to form reversed forks, but it promotes the accumulation of regressed forks by inhibiting RECQ1 fork restoration activity, thus preventing premature restart of the regressed forks. (**c**) Inhibition of PARP activity leads to replication run-off and increased DSBs formation upon Top1 inhibition, as RECQ1 can cause untimely restart of reversed fork. (**d**) PARP activity is no longer required in RECQ1-depleted cells were regressed forks accumulate because the cells lack the enzyme (RECQ1) necessary to promote fork restart. Homologous recombination (HR) might be required to promote fork restart in the absence of RECQ1 and PARP activity.

An intriguing aspect of these data is that PARP activity does not appear to be required to form reversed forks (Figure 4.1a), but rather to "accumulate" them, that is to maintain/protect them from a counteracting activity (RECQ1), which would otherwise restart reversed forks untimely, before Top1-DNA complex removal, leading to DSB formation (Figure 4.1c). Indeed, we show that, differently from control cells, PARP activity is dispensable to accumulate reversed forks and to avoid CPT-induced DSB in RECQ1 depleted cells (Figure 4.1d). We propose that PARP "signals" the presence of lesions on the template and inhibits locally RECQ1 thereby restraining the restart of reversed forks until Top1cc repair is complete. After the damage gets fixed, PARP1 is not longer activated and PARG-mediated PAR degradation might be responsible to set RECQ1 free to reset a functional replication fork (Figure 4.1b).

Which are the actors that might be required to promote fork regression rather than restart is still an open question, and a large number of helicases/translocases has been shown to catalyze this reaction *in vitro*. However, the particular structure of the stalled replication forks generated upon treatment with different types of genotoxic agents might dictate the differential requirement of motor enzymes to promote this reaction. Top1 inhibition by CPT derivatives was shown to trigger fork slowing due to the accumulation of positive supercoils ahead of the advancing replisome [115]. In this context, the torsional force can potentially drive spontaneous fork regression without the need of any specific factor to actively promote this reaction, as previously suggested by *in vitro* studies [105]. Moreover, little ssDNA is expected to form at these stalled structures since there should not be any polymerase-helicase uncoupling, ruling out an immediate checkpoint involvement as in the case of HU or UV treatment. Several evidences suggest indeed that CPT-induced fork slowing and reversal could result from local accumulation of torsional stress in vertebrates. First, Brdu Chip-chip analysis of synchronized, CPT-treated *S. cerevisiae* cells has been used to show that fork slowing and reversal are more frequent at chromosomal locations that are particularly susceptible to topological stress, such as highly transcribed or termination zones [117]. Indeed, Top1 was shown to prevent the genomic instability arising from the interference between transcription and replication [289]. Second, the checkpoint signals prevent the accumulation of reversed forks that arise as a consequence of torsional stress generated ahead of replication forks encountering transcribed genes in budding yeast,

by releasing their tethering to nuclear pores [108]. The same group was able to show a checkpoint-independent accumulation of cruciform structures by genetic inactivation of Top1 and Top2 [108]. Collectively, these findings suggest that fork reversal can occur spontaneously as a thermodynamic favorable event to dissipate the torsional stress accumulating ahead of the advancing replisome following Top1 inhibition.

In addition to CPT derivatives, oxidative or alkylating modifications of DNA were shown to trap Top1-DNA covalent complexes by perturbing the correct positioning of the two ends of the SSB, thus impeding the religation step [290, 291, 292]. Intriguingly, co-IP experiments showed that RECQ1-PARP1 interaction increases not only after Top1 inhibition, but also upon MMS and H_2O_2 treatment. Moreover MMC, an interstrand cross-linking agent that blocks replication impeding fork unwinding, increases RECQ1-PARP1 association as well. On the contrary, we were not able to observe an increased interaction between RECQ1 and PARP1 upon HU or aphidicolin treatment (data not shown). This result is unlikely to be due to a poor PARP1 activation since it has been already shown that PARP is activated *in vitro* and *in vivo* by HU-stalled forks to promote HR repair [256]. The fact that the interaction between RECQ1 and PARP1 is conserved in the presence of different genotoxic agents suggests that these two factors play a conserved role in mediating fork reversal and restart upon treatment with all these drugs. However, the RECQ1-PARP1 pathway might be regulated by different factors or events such as protein-protein interactions and post-translational modifications, depending on the particular structure of the stalled fork. For example, lysine acetylation is a mechanism that prevents PAR-protein binding by shielding the positive interacting surface, and thus introducing a further layer of regulation to PARP1-mediated signaling than the simple PARG-mediated PAR degradation [293]. Recently, RECQ1 was shown to be acetylated at two lysines located on its WH domain following etoposide treatment [294]; the WH domain is also crucial for RECQ1 interaction with PAR/PARP1 as demonstrated from this work. An intriguing possibility is that RECQ1 acetylation prevents PAR binding, counteracting the inhibitory effect on its branch migration activity. Further experiments are needed to prove this hypothesis and/or to identify factors that modulate the activities of RECQ1 and PARP in fork reversal and restart.

Our results also provide new data on the biological processes in which PARP1 is involved to maintain the genome stability. Poly(ADP-ribose) is a flexible, short-life modification which not only acts as chromatin docking site for protein recruitment, but, due to its negatively charged nature, can modify the biochemical properties of proteins, such as their affinity for DNA and RNA or their ability to interact with other proteins [231]. In our case, PAR formation is important to recruit and concentrate RECQ1 molecules on CPT-damaged replicative chromatin, and to keep them in an "inactive" state. Indeed, PAR inhibits RECQ1 oligomeric association with DNA, possibly preventing the interaction of the WH domain, with DNA or with other RECQ1 molecules. For this reason, it is possible that PAR inhibits the fork restoration activity of RECQ1 by preventing RECQ1 oligomer association with structured DNA, which has been previously proved to be critical for the branch migration activity of RECQ1 [128, 135]. Further investigation will be needed to validate this hypothesis.

RecQ helicases are DNA unwinding enzymes essential for the maintenance of genome stability in many organisms [122]. Why human cells should encode five RecQ homologs, while microorganisms like *E. coli, S. cerevisiae,* and *S. pombe* posses only one or two remains unexplained. Our previous studies identified important and distinct roles of RECQ1 and RECQ4 during DNA replication [202]. These data, combined with previous observation that RECQ1 depletion leads to increased DNA damage and affects cellular proliferation [214, 218], suggest that RECQ1 plays a role distinct from the other human RecQ helicases in the stabilization and/or repair of replication forks. Our discovery that RECQ1 is required for replication fork restoration after Top1 poisoning provides the first indication of a specific cellular function for RECQ1. U-2 OS cells lacking BLM or WRN do not show similar defects in replication fork restoration upon Top1 inhibition, suggesting that RECQ1 is the only RecQ helicase responsible to promote replication fork restart upon CPT-induced fork reversal. In agreement with this conclusion, chromatography-fractionated nuclear extract from RECQ1-depleted HEK 293T cells showed impaired HJ branch migration activity *in vitro*; this effect was not recapitulated by the lack of other RecQ helicases, such as WRN and BLM, or other HR enzymes such as RAD54, thus indicating RECQ1 as the major branch migrating protein in human cells [223]. Moreover, RECQ1 shows a striking preference for fork restoration *versus* regression while other helicases/translocases have

been shown to indiscriminately perform both reactions [30, 91, 153, 154]. However, we cannot rule out the possibility as yet that other motor proteins are involved in different steps of the same process.

Important avenues for future studies will be to determine whether reversed forks are detected in response to genotoxic agents other than Top1 inhibitors and whether other helicases are implicated in replication fork reversal and/or restart depending on the particular type of DNA damage. In this regard, WRN- and BLM-deficient cells display increased sensitivity to selected genotoxic agents [295], while RECQ1-deficient cells are markedly sensitive to CPT and etoposide supporting the notion that these three RecQ helicases play distinct roles in replication stress response. The fact that RECQ1-depleted cells show an increased sensitivity to etoposide opens the interesting possibility that a similar mechanism of fork reversal and restart might take place upon treatment with Top2 poisons. EM analysis of replication intermediates after treatment with different classes of chemotherapeutic drugs will provide early clues to the most interesting combinations of drugs and RecQ helicases to pursue in future studies.

The data reported in this thesis also provide new mechanistic insight to predict the efficiency of combinatorial anticancer therapies with PARP and Top1 inhibitors. These combinations are currently in clinical trials [119]. The fact that PARP inhibition is dominant over RECQ1 depletion on Top1 sensitivity is somehow surprising, considering that PARP activity is irrelevant in preventing replisome run-off at Top1cc and DSB formation in absence of RECQ1. A possible explanation is that PARP activity regulates additional biological processes associated with Top1 poisoning in addition to fork reversal and restart, such as Top1-DNA covalent complex removal [296], chromatin remodeling [240, 241] or even proper establishment of the HRR [256]. Indeed a genome-wide siRNA screen on HeLa cells has identified PARP1 as one of the genes, along with key recombination factors, displaying the strongest sensitive phenotype upon camptothecin exposure [286]. Several groups have previously shown that in chicken DT40 cells PARP1 activity is essential to counteract the toxic engagement of NHEJ in repairing DSBs arising from replication failure, likely by decreasing the strong affinity for DNA of Ku heterodimer through its poly(ADP-ribosyl)ation, and thus channelling the repair to the HR pathway [259, 260, 261]. Indeed increasing evidences suggest a conserved, inhibitory/competitive role of Ku for HRR [297,

[298]; in the absence of PARP activity unrestricted binding of Ku70/86 heterodimer to DSBs arising from replication fork breakage might prevent access to the end resection machinery required to generate a proper 5'-ssDNA for RAD51 loading, and/or trigger aberrant fusion of breaks located in different chromosomes. Given the particular structure of a regressed fork, the double-stranded end (DSE) of its extruded arm might be recognized by different DNA repair factors as a broken chromosome. Hence, PARP1 activity would be crucial to avoid aberrant NHEJ repair and allow the proper HR-mediated processing of reversed forks. In agreement with this conclusion, we observed a significant decrease of RAD51 foci formation upon Top1 and PARP inhibition, even in the absence of RECQ1. In this regard, it is also important to mention that Ku heterodimer was identified by mass spectrometry as one of the most abundant factors present the RECQ1 complex. Defining the role of the Ku heterodimer and HRR in the process of PARP1/RECQ1-mediated fork regression and restart is an essential topic for future investigations.

Our results also suggest that RECQ1 itself might represent a new target to be exploited in conjunction with Top1 for chemotherapy. Inducing fork reversal (Top1 poisons) and inhibiting reversed fork reactivation (RECQ1 depletion) is expected to synergize, explaining the observed CPT-sensitivity of RECQ1-depleted cells. RECQ1 is overexpressed in several kinds of tumors [214] and its depletion has been show to trigger mitotic catastrophe specifically in cancer cells [219]. One explanation might be the inability of RECQ1 depleted cells to restart reversed forks produced by chemotherapeutics or simply by oncogene-induced transcriptional perturbation of DNA replication and complete the DNA synthesis, thus leading to this form of mitotic apoptosis.

In last analysis, we showed that RECQ1 depletion leads to a dramatic increase in RAD51 foci formation upon Top1 inhibition, suggesting that the RECQ1-mediated mechanism of fork restart is a way to process reversed replication forks in a safe, non-recombinatorial way. Increasing evidences suggest that HRR can be considered as a "double-edged sword" and, even if crucial for completing DNA synthesis and guarantying cell survival upon replication stress, it represents an error-prone process that leads to complex genomic rearrangements, particularly due to the high content of repetitive sequences in mammalian genome [299, 300, 301, 302]. This aspect is particularly relevant for highly proliferating cancer cells, which depend on this pathway to deal with their constitutive replication stress at the

expense of genomic stability, thus acquiring mutations that further fuel their oncogenic potential. Therefore, cells have evolved specific mechanisms to overcome replication damage without the need of the HR pathway. Failure of such processes channels the repair of damaged replication forks into a potentially harmful homology-directed repair. In such a scenario, RECQ1 depletion triggers to an unscheduled accumulation of regressed replication forks, which are subsequently taken over and processed in a recombinogenic way, thus switching the nature of these structures from physiological to potentially pathological. Our preliminary findings confirm that regressed forks, if not properly restarted, represent indeed a recombinogenic substrate, as previously suggested for yeast [26]. Moreover seminal studies performed in prokaryotic cells have shown an extensive involvement of HR factors in the fork reversal/resetting process [75]. Due to the particular structure of a regressed fork which arbors a four way junction and a double-stranded end, it remains to verify if HRR can directly acts on these structures, or if the junction need to be processed by other factors, such as by selective-substrate endonucleases like Mus81-Eme1 or Slx1-SLx4, in order to recreate an one-side DSB. Our experimental findings such as accumulation of regressed forks and RAD51 foci formation in the absence of DSBs upon CPT treatment of RECQ1-depleted cells, favor for the first hypothesis and suggest the loading of RAD51 on the extruded arm of a regressed fork, probably upon proper 5'-3' resection, without the need of a DSB. Consistently, RAD51 was shown to be loaded on replication forks stalled by interstrand cross-linking agents, before the DSB formation mediated by FANCD2 and specific endonucleases [303]. All together these preliminary results open up new avenues of research on the HR-mediated mechanism of regressed fork processing in mammalian cells. More importantly, unscheduled accumulation of regressed forks upon RECQ1 depletion or inhibition might result in synthetic lethality in a HR-deficient background, thus providing a novel way to target and increase the efficacy of cancer therapies in HR-defective or -inhibited tumors.

REFERENCES

1. Negrini, S., V.G. Gorgoulis and T.D. Halazonetis, *Genomic instability--an evolving hallmark of cancer.* Nat Rev Mol Cell Biol, 2010. **11**(3): p. 220-8.
2. Bartkova, J., Z. Horejsi, K. Koed, A. Kramer, F. Tort, K. Zieger, P. Guldberg, M. Sehested, J.M. Nesland, C. Lukas, T. Orntoft, J. Lukas and J. Bartek, *DNA damage response as a candidate anti-cancer barrier in early human tumorigenesis.* Nature, 2005. **434**(7035): p. 864-70.
3. Gorgoulis, V.G., L.V. Vassiliou, P. Karakaidos, P. Zacharatos, A. Kotsinas, T. Liloglou, M. Venere, R.A. Ditullio, Jr., N.G. Kastrinakis, B. Levy, D. Kletsas, A. Yoneta, M. Herlyn, C. Kittas and T.D. Halazonetis, *Activation of the DNA damage checkpoint and genomic instability in human precancerous lesions.* Nature, 2005. **434**(7035): p. 907-13.
4. Di Micco, R., M. Fumagalli, A. Cicalese, S. Piccinin, P. Gasparini, C. Luise, C. Schurra, M. Garre, P.G. Nuciforo, A. Bensimon, R. Maestro, P.G. Pelicci and F. d'Adda di Fagagna, *Oncogene-induced senescence is a DNA damage response triggered by DNA hyper-replication.* Nature, 2006. **444**(7119): p. 638-42.
5. Lord, C.J. and A. Ashworth, *The DNA damage response and cancer therapy.* Nature, 2012. **481**(7381): p. 287-94.
6. Bouwman, P. and J. Jonkers, *The effects of deregulated DNA damage signalling on cancer chemotherapy response and resistance.* Nat Rev Cancer, 2012. **12**(9): p. 587-98.
7. Machida, Y.J., J.L. Hamlin and A. Dutta, *Right place, right time, and only once: replication initiation in metazoans.* Cell, 2005. **123**(1): p. 13-24.
8. Bell, S.P. and A. Dutta, *DNA replication in eukaryotic cells.* Annu Rev Biochem, 2002. **71**: p. 333-74.
9. Wohlschlegel, J.A., B.T. Dwyer, S.K. Dhar, C. Cvetic, J.C. Walter and A. Dutta, *Inhibition of eukaryotic DNA replication by geminin binding to Cdt1.* Science, 2000. **290**(5500): p. 2309-12.
10. Diffley, J.F., *Quality control in the initiation of eukaryotic DNA replication.* Philos Trans R Soc Lond B Biol Sci, 2011. **366**(1584): p. 3545-53.
11. Im, J.S., S.H. Ki, A. Farina, D.S. Jung, J. Hurwitz and J.K. Lee, *Assembly of the Cdc45-Mcm2-7-GINS complex in human cells requires the Ctf4/And-1, RecQL4, and Mcm10 proteins.* Proc Natl Acad Sci U S A, 2009. **106**(37): p. 15628-32.
12. Abdurashidova, G., S. Radulescu, O. Sandoval, S. Zahariev, M.B. Danailov, A. Demidovich, L. Santamaria, G. Biamonti, S. Riva and A. Falaschi, *Functional interactions of DNA topoisomerases with a human replication origin.* EMBO J, 2007. **26**(4): p. 998-1009.
13. Bermejo, R., Y. Doksani, T. Capra, Y.M. Katou, H. Tanaka, K. Shirahige and M. Foiani, *Top1- and Top2-mediated topological transitions at replication forks ensure fork progression and stability and prevent DNA damage checkpoint activation.* Genes Dev, 2007. **21**(15): p. 1921-36.
14. Tan, B.C., C.T. Chien, S. Hirose and S.C. Lee, *Functional cooperation between FACT and MCM helicase facilitates initiation of chromatin DNA replication.* EMBO J, 2006. **25**(17): p. 3975-85.

15. Groth, A., A. Corpet, A.J. Cook, D. Roche, J. Bartek, J. Lukas and G. Almouzni, *Regulation of replication fork progression through histone supply and demand.* Science, 2007. **318**(5858): p. 1928-31.
16. Branzei, D. and M. Foiani, *Maintaining genome stability at the replication fork.* Nat Rev Mol Cell Biol, 2010. **11**(3): p. 208-19.
17. Heller, R.C. and K.J. Marians, *Replisome assembly and the direct restart of stalled replication forks.* Nat Rev Mol Cell Biol, 2006. **7**(12): p. 932-43.
18. Woodward, A.M., T. Gohler, M.G. Luciani, M. Oehlmann, X. Ge, A. Gartner, D.A. Jackson and J.J. Blow, *Excess Mcm2-7 license dormant origins of replication that can be used under conditions of replicative stress.* J Cell Biol, 2006. **173**(5): p. 673-83.
19. Ge, X.Q., D.A. Jackson and J.J. Blow, *Dormant origins licensed by excess Mcm2-7 are required for human cells to survive replicative stress.* Genes Dev, 2007. **21**(24): p. 3331-41.
20. Ibarra, A., E. Schwob and J. Mendez, *Excess MCM proteins protect human cells from replicative stress by licensing backup origins of replication.* Proc Natl Acad Sci U S A, 2008. **105**(26): p. 8956-61.
21. Katou, Y., Y. Kanoh, M. Bando, H. Noguchi, H. Tanaka, T. Ashikari, K. Sugimoto and K. Shirahige, *S-phase checkpoint proteins Tof1 and Mrc1 form a stable replication-pausing complex.* Nature, 2003. **424**(6952): p. 1078-83.
22. Murga, M., S. Bunting, M.F. Montana, R. Soria, F. Mulero, M. Canamero, Y. Lee, P.J. McKinnon, A. Nussenzweig and O. Fernandez-Capetillo, *A mouse model of ATR-Seckel shows embryonic replicative stress and accelerated aging.* Nat Genet, 2009. **41**(8): p. 891-8.
23. Zou, L. and S.J. Elledge, *Sensing DNA damage through ATRIP recognition of RPA-ssDNA complexes.* Science, 2003. **300**(5625): p. 1542-8.
24. Lopez-Contreras, A.J. and O. Fernandez-Capetillo, *The ATR barrier to replication-born DNA damage.* DNA Repair (Amst), 2010. **9**(12): p. 1249-55.
25. Lopes, M., M. Foiani and J.M. Sogo, *Multiple mechanisms control chromosome integrity after replication fork uncoupling and restart at irreparable UV lesions.* Mol Cell, 2006. **21**(1): p. 15-27.
26. Sogo, J.M., M. Lopes and M. Foiani, *Fork reversal and ssDNA accumulation at stalled replication forks owing to checkpoint defects.* Science, 2002. **297**(5581): p. 599-602.
27. Errico, A. and V. Costanzo, *Mechanisms of replication fork protection: a safeguard for genome stability.* Crit Rev Biochem Mol Biol, 2012. **47**(3): p. 222-35.
28. Chapman, J.R., M.R. Taylor and S.J. Boulton, *Playing the end game: DNA double-strand break repair pathway choice.* Mol Cell, 2012. **47**(4): p. 497-510.
29. Heyer, W.D., K.T. Ehmsen and J. Liu, *Regulation of homologous recombination in eukaryotes.* Annu Rev Genet, 2010. **44**: p. 113-39.
30. Gari, K., C. Decaillet, M. Delannoy, L. Wu and A. Constantinou, *Remodeling of DNA replication structures by the branch point translocase FANCM.* Proc Natl Acad Sci U S A, 2008. **105**(42): p. 16107-12.
31. Prakash, R., D. Satory, E. Dray, A. Papusha, J. Scheller, W. Kramer, L. Krejci, H. Klein, J.E. Haber, P. Sung and G. Ira, *Yeast Mph1 helicase dissociates Rad51-made*

D-loops: implications for crossover control in mitotic recombination. Genes Dev, 2009. **23**(1): p. 67-79.
32. Sun, W., S. Nandi, F. Osman, J.S. Ahn, J. Jakovleska, A. Lorenz and M.C. Whitby, *The FANCM ortholog Fml1 promotes recombination at stalled replication forks and limits crossing over during DNA double-strand break repair.* Mol Cell, 2008. **32**(1): p. 118-28.
33. Hashimoto, Y., F. Puddu and V. Costanzo, *RAD51- and MRE11-dependent reassembly of uncoupled CMG helicase complex at collapsed replication forks.* Nat Struct Mol Biol, 2012. **19**(1): p. 17-24.
34. Smith, C.E., B. Llorente and L.S. Symington, *Template switching during break-induced replication.* Nature, 2007. **447**(7140): p. 102-5.
35. Llorente, B., C.E. Smith and L.S. Symington, *Break-induced replication: what is it and what is it for?* Cell Cycle, 2008. **7**(7): p. 859-64.
36. Deem, A., A. Keszthelyi, T. Blackgrove, A. Vayl, B. Coffey, R. Mathur, A. Chabes and A. Malkova, *Break-induced replication is highly inaccurate.* PLoS Biol, 2011. **9**(2): p. e1000594.
37. Mimitou, E.P. and L.S. Symington, *DNA end resection--unraveling the tail.* DNA Repair (Amst), 2011. **10**(3): p. 344-8.
38. Chen, L., C.J. Nievera, A.Y. Lee and X. Wu, *Cell cycle-dependent complex formation of BRCA1.CtIP.MRN is important for DNA double-strand break repair.* J Biol Chem, 2008. **283**(12): p. 7713-20.
39. Huertas, P., F. Cortes-Ledesma, A.A. Sartori, A. Aguilera and S.P. Jackson, *CDK targets Sae2 to control DNA-end resection and homologous recombination.* Nature, 2008. **455**(7213): p. 689-92.
40. Pierce, A.J., P. Hu, M. Han, N. Ellis and M. Jasin, *Ku DNA end-binding protein modulates homologous repair of double-strand breaks in mammalian cells.* Genes Dev, 2001. **15**(24): p. 3237-42.
41. Zhu, Z., W.H. Chung, E.Y. Shim, S.E. Lee and G. Ira, *Sgs1 helicase and two nucleases Dna2 and Exo1 resect DNA double-strand break ends.* Cell, 2008. **134**(6): p. 981-94.
42. Mimitou, E.P. and L.S. Symington, *Sae2, Exo1 and Sgs1 collaborate in DNA double-strand break processing.* Nature, 2008. **455**(7214): p. 770-4.
43. Cejka, P., E. Cannavo, P. Polaczek, T. Masuda-Sasa, S. Pokharel, J.L. Campbell and S.C. Kowalczykowski, *DNA end resection by Dna2-Sgs1-RPA and its stimulation by Top3-Rmi1 and Mre11-Rad50-Xrs2.* Nature, 2010. **467**(7311): p. 112-6.
44. Nimonkar, A.V., J. Genschel, E. Kinoshita, P. Polaczek, J.L. Campbell, C. Wyman, P. Modrich and S.C. Kowalczykowski, *BLM-DNA2-RPA-MRN and EXO1-BLM-RPA-MRN constitute two DNA end resection machineries for human DNA break repair.* Genes Dev, 2011. **25**(4): p. 350-62.
45. Jensen, R.B., A. Carreira and S.C. Kowalczykowski, *Purified human BRCA2 stimulates RAD51-mediated recombination.* Nature, 2010. **467**(7316): p. 678-83.
46. Holloman, W.K., *Unraveling the mechanism of BRCA2 in homologous recombination.* Nat Struct Mol Biol, 2011. **18**(7): p. 748-54.
47. Moynahan, M.E., A.J. Pierce and M. Jasin, *BRCA2 is required for homology-directed repair of chromosomal breaks.* Mol Cell, 2001. **7**(2): p. 263-72.

48. Moynahan, M.E. and M. Jasin, *Mitotic homologous recombination maintains genomic stability and suppresses tumorigenesis.* Nat Rev Mol Cell Biol, 2010. **11**(3): p. 196-207.
49. Loveday, C., C. Turnbull, E. Ruark, R.M. Xicola, E. Ramsay, D. Hughes, M. Warren-Perry, K. Snape, D. Eccles, D.G. Evans, M. Gore, A. Renwick, S. Seal, A.C. Antoniou and N. Rahman, *Germline RAD51C mutations confer susceptibility to ovarian cancer.* Nat Genet, 2012. **44**(5): p. 475-6; author reply 476.
50. Loveday, C., C. Turnbull, E. Ramsay, D. Hughes, E. Ruark, J.R. Frankum, G. Bowden, B. Kalmyrzaev, M. Warren-Perry, K. Snape, J.W. Adlard, J. Barwell, J. Berg, A.F. Brady, C. Brewer, G. Brice, C. Chapman, J. Cook, R. Davidson, A. Donaldson, F. Douglas, L. Greenhalgh, A. Henderson, L. Izatt, A. Kumar, F. Lalloo, Z. Miedzybrodzka, P.J. Morrison, J. Paterson, M. Porteous, M.T. Rogers, S. Shanley, L. Walker, D. Eccles, D.G. Evans, A. Renwick, S. Seal, C.J. Lord, A. Ashworth, J.S. Reis-Filho, A.C. Antoniou and N. Rahman, *Germline mutations in RAD51D confer susceptibility to ovarian cancer.* Nat Genet, 2011. **43**(9): p. 879-82.
51. Lin, W.Y., N.J. Camp, L.A. Cannon-Albright, K. Allen-Brady, S. Balasubramanian, M.W. Reed, J.L. Hopper, C. Apicella, G.G. Giles, M.C. Southey, R.L. Milne, J.I. Arias-Perez, P. Menendez-Rodriguez, J. Benitez, M. Grundmann, N. Dubrowinskaja, T.W. Park-Simon, T. Dork, M. Garcia-Closas, J. Figueroa, M. Sherman, J. Lissowska, D.F. Easton, A.M. Dunning, P. Rajaraman, A.J. Sigurdson, M.M. Doody, M.S. Linet, P.D. Pharoah, M.K. Schmidt and A. Cox, *A role for XRCC2 gene polymorphisms in breast cancer risk and survival.* J Med Genet, 2011. **48**(7): p. 477-84.
52. Lee, J.A., C.M. Carvalho and J.R. Lupski, *A DNA replication mechanism for generating nonrecurrent rearrangements associated with genomic disorders.* Cell, 2007. **131**(7): p. 1235-47.
53. Paek, A.L., S. Kaochar, H. Jones, A. Elezaby, L. Shanks and T. Weinert, *Fusion of nearby inverted repeats by a replication-based mechanism leads to formation of dicentric and acentric chromosomes that cause genome instability in budding yeast.* Genes Dev, 2009. **23**(24): p. 2861-75.
54. Mizuno, K., S. Lambert, G. Baldacci, J.M. Murray and A.M. Carr, *Nearby inverted repeats fuse to generate acentric and dicentric palindromic chromosomes by a replication template exchange mechanism.* Genes Dev, 2009. **23**(24): p. 2876-86.
55. Liu, P., A. Erez, S.C. Nagamani, S.U. Dhar, K.E. Kolodziejska, A.V. Dharmadhikari, M.L. Cooper, J. Wiszniewska, F. Zhang, M.A. Withers, C.A. Bacino, L.D. Campos-Acevedo, M.R. Delgado, D. Freedenberg, A. Garnica, T.A. Grebe, D. Hernandez-Almaguer, L. Immken, S.R. Lalani, S.D. McLean, H. Northrup, F. Scaglia, L. Strathearn, P. Trapane, S.H. Kang, A. Patel, S.W. Cheung, P.J. Hastings, P. Stankiewicz, J.R. Lupski and W. Bi, *Chromosome catastrophes involve replication mechanisms generating complex genomic rearrangements.* Cell, 2011. **146**(6): p. 889-903.
56. Bi, W., T. Sapir, O.A. Shchelochkov, F. Zhang, M.A. Withers, J.V. Hunter, T. Levy, V. Shinder, D.A. Peiffer, K.L. Gunderson, M.M. Nezarati, V.A. Shotts, S.S. Amato, S.K. Savage, D.J. Harris, D.L. Day-Salvatore, M. Horner, X.Y. Lu, T. Sahoo, Y. Yanagawa, A.L. Beaudet, S.W. Cheung, S. Martinez, J.R. Lupski and O.

Reiner, *Increased LIS1 expression affects human and mouse brain development.* Nat Genet, 2009. **41**(2): p. 168-77.
57. Karpenshif, Y. and K.A. Bernstein, *From yeast to mammals: Recent advances in genetic control of homologous recombination.* DNA Repair (Amst), 2012. **11**(10): p. 781-8.
58. Hashimoto, Y., A. Ray Chaudhuri, M. Lopes and V. Costanzo, *Rad51 protects nascent DNA from Mre11-dependent degradation and promotes continuous DNA synthesis.* Nat Struct Mol Biol, 2010. **17**(11): p. 1305-11.
59. Costanzo, V., *Brca2, Rad51 and Mre11: performing balancing acts on replication forks.* DNA Repair (Amst), 2011. **10**(10): p. 1060-5.
60. Schlacher, K., N. Christ, N. Siaud, A. Egashira, H. Wu and M. Jasin, *Double-strand break repair-independent role for BRCA2 in blocking stalled replication fork degradation by MRE11.* Cell, 2011. **145**(4): p. 529-42.
61. Schlacher, K., H. Wu and M. Jasin, *A distinct replication fork protection pathway connects Fanconi anemia tumor suppressors to RAD51-BRCA1/2.* Cancer Cell, 2012. **22**(1): p. 106-16.
62. Li, X. and W.D. Heyer, *Homologous recombination in DNA repair and DNA damage tolerance.* Cell Res, 2008. **18**(1): p. 99-113.
63. Heller, R.C. and K.J. Marians, *Replication fork reactivation downstream of a blocked nascent leading strand.* Nature, 2006. **439**(7076): p. 557-62.
64. Yeeles, J.T. and K.J. Marians, *The Escherichia coli replisome is inherently DNA damage tolerant.* Science, 2011. **334**(6053): p. 235-8.
65. Pomerantz, R.T. and M. O'Donnell, *The replisome uses mRNA as a primer after colliding with RNA polymerase.* Nature, 2008. **456**(7223): p. 762-6.
66. Liberi, G., G. Maffioletti, C. Lucca, I. Chiolo, A. Baryshnikova, C. Cotta-Ramusino, M. Lopes, A. Pellicioli, J.E. Haber and M. Foiani, *Rad51-dependent DNA structures accumulate at damaged replication forks in sgs1 mutants defective in the yeast ortholog of BLM RecQ helicase.* Genes Dev, 2005. **19**(3): p. 339-50.
67. Sale, J.E., A.R. Lehmann and R. Woodgate, *Y-family DNA polymerases and their role in tolerance of cellular DNA damage.* Nat Rev Mol Cell Biol, 2012. **13**(3): p. 141-52.
68. Hoege, C., B. Pfander, G.L. Moldovan, G. Pyrowolakis and S. Jentsch, *RAD6-dependent DNA repair is linked to modification of PCNA by ubiquitin and SUMO.* Nature, 2002. **419**(6903): p. 135-41.
69. Andersen, P.L., F. Xu and W. Xiao, *Eukaryotic DNA damage tolerance and translesion synthesis through covalent modifications of PCNA.* Cell Res, 2008. **18**(1): p. 162-73.
70. Pfander, B., G.L. Moldovan, M. Sacher, C. Hoege and S. Jentsch, *SUMO-modified PCNA recruits Srs2 to prevent recombination during S phase.* Nature, 2005. **436**(7049): p. 428-33.
71. Atkinson, J. and P. McGlynn, *Replication fork reversal and the maintenance of genome stability.* Nucleic Acids Res, 2009. **37**(11): p. 3475-92.
72. Fujiwara, Y. and M. Tatsumi, *Replicative bypass repair of ultraviolet damage to DNA of mammalian cells: caffeine sensitive and caffeine resistant mechanisms.* Mutat Res, 1976. **37**(1): p. 91-110.

73. Higgins, N.P., K. Kato and B. Strauss, *A model for replication repair in mammalian cells.* J Mol Biol, 1976. **101**(3): p. 417-25.
74. Michel, B., G. Grompone, M.J. Flores and V. Bidnenko, *Multiple pathways process stalled replication forks.* Proc Natl Acad Sci U S A, 2004. **101**(35): p. 12783-8.
75. Michel, B., H. Boubakri, Z. Baharoglu, M. LeMasson and R. Lestini, *Recombination proteins and rescue of arrested replication forks.* DNA Repair (Amst), 2007. **6**(7): p. 967-80.
76. Lopes, M., C. Cotta-Ramusino, A. Pellicioli, G. Liberi, P. Plevani, M. Muzi-Falconi, C.S. Newlon and M. Foiani, *The DNA replication checkpoint response stabilizes stalled replication forks.* Nature, 2001. **412**(6846): p. 557-61.
77. McGlynn, P. and R.G. Lloyd, *Rescue of stalled replication forks by RecG: simultaneous translocation on the leading and lagging strand templates supports an active DNA unwinding model of fork reversal and Holliday junction formation.* Proc Natl Acad Sci U S A, 2001. **98**(15): p. 8227-34.
78. Singleton, M.R., S. Scaife and D.B. Wigley, *Structural analysis of DNA replication fork reversal by RecG.* Cell, 2001. **107**(1): p. 79-89.
79. Blastyak, A., L. Pinter, I. Unk, L. Prakash, S. Prakash and L. Haracska, *Yeast Rad5 protein required for postreplication repair has a DNA helicase activity specific for replication fork regression.* Mol Cell, 2007. **28**(1): p. 167-75.
80. Unk, I., I. Hajdu, A. Blastyak and L. Haracska, *Role of yeast Rad5 and its human orthologs, HLTF and SHPRH in DNA damage tolerance.* DNA Repair (Amst), 2010. **9**(3): p. 257-67.
81. Blastyak, A., I. Hajdu, I. Unk and L. Haracska, *Role of double-stranded DNA translocase activity of human HLTF in replication of damaged DNA.* Mol Cell Biol, 2010. **30**(3): p. 684-93.
82. Torres-Ramos, C.A., S. Prakash and L. Prakash, *Requirement of RAD5 and MMS2 for postreplication repair of UV-damaged DNA in Saccharomyces cerevisiae.* Mol Cell Biol, 2002. **22**(7): p. 2419-26.
83. Unk, I., I. Hajdu, K. Fatyol, B. Szakal, A. Blastyak, V. Bermudez, J. Hurwitz, L. Prakash, S. Prakash and L. Haracska, *Human SHPRH is a ubiquitin ligase for Mms2-Ubc13-dependent polyubiquitylation of proliferating cell nuclear antigen.* Proc Natl Acad Sci U S A, 2006. **103**(48): p. 18107-12.
84. Motegi, A., R. Sood, H. Moinova, S.D. Markowitz, P.P. Liu and K. Myung, *Human SHPRH suppresses genomic instability through proliferating cell nuclear antigen polyubiquitination.* J Cell Biol, 2006. **175**(5): p. 703-8.
85. Unk, I., I. Hajdu, K. Fatyol, J. Hurwitz, J.H. Yoon, L. Prakash, S. Prakash and L. Haracska, *Human HLTF functions as a ubiquitin ligase for proliferating cell nuclear antigen polyubiquitination.* Proc Natl Acad Sci U S A, 2008. **105**(10): p. 3768-73.
86. Minca, E.C. and D. Kowalski, *Multiple Rad5 activities mediate sister chromatid recombination to bypass DNA damage at stalled replication forks.* Mol Cell, 2010. **38**(5): p. 649-61.
87. Bugreev, D.V., O.M. Mazina and A.V. Mazin, *Rad54 protein promotes branch migration of Holliday junctions.* Nature, 2006. **442**(7102): p. 590-3.
88. Mazin, A.V., O.M. Mazina, D.V. Bugreev and M.J. Rossi, *Rad54, the motor of homologous recombination.* DNA Repair (Amst), 2010. **9**(3): p. 286-302.

89. Mazina, O.M., M.J. Rossi, J.S. Deakyne, F. Huang and A.V. Mazin, *Polarity and bypass of DNA heterology during branch migration of Holliday junctions by human RAD54, BLM, and RECQ1 proteins.* J Biol Chem, 2012. **287**(15): p. 11820-32.
90. Bugreev, D.V., M.J. Rossi and A.V. Mazin, *Cooperation of RAD51 and RAD54 in regression of a model replication fork.* Nucleic Acids Res, 2011. **39**(6): p. 2153-64.
91. Gari, K., C. Decaillet, A.Z. Stasiak, A. Stasiak and A. Constantinou, *The Fanconi anemia protein FANCM can promote branch migration of Holliday junctions and replication forks.* Mol Cell, 2008. **29**(1): p. 141-8.
92. Zheng, X.F., R. Prakash, D. Saro, S. Longerich, H. Niu and P. Sung, *Processing of DNA structures via DNA unwinding and branch migration by the S. cerevisiae Mph1 protein.* DNA Repair (Amst), 2011. **10**(10): p. 1034-43.
93. Deans, A.J. and S.C. West, *DNA interstrand crosslink repair and cancer.* Nat Rev Cancer, 2011. **11**(7): p. 467-80.
94. Yusufzai, T. and J.T. Kadonaga, *HARP is an ATP-driven annealing helicase.* Science, 2008. **322**(5902): p. 748-50.
95. Bansbach, C.E., R. Betous, C.A. Lovejoy, G.G. Glick and D. Cortez, *The annealing helicase SMARCAL1 maintains genome integrity at stalled replication forks.* Genes Dev, 2009. **23**(20): p. 2405-14.
96. Ciccia, A., A.L. Bredemeyer, M.E. Sowa, M.E. Terret, P.V. Jallepalli, J.W. Harper and S.J. Elledge, *The SIOD disorder protein SMARCAL1 is an RPA-interacting protein involved in replication fork restart.* Genes Dev, 2009. **23**(20): p. 2415-25.
97. Betous, R., A.C. Mason, R.P. Rambo, C.E. Bansbach, A. Badu-Nkansah, B.M. Sirbu, B.F. Eichman and D. Cortez, *SMARCAL1 catalyzes fork regression and Holliday junction migration to maintain genome stability during DNA replication.* Genes Dev, 2012. **26**(2): p. 151-62.
98. Robu, M.E., R.B. Inman and M.M. Cox, *RecA protein promotes the regression of stalled replication forks in vitro.* Proc Natl Acad Sci U S A, 2001. **98**(15): p. 8211-8.
99. Kadyrov, F.A. and J.W. Drake, *UvsX recombinase and Dda helicase rescue stalled bacteriophage T4 DNA replication forks in vitro.* J Biol Chem, 2004. **279**(34): p. 35735-40.
100. Yoon, D., Y. Wang, K. Stapleford, L. Wiesmuller and J. Chen, *P53 inhibits strand exchange and replication fork regression promoted by human Rad51.* J Mol Biol, 2004. **336**(3): p. 639-54.
101. Robu, M.E., R.B. Inman and M.M. Cox, *Situational repair of replication forks: roles of RecG and RecA proteins.* J Biol Chem, 2004. **279**(12): p. 10973-81.
102. Michel, B., M.J. Flores, E. Viguera, G. Grompone, M. Seigneur and V. Bidnenko, *Rescue of arrested replication forks by homologous recombination.* Proc Natl Acad Sci U S A, 2001. **98**(15): p. 8181-8.
103. Courcelle, J., J.R. Donaldson, K.H. Chow and C.T. Courcelle, *DNA damage-induced replication fork regression and processing in Escherichia coli.* Science, 2003. **299**(5609): p. 1064-7.
104. Courcelle, C.T., K.H. Chow, A. Casey and J. Courcelle, *Nascent DNA processing by RecJ favors lesion repair over translesion synthesis at arrested replication forks in Escherichia coli.* Proc Natl Acad Sci U S A, 2006. **103**(24): p. 9154-9.

105. Postow, L., N.J. Crisona, B.J. Peter, C.D. Hardy and N.R. Cozzarelli, *Topological challenges to DNA replication: conformations at the fork.* Proc Natl Acad Sci U S A, 2001. **98**(15): p. 8219-26.
106. De Septenville, A.L., S. Duigou, H. Boubakri and B. Michel, *Replication fork reversal after replication-transcription collision.* PLoS Genet, 2012. **8**(4): p. e1002622.
107. Bermejo, R., M.S. Lai and M. Foiani, *Preventing replication stress to maintain genome stability: resolving conflicts between replication and transcription.* Mol Cell, 2012. **45**(6): p. 710-8.
108. Bermejo, R., T. Capra, R. Jossen, A. Colosio, C. Frattini, W. Carotenuto, A. Cocito, Y. Doksani, H. Klein, B. Gomez-Gonzalez, A. Aguilera, Y. Katou, K. Shirahige and M. Foiani, *The replication checkpoint protects fork stability by releasing transcribed genes from nuclear pores.* Cell, 2011. **146**(2): p. 233-46.
109. Lopes, M., C. Cotta-Ramusino, G. Liberi and M. Foiani, *Branch migrating sister chromatid junctions form at replication origins through Rad51/Rad52-independent mechanisms.* Mol Cell, 2003. **12**(6): p. 1499-510.
110. Cotta-Ramusino, C., D. Fachinetti, C. Lucca, Y. Doksani, M. Lopes, J. Sogo and M. Foiani, *Exo1 processes stalled replication forks and counteracts fork reversal in checkpoint-defective cells.* Mol Cell, 2005. **17**(1): p. 153-9.
111. Wang, J.C., *Cellular roles of DNA topoisomerases: a molecular perspective.* Nat Rev Mol Cell Biol, 2002. **3**(6): p. 430-40.
112. Pommier, Y., *Topoisomerase I inhibitors: camptothecins and beyond.* Nat Rev Cancer, 2006. **6**(10): p. 789-802.
113. Pommier, Y., E. Leo, H. Zhang and C. Marchand, *DNA topoisomerases and their poisoning by anticancer and antibacterial drugs.* Chem Biol, 2010. **17**(5): p. 421-33.
114. Strumberg, D., A.A. Pilon, M. Smith, R. Hickey, L. Malkas and Y. Pommier, *Conversion of topoisomerase I cleavage complexes on the leading strand of ribosomal DNA into 5'-phosphorylated DNA double-strand breaks by replication runoff.* Mol Cell Biol, 2000. **20**(11): p. 3977-87.
115. Koster, D.A., K. Palle, E.S. Bot, M.A. Bjornsti and N.H. Dekker, *Antitumour drugs impede DNA uncoiling by topoisomerase I.* Nature, 2007. **448**(7150): p. 213-7.
116. Koster, D.A., A. Crut, S. Shuman, M.A. Bjornsti and N.H. Dekker, *Cellular strategies for regulating DNA supercoiling: a single-molecule perspective.* Cell, 2010. **142**(4): p. 519-30.
117. Ray Chaudhuri, A., Y. Hashimoto, R. Herrador, K.J. Neelsen, D. Fachinetti, R. Bermejo, A. Cocito, V. Costanzo and M. Lopes, *Topoisomerase I poisoning results in PARP-mediated replication fork reversal.* Nat Struct Mol Biol, 2012. **19**(4): p. 417-23.
118. Curtin, N.J., *PARP inhibitors for cancer therapy.* Expert Rev Mol Med, 2005. **7**(4): p. 1-20.
119. Kummar, S., A. Chen, J. Ji, Y. Zhang, J.M. Reid, M. Ames, L. Jia, M. Weil, G. Speranza, A.J. Murgo, R. Kinders, L. Wang, R.E. Parchment, J. Carter, H. Stotler, L. Rubinstein, M. Hollingshead, G. Melillo, Y. Pommier, W. Bonner, J.E. Tomaszewski and J.H. Doroshow, *Phase I study of PARP inhibitor ABT-888 in*

combination with topotecan in adults with refractory solid tumors and lymphomas. Cancer Res, 2011. **71**(17): p. 5626-34.
120. Seigneur, M., V. Bidnenko, S.D. Ehrlich and B. Michel, *RuvAB acts at arrested replication forks.* Cell, 1998. **95**(3): p. 419-30.
121. Hu, J., L. Sun, F. Shen, Y. Chen, Y. Hua, Y. Liu, M. Zhang, Y. Hu, Q. Wang, W. Xu, F. Sun, J. Ji, J.M. Murray, A.M. Carr and D. Kong, *The intra-S phase checkpoint targets Dna2 to prevent stalled replication forks from reversing.* Cell, 2012. **149**(6): p. 1221-32.
122. Chu, W.K. and I.D. Hickson, *RecQ helicases: multifunctional genome caretakers.* Nat Rev Cancer, 2009. **9**(9): p. 644-54.
123. Bernstein, D.A., M.C. Zittel and J.L. Keck, *High-resolution structure of the E.coli RecQ helicase catalytic core.* EMBO J, 2003. **22**(19): p. 4910-21.
124. Bernstein, K.A., S. Gangloff and R. Rothstein, *The RecQ DNA helicases in DNA repair.* Annu Rev Genet, 2010. **44**: p. 393-417.
125. Janscak, P., P.L. Garcia, F. Hamburger, Y. Makuta, K. Shiraishi, Y. Imai, H. Ikeda and T.A. Bickle, *Characterization and mutational analysis of the RecQ core of the bloom syndrome protein.* J Mol Biol, 2003. **330**(1): p. 29-42.
126. Guo, R.B., P. Rigolet, L. Zargarian, S. Fermandjian and X.G. Xi, *Structural and functional characterizations reveal the importance of a zinc binding domain in Bloom's syndrome helicase.* Nucleic Acids Res, 2005. **33**(10): p. 3109-24.
127. Vindigni, A., F. Marino and O. Gileadi, *Probing the structural basis of RecQ helicase function.* Biophys Chem, 2010. **149**(3): p. 67-77.
128. Pike, A.C., B. Shrestha, V. Popuri, N. Burgess-Brown, L. Muzzolini, S. Costantini, A. Vindigni and O. Gileadi, *Structure of the human RECQ1 helicase reveals a putative strand-separation pin.* Proc Natl Acad Sci U S A, 2009. **106**(4): p. 1039-44.
129. Lucic, B., Y. Zhang, O. King, R. Mendoza-Maldonado, M. Berti, F.H. Niesen, N.A. Burgess-Brown, A.C. Pike, C.D. Cooper, O. Gileadi and A. Vindigni, *A prominent beta-hairpin structure in the winged-helix domain of RECQ1 is required for DNA unwinding and oligomer formation.* Nucleic Acids Res, 2011. **39**(5): p. 1703-17.
130. Kitano, K., S.Y. Kim and T. Hakoshima, *Structural basis for DNA strand separation by the unconventional winged-helix domain of RecQ helicase WRN.* Structure, 2010. **18**(2): p. 177-87.
131. Lee, J.W., J. Harrigan, P.L. Opresko and V.A. Bohr, *Pathways and functions of the Werner syndrome protein.* Mech Ageing Dev, 2005. **126**(1): p. 79-86.
132. Bernstein, D.A. and J.L. Keck, *Conferring substrate specificity to DNA helicases: role of the RecQ HRDC domain.* Structure, 2005. **13**(8): p. 1173-82.
133. Wu, L., K.L. Chan, C. Ralf, D.A. Bernstein, P.L. Garcia, V.A. Bohr, A. Vindigni, P. Janscak, J.L. Keck and I.D. Hickson, *The HRDC domain of BLM is required for the dissolution of double Holliday junctions.* EMBO J, 2005. **24**(14): p. 2679-87.
134. Perry, J.J., S.M. Yannone, L.G. Holden, C. Hitomi, A. Asaithamby, S. Han, P.K. Cooper, D.J. Chen and J.A. Tainer, *WRN exonuclease structure and molecular mechanism imply an editing role in DNA end processing.* Nat Struct Mol Biol, 2006. **13**(5): p. 414-22.
135. Muzzolini, L., F. Beuron, A. Patwardhan, V. Popuri, S. Cui, B. Niccolini, M. Rappas, P.S. Freemont and A. Vindigni, *Different quaternary structures of human*

RECQ1 are associated with its dual enzymatic activity. PLoS Biol, 2007. **5**(2): p. e20.

136. Perry, J.J., A. Asaithamby, A. Barnebey, F. Kiamanesch, D.J. Chen, S. Han, J.A. Tainer and S.M. Yannone, *Identification of a coiled coil in werner syndrome protein that facilitates multimerization and promotes exonuclease processivity.* J Biol Chem, 2010. **285**(33): p. 25699-707.
137. Popuri, V., C.Z. Bachrati, L. Muzzolini, G. Mosedale, S. Costantini, E. Giacomini, I.D. Hickson and A. Vindigni, *The Human RecQ helicases, BLM and RECQ1, display distinct DNA substrate specificities.* J Biol Chem, 2008. **283**(26): p. 17766-76.
138. Monnat, R.J., Jr., *Human RECQ helicases: roles in DNA metabolism, mutagenesis and cancer biology.* Semin Cancer Biol, 2010. **20**(5): p. 329-39.
139. Luo, G., I.M. Santoro, L.D. McDaniel, I. Nishijima, M. Mills, H. Youssoufian, H. Vogel, R.A. Schultz and A. Bradley, *Cancer predisposition caused by elevated mitotic recombination in Bloom mice.* Nat Genet, 2000. **26**(4): p. 424-9.
140. Chaganti, R.S., S. Schonberg and J. German, *A manyfold increase in sister chromatid exchanges in Bloom's syndrome lymphocytes.* Proc Natl Acad Sci U S A, 1974. **71**(11): p. 4508-12.
141. Wu, L. and I.D. Hickson, *The Bloom's syndrome helicase suppresses crossing over during homologous recombination.* Nature, 2003. **426**(6968): p. 870-4.
142. Wu, L., C.Z. Bachrati, J. Ou, C. Xu, J. Yin, M. Chang, W. Wang, L. Li, G.W. Brown and I.D. Hickson, *BLAP75/RMI1 promotes the BLM-dependent dissolution of homologous recombination intermediates.* Proc Natl Acad Sci U S A, 2006. **103**(11): p. 4068-73.
143. Singh, T.R., A.M. Ali, V. Busygina, S. Raynard, Q. Fan, C.H. Du, P.R. Andreassen, P. Sung and A.R. Meetei, *BLAP18/RMI2, a novel OB-fold-containing protein, is an essential component of the Bloom helicase-double Holliday junction dissolvasome.* Genes Dev, 2008. **22**(20): p. 2856-68.
144. Xu, D., R. Guo, A. Sobeck, C.Z. Bachrati, J. Yang, T. Enomoto, G.W. Brown, M.E. Hoatlin, I.D. Hickson and W. Wang, *RMI, a new OB-fold complex essential for Bloom syndrome protein to maintain genome stability.* Genes Dev, 2008. **22**(20): p. 2843-55.
145. Chan, K.L., T. Palmai-Pallag, S. Ying and I.D. Hickson, *Replication stress induces sister-chromatid bridging at fragile site loci in mitosis.* Nat Cell Biol, 2009. **11**(6): p. 753-60.
146. Gravel, S., J.R. Chapman, C. Magill and S.P. Jackson, *DNA helicases Sgs1 and BLM promote DNA double-strand break resection.* Genes Dev, 2008. **22**(20): p. 2767-72.
147. Niu, H., W.H. Chung, Z. Zhu, Y. Kwon, W. Zhao, P. Chi, R. Prakash, C. Seong, D. Liu, L. Lu, G. Ira and P. Sung, *Mechanism of the ATP-dependent DNA end-resection machinery from Saccharomyces cerevisiae.* Nature, 2010. **467**(7311): p. 108-11.
148. Wu, L., *Role of the BLM helicase in replication fork management.* DNA Repair (Amst), 2007. **6**(7): p. 936-44.

149. Davies, S.L., P.S. North and I.D. Hickson, *Role for BLM in replication-fork restart and suppression of origin firing after replicative stress.* Nat Struct Mol Biol, 2007. **14**(7): p. 677-9.
150. Chabosseau, P., G. Buhagiar-Labarchede, R. Onclercq-Delic, S. Lambert, M. Debatisse, O. Brison and M. Amor-Gueret, *Pyrimidine pool imbalance induced by BLM helicase deficiency contributes to genetic instability in Bloom syndrome.* Nat Commun, 2011. **2**: p. 368.
151. Bugreev, D.V., X. Yu, E.H. Egelman and A.V. Mazin, *Novel pro- and anti-recombination activities of the Bloom's syndrome helicase.* Genes Dev, 2007. **21**(23): p. 3085-94.
152. Ralf, C., I.D. Hickson and L. Wu, *The Bloom's syndrome helicase can promote the regression of a model replication fork.* J Biol Chem, 2006. **281**(32): p. 22839-46.
153. Machwe, A., L. Xiao, J. Groden and D.K. Orren, *The Werner and Bloom syndrome proteins catalyze regression of a model replication fork.* Biochemistry, 2006. **45**(47): p. 13939-46.
154. Machwe, A., R. Karale, X. Xu, Y. Liu and D.K. Orren, *The Werner and Bloom syndrome proteins help resolve replication blockage by converting (regressed) holliday junctions to functional replication forks.* Biochemistry, 2011. **50**(32): p. 6774-88.
155. Salk, D., E. Bryant, K. Au, H. Hoehn and G.M. Martin, *Systematic growth studies, cocultivation, and cell hybridization studies of Werner syndrome cultured skin fibroblasts.* Hum Genet, 1981. **58**(3): p. 310-6.
156. Chang, S., A.S. Multani, N.G. Cabrera, M.L. Naylor, P. Laud, D. Lombard, S. Pathak, L. Guarente and R.A. DePinho, *Essential role of limiting telomeres in the pathogenesis of Werner syndrome.* Nat Genet, 2004. **36**(8): p. 877-82.
157. Crabbe, L., A. Jauch, C.M. Naeger, H. Holtgreve-Grez and J. Karlseder, *Telomere dysfunction as a cause of genomic instability in Werner syndrome.* Proc Natl Acad Sci U S A, 2007. **104**(7): p. 2205-10.
158. Wyllie, F.S., C.J. Jones, J.W. Skinner, M.F. Haughton, C. Wallis, D. Wynford-Thomas, R.G. Faragher and D. Kipling, *Telomerase prevents the accelerated cell ageing of Werner syndrome fibroblasts.* Nat Genet, 2000. **24**(1): p. 16-7.
159. Crabbe, L., R.E. Verdun, C.I. Haggblom and J. Karlseder, *Defective telomere lagging strand synthesis in cells lacking WRN helicase activity.* Science, 2004. **306**(5703): p. 1951-3.
160. Mohaghegh, P., J.K. Karow, R.M. Brosh, Jr., V.A. Bohr and I.D. Hickson, *The Bloom's and Werner's syndrome proteins are DNA structure-specific helicases.* Nucleic Acids Res, 2001. **29**(13): p. 2843-9.
161. Opresko, P.L., M. Otterlei, J. Graakjaer, P. Bruheim, L. Dawut, S. Kolvraa, A. May, M.M. Seidman and V.A. Bohr, *The Werner syndrome helicase and exonuclease cooperate to resolve telomeric D loops in a manner regulated by TRF1 and TRF2.* Mol Cell, 2004. **14**(6): p. 763-74.
162. Pirzio, L.M., P. Pichierri, M. Bignami and A. Franchitto, *Werner syndrome helicase activity is essential in maintaining fragile site stability.* J Cell Biol, 2008. **180**(2): p. 305-14.
163. Sidorova, J.M., *Roles of the Werner syndrome RecQ helicase in DNA replication.* DNA Repair (Amst), 2008. **7**(11): p. 1776-86.

164. Sidorova, J.M., N. Li, A. Folch and R.J. Monnat, Jr., *The RecQ helicase WRN is required for normal replication fork progression after DNA damage or replication fork arrest.* Cell Cycle, 2008. **7**(6): p. 796-807.
165. Kamath-Loeb, A.S., J.C. Shen, M.W. Schmitt and L.A. Loeb, *The Werner syndrome exonuclease facilitates DNA degradation and high fidelity DNA polymerization by human DNA polymerase delta.* J Biol Chem, 2012. **287**(15): p. 12480-90.
166. Brosh, R.M., Jr., C. von Kobbe, J.A. Sommers, P. Karmakar, P.L. Opresko, J. Piotrowski, I. Dianova, G.L. Dianov and V.A. Bohr, *Werner syndrome protein interacts with human flap endonuclease 1 and stimulates its cleavage activity.* EMBO J, 2001. **20**(20): p. 5791-801.
167. Yan, H., T. Toczylowski, J. McCane, C. Chen and S. Liao, *Replication protein A promotes 5'-->3' end processing during homology-dependent DNA double-strand break repair.* J Cell Biol, 2011. **192**(2): p. 251-61.
168. Tomimatsu, N., B. Mukherjee, K. Deland, A. Kurimasa, E. Bolderson, K.K. Khanna and S. Burma, *Exo1 plays a major role in DNA end resection in humans and influences double-strand break repair and damage signaling decisions.* DNA Repair (Amst), 2012. **11**(4): p. 441-8.
169. Ouyang, K.J., L.L. Woo and N.A. Ellis, *Homologous recombination and maintenance of genome integrity: cancer and aging through the prism of human RecQ helicases.* Mech Ageing Dev, 2008. **129**(7-8): p. 425-40.
170. Franchitto, A., L.M. Pirzio, E. Prosperi, O. Sapora, M. Bignami and P. Pichierri, *Replication fork stalling in WRN-deficient cells is overcome by prompt activation of a MUS81-dependent pathway.* J Cell Biol, 2008. **183**(2): p. 241-52.
171. Murfuni, I., S. Nicolai, S. Baldari, M. Crescenzi, M. Bignami, A. Franchitto and P. Pichierri, *The WRN and MUS81 proteins limit cell death and genome instability following oncogene activation.* Oncogene, 2012.
172. Kawabe, Y., M. Seki, A. Yoshimura, K. Nishino, T. Hayashi, T. Takeuchi, S. Iguchi, Y. Kusa, M. Ohtsuki, T. Tsuyama, O. Imamura, T. Matsumoto, Y. Furuichi, S. Tada and T. Enomoto, *Analyses of the interaction of WRNIP1 with Werner syndrome protein (WRN) in vitro and in the cell.* DNA Repair (Amst), 2006. **5**(7): p. 816-28.
173. Phillips, L.G. and J.E. Sale, *The Werner's Syndrome protein collaborates with REV1 to promote replication fork progression on damaged DNA.* DNA Repair (Amst), 2010. **9**(10): p. 1064-72.
174. Kamath-Loeb, A.S., L. Lan, S. Nakajima, A. Yasui and L.A. Loeb, *Werner syndrome protein interacts functionally with translesion DNA polymerases.* Proc Natl Acad Sci U S A, 2007. **104**(25): p. 10394-9.
175. Kobayashi, J., M. Okui, A. Asaithamby, S. Burma, B.P. Chen, K. Tanimoto, S. Matsuura, K. Komatsu and D.J. Chen, *WRN participates in translesion synthesis pathway through interaction with NBS1.* Mech Ageing Dev, 2010. **131**(6): p. 436-44.
176. Lee, S.J., A. Gartner, M. Hyun, B. Ahn and H.S. Koo, *The Caenorhabditis elegans Werner syndrome protein functions upstream of ATR and ATM in response to DNA replication inhibition and double-strand DNA breaks.* PLoS Genet, 2010. **6**(1): p. e1000801.

177. Cheng, W.H., D. Muftic, M. Muftuoglu, L. Dawut, C. Morris, T. Helleday, Y. Shiloh and V.A. Bohr, *WRN is required for ATM activation and the S-phase checkpoint in response to interstrand cross-link-induced DNA double-strand breaks.* Mol Biol Cell, 2008. **19**(9): p. 3923-33.
178. Patro, B.S., R. Frohlich, V.A. Bohr and T. Stevnsner, *WRN helicase regulates the ATR-CHK1-induced S-phase checkpoint pathway in response to topoisomerase-I-DNA covalent complexes.* J Cell Sci, 2011. **124**(Pt 23): p. 3967-79.
179. Ammazzalorso, F., L.M. Pirzio, M. Bignami, A. Franchitto and P. Pichierri, *ATR and ATM differently regulate WRN to prevent DSBs at stalled replication forks and promote replication fork recovery.* EMBO J, 2010. **29**(18): p. 3156-69.
180. Pichierri, P., S. Nicolai, L. Cignolo, M. Bignami and A. Franchitto, *The RAD9-RAD1-HUS1 (9.1.1) complex interacts with WRN and is crucial to regulate its response to replication fork stalling.* Oncogene, 2012. **31**(23): p. 2809-23.
181. Constantinou, A., M. Tarsounas, J.K. Karow, R.M. Brosh, V.A. Bohr, I.D. Hickson and S.C. West, *Werner's syndrome protein (WRN) migrates Holliday junctions and co-localizes with RPA upon replication arrest.* EMBO Rep, 2000. **1**(1): p. 80-4.
182. Machwe, A., L. Xiao, R.G. Lloyd, E. Bolt and D.K. Orren, *Replication fork regression in vitro by the Werner syndrome protein (WRN): holliday junction formation, the effect of leading arm structure and a potential role for WRN exonuclease activity.* Nucleic Acids Res, 2007. **35**(17): p. 5729-47.
183. Li, B. and L. Comai, *Functional interaction between Ku and the werner syndrome protein in DNA end processing.* J Biol Chem, 2000. **275**(50): p. 39800.
184. Li, B. and L. Comai, *Displacement of DNA-PKcs from DNA ends by the Werner syndrome protein.* Nucleic Acids Res, 2002. **30**(17): p. 3653-61.
185. Kusumoto, R., L. Dawut, C. Marchetti, J. Wan Lee, A. Vindigni, D. Ramsden and V.A. Bohr, *Werner protein cooperates with the XRCC4-DNA ligase IV complex in end-processing.* Biochemistry, 2008. **47**(28): p. 7548-56.
186. Karmakar, P. and V.A. Bohr, *Cellular dynamics and modulation of WRN protein is DNA damage specific.* Mech Ageing Dev, 2005. **126**(11): p. 1146-58.
187. Szekely, A.M., F. Bleichert, A. Numann, S. Van Komen, E. Manasanch, A. Ben Nasr, A. Canaan and S.M. Weissman, *Werner protein protects nonproliferating cells from oxidative DNA damage.* Mol Cell Biol, 2005. **25**(23): p. 10492-506.
188. von Kobbe, C., J.A. Harrigan, A. May, P.L. Opresko, L. Dawut, W.H. Cheng and V.A. Bohr, *Central role for the Werner syndrome protein/poly(ADP-ribose) polymerase 1 complex in the poly(ADP-ribosyl)ation pathway after DNA damage.* Mol Cell Biol, 2003. **23**(23): p. 8601-13.
189. von Kobbe, C., J.A. Harrigan, V. Schreiber, P. Stiegler, J. Piotrowski, L. Dawut and V.A. Bohr, *Poly(ADP-ribose) polymerase 1 regulates both the exonuclease and helicase activities of the Werner syndrome protein.* Nucleic Acids Res, 2004. **32**(13): p. 4003-14.
190. Lebel, M., J. Lavoie, I. Gaudreault, M. Bronsard and R. Drouin, *Genetic cooperation between the Werner syndrome protein and poly(ADP-ribose) polymerase-1 in preventing chromatid breaks, complex chromosomal rearrangements, and cancer in mice.* Am J Pathol, 2003. **162**(5): p. 1559-69.
191. Saleh-Gohari, N., H.E. Bryant, N. Schultz, K.M. Parker, T.N. Cassel and T. Helleday, *Spontaneous homologous recombination is induced by collapsed*

replication forks that are caused by endogenous DNA single-strand breaks. Mol Cell Biol, 2005. **25**(16): p. 7158-69.

192. Sekelsky, J.J., M.H. Brodsky, G.M. Rubin and R.S. Hawley, *Drosophila and human RecQ5 exist in different isoforms generated by alternative splicing.* Nucleic Acids Res, 1999. **27**(18): p. 3762-9.
193. Hu, Y., X. Lu, E. Barnes, M. Yan, H. Lou and G. Luo, *Recql5 and Blm RecQ DNA helicases have nonredundant roles in suppressing crossovers.* Mol Cell Biol, 2005. **25**(9): p. 3431-42.
194. Hu, Y., S. Raynard, M.G. Sehorn, X. Lu, W. Bussen, L. Zheng, J.M. Stark, E.L. Barnes, P. Chi, P. Janscak, M. Jasin, H. Vogel, P. Sung and G. Luo, *RECQL5/Recql5 helicase regulates homologous recombination and suppresses tumor formation via disruption of Rad51 presynaptic filaments.* Genes Dev, 2007. **21**(23): p. 3073-84.
195. Schwendener, S., S. Raynard, S. Paliwal, A. Cheng, R. Kanagaraj, I. Shevelev, J.M. Stark, P. Sung and P. Janscak, *Physical interaction of RECQ5 helicase with RAD51 facilitates its anti-recombinase activity.* J Biol Chem, 2010. **285**(21): p. 15739-45.
196. Islam, M.N., N. Paquet, D. Fox, 3rd, E. Dray, X.F. Zheng, H. Klein, P. Sung and W. Wang, *A variant of the breast cancer type 2 susceptibility protein (BRC) repeat is essential for the RECQL5 helicase to interact with RAD51 recombinase for genome stabilization.* J Biol Chem, 2012. **287**(28): p. 23808-18.
197. Aygun, O., J. Svejstrup and Y. Liu, *A RECQ5-RNA polymerase II association identified by targeted proteomic analysis of human chromatin.* Proc Natl Acad Sci U S A, 2008. **105**(25): p. 8580-4.
198. Li, M., X. Xu and Y. Liu, *The SET2-RPB1 interaction domain of human RECQ5 is important for transcription-associated genome stability.* Mol Cell Biol, 2011. **31**(10): p. 2090-9.
199. Ichikawa, K., T. Noda and Y. Furuichi, *[Preparation of the gene targeted knockout mice for human premature aging diseases, Werner syndrome, and Rothmund-Thomson syndrome caused by the mutation of DNA helicases].* Nihon Yakurigaku Zasshi, 2002. **119**(4): p. 219-26.
200. Hoki, Y., R. Araki, A. Fujimori, T. Ohhata, H. Koseki, R. Fukumura, M. Nakamura, H. Takahashi, Y. Noda, S. Kito and M. Abe, *Growth retardation and skin abnormalities of the Recql4-deficient mouse.* Hum Mol Genet, 2003. **12**(18): p. 2293-9.
201. Sangrithi, M.N., J.A. Bernal, M. Madine, A. Philpott, J. Lee, W.G. Dunphy and A.R. Venkitaraman, *Initiation of DNA replication requires the RECQL4 protein mutated in Rothmund-Thomson syndrome.* Cell, 2005. **121**(6): p. 887-98.
202. Thangavel, S., R. Mendoza-Maldonado, E. Tissino, J.M. Sidorova, J. Yin, W. Wang, R.J. Monnat, Jr., A. Falaschi and A. Vindigni, *Human RECQ1 and RECQ4 helicases play distinct roles in DNA replication initiation.* Mol Cell Biol, 2010. **30**(6): p. 1382-96.
203. Xu, X., P.J. Rochette, E.A. Feyissa, T.V. Su and Y. Liu, *MCM10 mediates RECQ4 association with MCM2-7 helicase complex during DNA replication.* EMBO J, 2009. **28**(19): p. 3005-14.
204. Xu, X. and Y. Liu, *Dual DNA unwinding activities of the Rothmund-Thomson syndrome protein, RECQ4.* EMBO J, 2009. **28**(5): p. 568-77.

205. Fu, Y.V., H. Yardimci, D.T. Long, T.V. Ho, A. Guainazzi, V.P. Bermudez, J. Hurwitz, A. van Oijen, O.D. Scharer and J.C. Walter, *Selective bypass of a lagging strand roadblock by the eukaryotic replicative DNA helicase.* Cell, 2011. **146**(6): p. 931-41.
206. Liu, Y., *Rothmund-Thomson syndrome helicase, RECQ4: on the crossroad between DNA replication and repair.* DNA Repair (Amst), 2010. **9**(3): p. 325-30.
207. Woo, L.L., K. Futami, A. Shimamoto, Y. Furuichi and K.M. Frank, *The Rothmund-Thomson gene product RECQL4 localizes to the nucleolus in response to oxidative stress.* Exp Cell Res, 2006. **312**(17): p. 3443-57.
208. Schurman, S.H., M. Hedayati, Z. Wang, D.K. Singh, E. Speina, Y. Zhang, K. Becker, M. Macris, P. Sung, D.M. Wilson, 3rd, D.L. Croteau and V.A. Bohr, *Direct and indirect roles of RECQL4 in modulating base excision repair capacity.* Hum Mol Genet, 2009. **18**(18): p. 3470-83.
209. Ghosh, A.K., M.L. Rossi, D.K. Singh, C. Dunn, M. Ramamoorthy, D.L. Croteau, Y. Liu and V.A. Bohr, *RECQL4, the protein mutated in Rothmund-Thomson syndrome, functions in telomere maintenance.* J Biol Chem, 2012. **287**(1): p. 196-209.
210. De, S., J. Kumari, R. Mudgal, P. Modi, S. Gupta, K. Futami, H. Goto, N.M. Lindor, Y. Furuichi, D. Mohanty and S. Sengupta, *RECQL4 is essential for the transport of p53 to mitochondria in normal human cells in the absence of exogenous stress.* J Cell Sci, 2012. **125**(Pt 10): p. 2509-22.
211. Croteau, D.L., M.L. Rossi, C. Canugovi, J. Tian, P. Sykora, M. Ramamoorthy, Z.M. Wang, D.K. Singh, M. Akbari, R. Kasiviswanathan, W.C. Copeland and V.A. Bohr, *RECQL4 localizes to mitochondria and preserves mitochondrial DNA integrity.* Aging Cell, 2012. **11**(3): p. 456-66.
212. Puranam, K.L. and P.J. Blackshear, *Cloning and characterization of RECQL, a potential human homologue of the Escherichia coli DNA helicase RecQ.* J Biol Chem, 1994. **269**(47): p. 29838-45.
213. Kawabe, T., N. Tsuyama, S. Kitao, K. Nishikawa, A. Shimamoto, M. Shiratori, T. Matsumoto, K. Anno, T. Sato, Y. Mitsui, M. Seki, T. Enomoto, M. Goto, N.A. Ellis, T. Ide, Y. Furuichi and M. Sugimoto, *Differential regulation of human RecQ family helicases in cell transformation and cell cycle.* Oncogene, 2000. **19**(41): p. 4764-72.
214. Mendoza-Maldonado, R., V. Faoro, S. Bajpai, M. Berti, F. Odreman, M. Vindigni, T. Ius, A. Ghasemian, S. Bonin, M. Skrap, G. Stanta and A. Vindigni, *The human RECQ1 helicase is highly expressed in glioblastoma and plays an important role in tumor cell proliferation.* Mol Cancer, 2011. **10**: p. 83.
215. Suijkerbuijk, R.F., R.J. Sinke, A.M. Meloni, J.M. Parrington, J. van Echten, B. de Jong, J.W. Oosterhuis, A.A. Sandberg and A. Geurts van Kessel, *Overrepresentation of chromosome 12p sequences and karyotypic evolution in i(12p)-negative testicular germ-cell tumors revealed by fluorescence in situ hybridization.* Cancer Genet Cytogenet, 1993. **70**(2): p. 85-93.
216. Li, D., M. Frazier, D.B. Evans, K.R. Hess, C.H. Crane, L. Jiao and J.L. Abbruzzese, *Single nucleotide polymorphisms of RecQ1, RAD54L, and ATM genes are associated with reduced survival of pancreatic cancer.* J Clin Oncol, 2006. **24**(11): p. 1720-8.

217. Sharma, S., D.J. Stumpo, A.S. Balajee, C.B. Bock, P.M. Lansdorp, R.M. Brosh, Jr. and P.J. Blackshear, *RECQL, a member of the RecQ family of DNA helicases, suppresses chromosomal instability.* Mol Cell Biol, 2007. **27**(5): p. 1784-94.
218. Sharma, S. and R.M. Brosh, Jr., *Human RECQ1 is a DNA damage responsive protein required for genotoxic stress resistance and suppression of sister chromatid exchanges.* PloS one, 2007. **2**(12): p. e1297.
219. Futami, K., E. Kumagai, H. Makino, H. Goto, M. Takagi, A. Shimamoto and Y. Furuichi, *Induction of mitotic cell death in cancer cells by small interference RNA suppressing the expression of RecQL1 helicase.* Cancer Sci, 2008. **99**(1): p. 71-80.
220. Futami, K., E. Kumagai, H. Makino, A. Sato, M. Takagi, A. Shimamoto and Y. Furuichi, *Anticancer activity of RecQL1 helicase siRNA in mouse xenograft models.* Cancer Sci, 2008. **99**(6): p. 1227-36.
221. Futami, K., S. Ogasawara, H. Goto, H. Yano and Y. Furuichi, *RecQL1 DNA repair helicase: A potential tumor marker and therapeutic target against hepatocellular carcinoma.* Int J Mol Med, 2010. **25**(4): p. 537-45.
222. Bugreev, D.V., R.M. Brosh, Jr. and A.V. Mazin, *RECQ1 possesses DNA branch migration activity.* J Biol Chem, 2008. **283**(29): p. 20231-42.
223. LeRoy, G., R. Carroll, S. Kyin, M. Seki and M.D. Cole, *Identification of RecQL1 as a Holliday junction processing enzyme in human cell lines.* Nucleic Acids Res, 2005. **33**(19): p. 6251-7.
224. Wang, W., M. Seki, Y. Narita, T. Nakagawa, A. Yoshimura, M. Otsuki, Y. Kawabe, S. Tada, H. Yagi, Y. Ishii and T. Enomoto, *Functional relation among RecQ family helicases RecQL1, RecQL5, and BLM in cell growth and sister chromatid exchange formation.* Mol Cell Biol, 2003. **23**(10): p. 3527-35.
225. Wang, Y., H. Li, Q. Tang, G.G. Maul and Y. Yuan, *Kaposi's sarcoma-associated herpesvirus ori-Lyt-dependent DNA replication: involvement of host cellular factors.* J Virol, 2008. **82**(6): p. 2867-82.
226. Wang, P., A.J. Rennekamp, Y. Yuan and P.M. Lieberman, *Topoisomerase I and RecQL1 function in Epstein-Barr virus lytic reactivation.* J Virol, 2009. **83**(16): p. 8090-8.
227. Cogoni, C. and G. Macino, *Posttranscriptional gene silencing in Neurospora by a RecQ DNA helicase.* Science, 1999. **286**(5448): p. 2342-4.
228. Lau, N.C., A.G. Seto, J. Kim, S. Kuramochi-Miyagawa, T. Nakano, D.P. Bartel and R.E. Kingston, *Characterization of the piRNA complex from rat testes.* Science, 2006. **313**(5785): p. 363-7.
229. Thomson, T. and H. Lin, *The biogenesis and function of PIWI proteins and piRNAs: progress and prospect.* Annu Rev Cell Dev Biol, 2009. **25**: p. 355-76.
230. Esteller, M., *Non-coding RNAs in human disease.* Nat Rev Genet, 2011. **12**(12): p. 861-74.
231. Gibson, B.A. and W.L. Kraus, *New insights into the molecular and cellular functions of poly(ADP-ribose) and PARPs.* Nat Rev Mol Cell Biol, 2012. **13**(7): p. 411-24.
232. Ali, A.A., G. Timinszky, R. Arribas-Bosacoma, M. Kozlowski, P.O. Hassa, M. Hassler, A.G. Ladurner, L.H. Pearl and A.W. Oliver, *The zinc-finger domains of PARP1 cooperate to recognize DNA strand breaks.* Nat Struct Mol Biol, 2012. **19**(7): p. 685-92.

233. Langelier, M.F., J.L. Planck, S. Roy and J.M. Pascal, *Structural basis for DNA damage-dependent poly(ADP-ribosyl)ation by human PARP-1*. Science, 2012. **336**(6082): p. 728-32.
234. Ferro, A.M. and B.M. Olivera, *Poly(ADP-ribosylation) in vitro. Reaction parameters and enzyme mechanism.* J Biol Chem, 1982. **257**(13): p. 7808-13.
235. Koh, D.W., V.L. Dawson and T.M. Dawson, *The road to survival goes through PARG.* Cell Cycle, 2005. **4**(3): p. 397-9.
236. Pleschke, J.M., H.E. Kleczkowska, M. Strohm and F.R. Althaus, *Poly(ADP-ribose) binds to specific domains in DNA damage checkpoint proteins.* J Biol Chem, 2000. **275**(52): p. 40974-80.
237. Ahel, I., D. Ahel, T. Matsusaka, A.J. Clark, J. Pines, S.J. Boulton and S.C. West, *Poly(ADP-ribose)-binding zinc finger motifs in DNA repair/checkpoint proteins.* Nature, 2008. **451**(7174): p. 81-5.
238. Eustermann, S., C. Brockmann, P.V. Mehrotra, J.C. Yang, D. Loakes, S.C. West, I. Ahel and D. Neuhaus, *Solution structures of the two PBZ domains from human APLF and their interaction with poly(ADP-ribose).* Nat Struct Mol Biol, 2010. **17**(2): p. 241-3.
239. Karras, G.I., G. Kustatscher, H.R. Buhecha, M.D. Allen, C. Pugieux, F. Sait, M. Bycroft and A.G. Ladurner, *The macro domain is an ADP-ribose binding module.* EMBO J, 2005. **24**(11): p. 1911-20.
240. Ahel, D., Z. Horejsi, N. Wiechens, S.E. Polo, E. Garcia-Wilson, I. Ahel, H. Flynn, M. Skehel, S.C. West, S.P. Jackson, T. Owen-Hughes and S.J. Boulton, *Poly(ADP-ribose)-dependent regulation of DNA repair by the chromatin remodeling enzyme ALC1.* Science, 2009. **325**(5945): p. 1240-3.
241. Timinszky, G., S. Till, P.O. Hassa, M. Hothorn, G. Kustatscher, B. Nijmeijer, J. Colombelli, M. Altmeyer, E.H. Stelzer, K. Scheffzek, M.O. Hottiger and A.G. Ladurner, *A macrodomain-containing histone rearranges chromatin upon sensing PARP1 activation.* Nat Struct Mol Biol, 2009. **16**(9): p. 923-9.
242. Gottschalk, A.J., G. Timinszky, S.E. Kong, J. Jin, Y. Cai, S.K. Swanson, M.P. Washburn, L. Florens, A.G. Ladurner, J.W. Conaway and R.C. Conaway, *Poly(ADP-ribosyl)ation directs recruitment and activation of an ATP-dependent chromatin remodeler.* Proc Natl Acad Sci U S A, 2009. **106**(33): p. 13770-4.
243. Wang, Z., G.A. Michaud, Z. Cheng, Y. Zhang, T.R. Hinds, E. Fan, F. Cong and W. Xu, *Recognition of the iso-ADP-ribose moiety in poly(ADP-ribose) by WWE domains suggests a general mechanism for poly(ADP-ribosyl)ation-dependent ubiquitination.* Genes Dev, 2012. **26**(3): p. 235-40.
244. Kalisch, T., J.C. Ame, F. Dantzer and V. Schreiber, *New readers and interpretations of poly(ADP-ribosyl)ation.* Trends Biochem Sci, 2012. **37**(9): p. 381-90.
245. Horton, J.K., M. Watson, D.F. Stefanick, D.T. Shaughnessy, J.A. Taylor and S.H. Wilson, *XRCC1 and DNA polymerase beta in cellular protection against cytotoxic DNA single-strand breaks.* Cell Res, 2008. **18**(1): p. 48-63.
246. Mehrotra, P.V., D. Ahel, D.P. Ryan, R. Weston, N. Wiechens, R. Kraehenbuehl, T. Owen-Hughes and I. Ahel, *DNA repair factor APLF is a histone chaperone.* Mol Cell, 2011. **41**(1): p. 46-55.

247. Li, B., S. Navarro, N. Kasahara and L. Comai, *Identification and biochemical characterization of a Werner's syndrome protein complex with Ku70/80 and poly(ADP-ribose) polymerase-1.* J Biol Chem, 2004. **279**(14): p. 13659-67.
248. Ruscetti, T., B.E. Lehnert, J. Halbrook, H. Le Trong, M.F. Hoekstra, D.J. Chen and S.R. Peterson, *Stimulation of the DNA-dependent protein kinase by poly(ADP-ribose) polymerase.* J Biol Chem, 1998. **273**(23): p. 14461-7.
249. Ariumi, Y., M. Masutani, T.D. Copeland, T. Mimori, T. Sugimura, K. Shimotohno, K. Ueda, M. Hatanaka and M. Noda, *Suppression of the poly(ADP-ribose) polymerase activity by DNA-dependent protein kinase in vitro.* Oncogene, 1999. **18**(32): p. 4616-25.
250. Audebert, M., B. Salles and P. Calsou, *Involvement of poly(ADP-ribose) polymerase-1 and XRCC1/DNA ligase III in an alternative route for DNA double-strand breaks rejoining.* J Biol Chem, 2004. **279**(53): p. 55117-26.
251. Wang, M., W. Wu, B. Rosidi, L. Zhang, H. Wang and G. Iliakis, *PARP-1 and Ku compete for repair of DNA double strand breaks by distinct NHEJ pathways.* Nucleic Acids Res, 2006. **34**(21): p. 6170-82.
252. Xie, A., A. Kwok and R. Scully, *Role of mammalian Mre11 in classical and alternative nonhomologous end joining.* Nat Struct Mol Biol, 2009. **16**(8): p. 814-8.
253. Henrie, M.S., A. Kurimasa, S. Burma, J. Menissier-de Murcia, G. de Murcia, G.C. Li and D.J. Chen, *Lethality in PARP-1/Ku80 double mutant mice reveals physiological synergy during early embryogenesis.* DNA Repair (Amst), 2003. **2**(2): p. 151-8.
254. Tong, W.M., U. Cortes, M.P. Hande, H. Ohgaki, L.R. Cavalli, P.M. Lansdorp, B.R. Haddad and Z.Q. Wang, *Synergistic role of Ku80 and poly(ADP-ribose) polymerase in suppressing chromosomal aberrations and liver cancer formation.* Cancer Res, 2002. **62**(23): p. 6990-6.
255. Schultz, N., E. Lopez, N. Saleh-Gohari and T. Helleday, *Poly(ADP-ribose) polymerase (PARP-1) has a controlling role in homologous recombination.* Nucleic Acids Res, 2003. **31**(17): p. 4959-64.
256. Bryant, H.E., E. Petermann, N. Schultz, A.S. Jemth, O. Loseva, N. Issaeva, F. Johansson, S. Fernandez, P. McGlynn and T. Helleday, *PARP is activated at stalled forks to mediate Mre11-dependent replication restart and recombination.* EMBO J, 2009. **28**(17): p. 2601-15.
257. Ying, S., F.C. Hamdy and T. Helleday, *Mre11-dependent degradation of stalled DNA replication forks is prevented by BRCA2 and PARP1.* Cancer Res, 2012. **72**(11): p. 2814-21.
258. Petermann, E., M.L. Orta, N. Issaeva, N. Schultz and T. Helleday, *Hydroxyurea-stalled replication forks become progressively inactivated and require two different RAD51-mediated pathways for restart and repair.* Mol Cell, 2010. **37**(4): p. 492-502.
259. Hochegger, H., D. Dejsuphong, T. Fukushima, C. Morrison, E. Sonoda, V. Schreiber, G.Y. Zhao, A. Saberi, M. Masutani, N. Adachi, H. Koyama, G. de Murcia and S. Takeda, *Parp-1 protects homologous recombination from interference by Ku and Ligase IV in vertebrate cells.* EMBO J, 2006. **25**(6): p. 1305-14.

260. Saberi, A., H. Hochegger, D. Szuts, L. Lan, A. Yasui, J.E. Sale, Y. Taniguchi, Y. Murakawa, W. Zeng, K. Yokomori, T. Helleday, H. Teraoka, H. Arakawa, J.M. Buerstedde and S. Takeda, *RAD18 and poly(ADP-ribose) polymerase independently suppress the access of nonhomologous end joining to double-strand breaks and facilitate homologous recombination-mediated repair.* Mol Cell Biol, 2007. **27**(7): p. 2562-71.
261. Sugimura, K., S. Takebayashi, H. Taguchi, S. Takeda and K. Okumura, *PARP-1 ensures regulation of replication fork progression by homologous recombination on damaged DNA.* J Cell Biol, 2008. **183**(7): p. 1203-12.
262. Bryant, H.E., N. Schultz, H.D. Thomas, K.M. Parker, D. Flower, E. Lopez, S. Kyle, M. Meuth, N.J. Curtin and T. Helleday, *Specific killing of BRCA2-deficient tumours with inhibitors of poly(ADP-ribose) polymerase.* Nature, 2005. **434**(7035): p. 913-7.
263. Farmer, H., N. McCabe, C.J. Lord, A.N. Tutt, D.A. Johnson, T.B. Richardson, M. Santarosa, K.J. Dillon, I. Hickson, C. Knights, N.M. Martin, S.P. Jackson, G.C. Smith and A. Ashworth, *Targeting the DNA repair defect in BRCA mutant cells as a therapeutic strategy.* Nature, 2005. **434**(7035): p. 917-21.
264. Sourisseau, T., D. Maniotis, A. McCarthy, C. Tang, C.J. Lord, A. Ashworth and S. Linardopoulos, *Aurora-A expressing tumour cells are deficient for homology-directed DNA double strand-break repair and sensitive to PARP inhibition.* EMBO Mol Med, 2010. **2**(4): p. 130-42.
265. Johnson, N., Y.C. Li, Z.E. Walton, K.A. Cheng, D. Li, S.J. Rodig, L.A. Moreau, C. Unitt, R.T. Bronson, H.D. Thomas, D.R. Newell, A.D. D'Andrea, N.J. Curtin, K.K. Wong and G.I. Shapiro, *Compromised CDK1 activity sensitizes BRCA-proficient cancers to PARP inhibition.* Nat Med, 2011. **17**(7): p. 875-82.
266. Gottipati, P., B. Vischioni, N. Schultz, J. Solomons, H.E. Bryant, T. Djureinovic, N. Issaeva, K. Sleeth, R.A. Sharma and T. Helleday, *Poly(ADP-ribose) polymerase is hyperactivated in homologous recombination-defective cells.* Cancer Res, 2010. **70**(13): p. 5389-98.
267. Patel, A.G., J.N. Sarkaria and S.H. Kaufmann, *Nonhomologous end joining drives poly(ADP-ribose) polymerase (PARP) inhibitor lethality in homologous recombination-deficient cells.* Proc Natl Acad Sci U S A, 2011. **108**(8): p. 3406-11.
268. Bunting, S.F., E. Callen, N. Wong, H.T. Chen, F. Polato, A. Gunn, A. Bothmer, N. Feldhahn, O. Fernandez-Capetillo, L. Cao, X. Xu, C.X. Deng, T. Finkel, M. Nussenzweig, J.M. Stark and A. Nussenzweig, *53BP1 inhibits homologous recombination in Brca1-deficient cells by blocking resection of DNA breaks.* Cell, 2010. **141**(2): p. 243-54.
269. Aly, A. and S. Ganesan, *BRCA1, PARP, and 53BP1: conditional synthetic lethality and synthetic viability.* J Mol Cell Biol, 2011. **3**(1): p. 66-74.
270. Jackman, J. and P.M. O'Connor, *Methods for synchronizing cells at specific stages of the cell cycle.* Curr Protoc Cell Biol, 2001. **Chapter 8**: p. Unit 8 3.
271. Glatter, T., A. Wepf, R. Aebersold and M. Gstaiger, *An integrated workflow for charting the human interaction proteome: insights into the PP2A system.* Mol Syst Biol, 2009. **5**: p. 237.
272. Paolinelli, R., R. Mendoza-Maldonado, A. Cereseto and M. Giacca, *Acetylation by GCN5 regulates CDC6 phosphorylation in the S phase of the cell cycle.* Nat Struct Mol Biol, 2009. **16**(4): p. 412-20.

273. Sirbu, B.M., F.B. Couch and D. Cortez, *Monitoring the spatiotemporal dynamics of proteins at replication forks and in assembled chromatin using isolation of proteins on nascent DNA.* Nat Protoc, 2012. **7**(3): p. 594-605.
274. Smogorzewska, A., S. Matsuoka, P. Vinciguerra, E.R. McDonald, 3rd, K.E. Hurov, J. Luo, B.A. Ballif, S.P. Gygi, K. Hofmann, A.D. D'Andrea and S.J. Elledge, *Identification of the FANCI protein, a monoubiquitinated FANCD2 paralog required for DNA repair.* Cell, 2007. **129**(2): p. 289-301.
275. Franken, N.A., H.M. Rodermond, J. Stap, J. Haveman and C. van Bree, *Clonogenic assay of cells in vitro.* Nat Protoc, 2006. **1**(5): p. 2315-9.
276. Cui, S., D. Arosio, K.M. Doherty, R.M. Brosh, Jr., A. Falaschi and A. Vindigni, *Analysis of the unwinding activity of the dimeric RECQ1 helicase in the presence of human replication protein A.* Nucleic Acids Res, 2004. **32**(7): p. 2158-70.
277. Sidorova, J.M., N. Li, D.C. Schwartz, A. Folch and R.J. Monnat, Jr., *Microfluidic-assisted analysis of replicating DNA molecules.* Nat Protoc, 2009. **4**(6): p. 849-61.
278. Hanada, K., M. Budzowska, S.L. Davies, E. van Drunen, H. Onizawa, H.B. Beverloo, A. Maas, J. Essers, I.D. Hickson and R. Kanaar, *The structure-specific endonuclease Mus81 contributes to replication restart by generating double-strand DNA breaks.* Nat Struct Mol Biol, 2007. **14**(11): p. 1096-104.
279. Lopes, M., *Electron microscopy methods for studying in vivo DNA replication intermediates.* Methods Mol Biol, 2009. **521**: p. 605-31.
280. Sharma, S., P. Phatak, A. Stortchevoi, M. Jasin and J.R. Larocque, *RECQ1 plays a distinct role in cellular response to oxidative DNA damage.* DNA Repair (Amst), 2012. **11**(6): p. 537-49.
281. Gagne, J.P., M. Isabelle, K.S. Lo, S. Bourassa, M.J. Hendzel, V.L. Dawson, T.M. Dawson and G.G. Poirier, *Proteome-wide identification of poly(ADP-ribose) binding proteins and poly(ADP-ribose)-associated protein complexes.* Nucleic Acids Res, 2008. **36**(22): p. 6959-76.
282. Langelier, M.F., K.M. Servent, E.E. Rogers and J.M. Pascal, *A third zinc-binding domain of human poly(ADP-ribose) polymerase-1 coordinates DNA-dependent enzyme activation.* J Biol Chem, 2008. **283**(7): p. 4105-14.
283. Tao, Z., P. Gao, D.W. Hoffman and H.W. Liu, *Domain C of human poly(ADP-ribose) polymerase-1 is important for enzyme activity and contains a novel zinc-ribbon motif.* Biochemistry, 2008. **47**(21): p. 5804-13.
284. Sirbu, B.M., F.B. Couch, J.T. Feigerle, S. Bhaskara, S.W. Hiebert and D. Cortez, *Analysis of protein dynamics at active, stalled, and collapsed replication forks.* Genes Dev, 2011. **25**(12): p. 1320-7.
285. Mortusewicz, O., J.C. Ame, V. Schreiber and H. Leonhardt, *Feedback-regulated poly(ADP-ribosyl)ation by PARP-1 is required for rapid response to DNA damage in living cells.* Nucleic Acids Res, 2007. **35**(22): p. 7665-75.
286. O'Connell, B.C., B. Adamson, J.R. Lydeard, M.E. Sowa, A. Ciccia, A.L. Bredemeyer, M. Schlabach, S.P. Gygi, S.J. Elledge and J.W. Harper, *A genome-wide camptothecin sensitivity screen identifies a mammalian MMS22L-NFKBIL2 complex required for genomic stability.* Mol Cell, 2010. **40**(4): p. 645-57.
287. Raderschall, E., E.I. Golub and T. Haaf, *Nuclear foci of mammalian recombination proteins are located at single-stranded DNA regions formed after DNA damage.* Proc Natl Acad Sci U S A, 1999. **96**(5): p. 1921-6.

288. Davar, D., J.H. Beumer, L. Hamieh and H. Tawbi, *Role of PARP inhibitors in cancer biology and therapy.* Curr Med Chem, 2012. **19**(23): p. 3907-21.
289. Tuduri, S., L. Crabbe, C. Conti, H. Tourriere, H. Holtgreve-Grez, A. Jauch, V. Pantesco, J. De Vos, A. Thomas, C. Theillet, Y. Pommier, J. Tazi, A. Coquelle and P. Pasero, *Topoisomerase I suppresses genomic instability by preventing interference between replication and transcription.* Nat Cell Biol, 2009. **11**(11): p. 1315-24.
290. Pourquier, P., A.A. Pilon, G. Kohlhagen, A. Mazumder, A. Sharma and Y. Pommier, *Trapping of mammalian topoisomerase I and recombinations induced by damaged DNA containing nicks or gaps. Importance of DNA end phosphorylation and camptothecin effects.* J Biol Chem, 1997. **272**(42): p. 26441-7.
291. Pourquier, P., L.M. Ueng, G. Kohlhagen, A. Mazumder, M. Gupta, K.W. Kohn and Y. Pommier, *Effects of uracil incorporation, DNA mismatches, and abasic sites on cleavage and religation activities of mammalian topoisomerase I.* J Biol Chem, 1997. **272**(12): p. 7792-6.
292. Pourquier, P., J.L. Waltman, Y. Urasaki, N.A. Loktionova, A.E. Pegg, J.L. Nitiss and Y. Pommier, *Topoisomerase I-mediated cytotoxicity of N-methyl-N'-nitro-N-nitrosoguanidine: trapping of topoisomerase I by the O6-methylguanine.* Cancer Res, 2001. **61**(1): p. 53-8.
293. Altmeyer, M., S. Messner, P.O. Hassa, M. Fey and M.O. Hottiger, *Molecular mechanism of poly(ADP-ribosyl)ation by PARP1 and identification of lysine residues as ADP-ribose acceptor sites.* Nucleic Acids Res, 2009. **37**(11): p. 3723-38.
294. Choudhary, C., C. Kumar, F. Gnad, M.L. Nielsen, M. Rehman, T.C. Walther, J.V. Olsen and M. Mann, *Lysine acetylation targets protein complexes and co-regulates major cellular functions.* Science, 2009. **325**(5942): p. 834-40.
295. Mao, F.J., J.M. Sidorova, J.M. Lauper, M.J. Emond and R.J. Monnat, *The human WRN and BLM RecQ helicases differentially regulate cell proliferation and survival after chemotherapeutic DNA damage.* Cancer research, 2010. **70**(16): p. 6548-55.
296. Zhang, Y.W., M. Regairaz, J.A. Seiler, K.K. Agama, J.H. Doroshow and Y. Pommier, *Poly(ADP-ribose) polymerase and XPF-ERCC1 participate in distinct pathways for the repair of topoisomerase I-induced DNA damage in mammalian cells.* Nucleic Acids Res, 2011. **39**(9): p. 3607-20.
297. Symington, L.S. and J. Gautier, *Double-strand break end resection and repair pathway choice.* Annu Rev Genet, 2011. **45**: p. 247-71.
298. Foster, S.S., A. Balestrini and J.H. Petrini, *Functional interplay of the Mre11 nuclease and Ku in the response to replication-associated DNA damage.* Mol Cell Biol, 2011. **31**(21): p. 4379-89.
299. Hastings, P.J., G. Ira and J.R. Lupski, *A microhomology-mediated break-induced replication model for the origin of human copy number variation.* PLoS Genet, 2009. **5**(1): p. e1000327.
300. Lambert, S., K. Mizuno, J. Blaisonneau, S. Martineau, R. Chanet, K. Freon, J.M. Murray, A.M. Carr and G. Baldacci, *Homologous recombination restarts blocked replication forks at the expense of genome rearrangements by template exchange.* Mol Cell, 2010. **39**(3): p. 346-59.

301. Iraqui, I., Y. Chekkal, N. Jmari, V. Pietrobon, K. Freon, A. Costes and S.A. Lambert, *Recovery of arrested replication forks by homologous recombination is error-prone.* PLoS Genet, 2012. **8**(10): p. e1002976.
302. Mizuno, K., I. Miyabe, S.A. Schalbetter, A.M. Carr and J.M. Murray, *Recombination-restarted replication makes inverted chromosome fusions at inverted repeats.* Nature, 2012.
303. Long, D.T., M. Raschle, V. Joukov and J.C. Walter, *Mechanism of RAD51-dependent DNA interstrand cross-link repair.* Science, 2011. **333**(6038): p. 84-7.